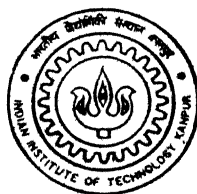


# EFFECT OF $\beta$ PROCESSING ON MICROSTRUCTURAL EVOLUTION OF Ti-6Al-4V ALLOY

by  
DEBRUPA MONDAL

TH  
MME/2000/M  
M744C



DEPARTMENT OF MATERIALS AND METALLURGICAL ENGINEERING  
INDIAN INSTITUTE OF TECHNOLOGY KANPUR  
April, 2000

**EFFECT OF  $\beta$  PROCESSING ON MICROSTRUCTURAL EVOLUTION OF  
Ti-6Al-4V ALLOY**

200001

A Thesis Submitted in Partial Fulfilment of the Requirements  
for the Degree of  
**MASTER OF TECHNOLOGY**

By  
**DEBRUPA MONDAL**

To the  
**DEPARTMENT OF MATERIALS AND METALLURGICAL ENGINEERING  
INDIAN INSTITUTE OF TECHNOLOGY KANPUR  
APRIL, 2000**

22 MAY 2000 / MME  
CENTRAL LIBRARY  
I. I. T., KANPUR

**A 130905**

TH  
MME. / 2000 / M


M1744c



A130905

# CERTIFICATE

This is to certify that the thesis entitled, '**Effect of  $\beta$ -Processing on Microstructural Evolution of Ti-6Al-4V Alloy**', is the record of the work carried out by under my supervision and has not been submitted else where for the award of the degree.



(Prof. S. Bhargava.)

Department of Materials and Metallurgical Engineering

Indian Institute of Technology

Kanpur

April, 2000.



**DEDICATED**

**TO**

***My Parents  
And  
Brother***

## ACKNOWLEDGEMENT

<b>ABSTRACT</b>	1 - 2
<b>Chapter 1. Introduction</b>	3 - 5
<b>Chapter 2. Literature Review</b>	6 - 45
2.1 Titanium and its Alloy	
2.1.1 Properties and Application of Ti and its Alloys	
2.1.2 Classification of Ti Alloys	
2.1.3 Importance of ( $\alpha$ + $\beta$ ) Alloys	
2.1.4 Microstructural Features Ti-Alloys	
2.1.5 Microstructure and Property Control	
2.1.5.1 Effect of Heat Treatment	
2.1.5.2 Effect of Working	
2.1.5.3 Effect of Thermo-Mechanical Treatment	
2.2 Texture in ( $\alpha$ + $\beta$ ) Ti-Alloys	
2.3 Deformation Characteristics of Ti and its Alloys	
2.4 Forming Characteristics of Ti-Alloys	
2.5 Superplasticity and Ti Alloys	
<b>Chapter 3. Experimental Procedure</b>	46 - 52
3.1 Starting Material	
3.2 Determination of $\beta$ -Transus Temperature	
3.3 Thermo-Mechanical Treatment	
3.3.1 Equipments for Thermo-Mechanical Processing	
3.3.2 Working Schedule	
3.4 Microstructural Characterization	
3.5 Quantitative Metallographic Measurements	
<b>Chapter 4. Results and Discussions</b>	53 – 128
4.1 Structure of the As Received Alloy	

- 4.3 Effect of Temperature on  $\beta$  Grain Size
- 4.4 Effect of Thermomechanical Processing Variables on Conditioning of  $\beta$  Grains
  - 4.4.1 Effect of Cooling Rate on the Structure
  - 4.4.2 Effect of Thickness Reduction on  $\beta$  Grain Characteristics
  - 4.4.3 Effect of Recrystallization Annealing on the Microstructure
  - 4.4.4 Comparison of Different Structures Produced by  $\beta$  Processing
- 4.5 Effect of Thermomechanical Processing in  $(\alpha+\beta)$  Phase Field on Microstructural Refinement of The Alloy
  - 4.5.1 Effect of Thermomechanical Processing Variables on the Microstructures of the Samples Treated Through Route I
  - 4.5.2 Effect of Thermomechanical Processing Variables on the Microstructures of the Samples Treated Through Route II
  - 4.5.3 Effect of Thermomechanical Processing Variables on the Microstructures of the Samples Treated Through Route III
  - 4.5.4 Effect of Thermomechanical Processing Variables on the Microstructures of the Samples Treated Through Route IV
  - 4.5.5 Effect of Thermomechanical Processing Variables on the Microstructures of the Samples Treated Through Route V

- 4.6 Effect of Mill Annealing Treatment on the Evolution of the Equiaxed  $\alpha$  Structure in Heavily ( $\alpha+\beta$ ) Deformed Ti-6-4 Alloy
- 4.7 Mechanism of Evolution of Equiaxed  $\alpha$  Structure in Ti-6-4 Alloy

<b>Chapter 5. Conclusions</b>	129 - 130
<b>References</b>	131 - 137

## **ACKNOWLEDGEMENT**

I wish to express my deep sense of gratitude and indebtedness to Dr. S. Bhargava for his valuable guidance, encouragement and inspirational discussions throughout the course of this investigation. It has truly been a learning experience to associate with him and work towards the completion of this work.

I am really grateful to Dr. S. Sangal (ex-DPGC convenor), Dr. R. Balasubramaniam (DPGC convenor), Dr. K. N. Rai (faculty-member, DPGC) for granting me semester leave and permitting me to do some of the works of my thesis outside IITK and also to my present employer INDAL, Belur for granting me leave for the completion of my M.Tech Thesis.

I am thankful to Mr. Manasij Kumar Yadava and Dr. Satyam Suwas for their endless help and moral support extended to me at different time.

I am also thankful to Dr. Mungole, Mr. K.P.Mukherjee, late Mr. Pal, the metallurgical workshop staffs and especially to Mr. Kumar for their assistance in the experimental works.

I must thank my father, mother and brother for their whole-hearted help in keeping up my spirit for completing my works.

And, last but not the least, I must mention the name of Indranil Lahiri, who is not only my co-worker and best friend, but without his assistance and encouragement it was totally impossible for me to complete the thesis-work.

April'2000

I.I.T., Kanpur

Debrupa Mondal

## ABSTRACT

Ti-6Al-4V alloy is one of the most important ( $\alpha+\beta$ ) titanium alloy having wide application in space, aeronautical and chemical industries. Further, in the extra-low interstitial (ELI) condition, Ti-6Al-4V alloy shows excellent fracture toughness in cryogenic environments. The flow stress of this alloy, however, is extremely sensitive to temperature and production of its net- or near-net shape parts by the conventional forging methods is virtually not possible. This alloy, however, shows excellent superplastic behaviour in the equiaxed  $\alpha$  microstructural state and hence can be easily isothermally forged or superplastically formed. The challenge thus lies in obtaining a very fine equiaxed  $\alpha$  microstructural condition by an appropriate thermo-mechanical processing schedule. The conventional thermo-mechanical processing route for this alloy consists of heavy hot deformation in the ( $\alpha+\beta$ ) phase field followed by mill annealing at a lower temperature to obtain a fine equiaxed  $\alpha$  phase structure surrounded by the  $\beta$  phase.

Evolution of the equiaxed  $\alpha$  structure, however, is expected to be influenced by the conditioning of prior  $\beta$  grains. The present study deals with the microstructural evolution of an ELI grade Ti-6Al-4V alloy as influenced by its thermo-mechanical processing involving different routes affecting the conditioning of prior  $\beta$  grains as well as the aspect ratio of the lamellar  $\alpha$  prior to rolling in ( $\alpha+\beta$ ) field.

For obtaining differently conditioned  $\beta$  grains, plates of the given Ti-6Al-4V alloy, before their rolling in the ( $\alpha+\beta$ ) field, were subjected to five thermo-mechanical treatments involving heating in the  $\beta$  phase field at 980°C followed by (a) furnace cooling (Route I), (b) water quenching with no deformation in the  $\beta$  phase field (Route II), (c) water quenching with 30% deformation in the  $\beta$  phase field (Route III), (d) water quenching with 60% deformation in the  $\beta$  phase field (Route IV) and (e) recrystallization of the 60% deformed sample for 30 seconds at 960°C, which is 10°C above the  $\beta$ -transus temperature, followed by water quenching (Route V). Samples obtained from

these routes were further hot rolled at three different temperatures of 820°C, 880°C and 920°C to give thickness reductions of 0%, 25%, 50% and 75% at each temperature in the ( $\alpha$ + $\beta$ ) field. Some of these samples were subsequently mill-annealed at the temperatures of 250°C, 150°C and 100°C below the  $\beta$ -transus temperature

An extensive metallographic work involving quantitative measurements on lengths and thicknesses of  $\alpha$  lamellae and martensitic needles in differently processed Ti-6Al-4V alloy was done. Results of the present study show that the unconventional routes involving thermo-mechanical processing in the  $\beta$  field produce considerably finer structures than those obtained by the conventional route. Microstructures obtained by each of these new routes were found to have an average  $\alpha$  phase size < 3 $\mu$ m. Thickness of the  $\alpha$  lamellae decreases as the temperature of treatment in the two phase field increases from 820°C to 920°C. Recrystallization behaviour of  $\alpha$  lamellae at 880°C shows that samples treated through route III and route IV in the  $\beta$  phase field produces the finest equiaxed structure on annealing at 850°C for 30 minutes.

# CHAPTER 1

## INTRODUCTION

---

During late 1940s and early 1950s Ti and its alloys caught the attention of the scientists and technologists due to their good high temperature properties and high strength-to-weight ratio which made them candidate materials for aeronautical industries. Till date, these alloys have found widespread application in the chemical and related industries also, where advantage is taken of its excellent corrosion resistance and in making medical implants due to good bio-compatibility[4,71].

Titanium alloys are generally classified into three major classes depending on the phases present in the alloy at room temperature and are referred to as  $\alpha$  alloys,  $\alpha+\beta$  alloys and  $\beta$  alloys. The group  $\alpha+\beta$  alloys consists of largest number of commercial alloys. These are alloys whose compositions are such that they support a mixture of  $\alpha$  and  $\beta$  phases in the microstructure at room temperature. They also have high room temperature strength and moderate elevated temperature strength. The properties of  $\alpha+\beta$  alloys can be controlled by heat treatment and thermo-mechanical treatment, which are used to control the microstructural and precipitational states of the phase components.

In the  $\alpha+\beta$  titanium alloys morphology of the primary  $\alpha$  phase is of high importance from the point of view of controlling the static and dynamic mechanical properties. Equiaxed microstructures often show a higher tensile ductility at low temperature, superior fatigue strength, increasing fatigue crack initiation resistance and good elevated temperature flow characteristics, especially when the  $\alpha$  grain size is reduced, whereas lamellar structures have improved fatigue crack propagation resistance, creep strength and fracture toughness values[72]. Slow cooling into the  $\alpha+\beta$  phase field leads to a very coarse lamellar arrangement while water quenching from the  $\beta$  phase field followed by an annealing treatment in the two phase field leads to a finer lamellar



followed by an annealing treatment in the two phase field leads to a finer lamellar structure. Equiaxed microstructures require an additional deformation treatment within the  $\alpha+\beta$  phase field followed by mill annealing at about 700°C. Generally, it has been observed that the rate at which lamellar  $\alpha$  transforms to equiaxed  $\alpha$  is a function of annealing temperature, time and the amount of work the alpha phase has received. The bi-modal structures, mixtures of lamellar and equiaxed  $\alpha$ , are reported to have advantages in terms of yield stress, tensile ductility and fatigue strength and also a proper balance between strength and toughness [79,81]. Another important factor with respect to mechanical properties is the existence of grain boundary  $\alpha$ , which can be considered as a continuous, thin, soft layer along prior  $\beta$  grain boundaries. It was observed that the grain boundary  $\alpha$  is the site where voids nucleate most easily reducing its toughness[80].

Processing history of the alloys govern the microstructures of the titanium alloys and hence the mechanical properties. It is seen that the strength in the  $\alpha+\beta$  worked and  $\beta$  worked material are comparable, but the tensile ductility is better for the former one with much better fracture toughness and fatigue strength for the latter one[81]. It is also observed that as the cooling rate from the  $\beta$  annealing temperature is decreased, strength decreases, ductility increases and the fracture mode after an  $\alpha+\beta$  annealing treatment changes from predominantly intergranular to a ductile transgranular one[82].

Though  $\alpha+\beta$  titanium alloys possess good mechanical properties, they have poor workability. Hence, superplastic forming has emerged as one of the commercially viable production route. The microstructure of the alloy has important bearing on the superplastic properties and one of the essential requirements of superplasticity in these alloys is that the structure should consist of  $\alpha+\beta$  structure in which the primary  $\alpha$  exists in a very fine equiaxed morphology. Therefore obtaining fine equiaxed structure in the material, so that they can be further processed by superplastic forming, has become one of the major objectives in processing of  $\alpha+\beta$  titanium alloys.

The scope of refining the structure by proper  $\beta$  treatment prior to the conventional thermo-mechanical processing is not investigated thoroughly for this alloy though it has the possibility to show better superplastic formability and some other mechanical properties, as discussed earlier. The results and understanding of the refinement process for development of suitable microstructures can lead to more precision shapes to be formed by superplastic forming in this alloy with good strength, fatigue properties.

The present study was undertaken

- (i) to investigate the microstructural refinement in Ti-6Al-4V alloy by involving the conditioning of  $\beta$  grains and acicular  $\alpha$  prior to hot rolling in the  $\alpha+\beta$  field,
- (ii) to present the mechanism of recrystallization for this alloy and to pinpoint the effect of deformation and temperature during two-phase treatment on the evolution of microstructure.

# LITERATURE REVIEW

---

## 2.1 TITANIUM AND ITS ALLOYS

### 2.1.1 Properties and Applications of Ti and its Alloys

Titanium shows an outstanding combination of mechanical, chemical and physical properties. Titanium metal is found in two allotropic forms. The low temperature form, known as  $\alpha$ -titanium, is stable below 882.5°C and has a hexagonal close-packed structure. The high temperature form, stable above 882.5°C, has a body centred cubic structure and is known as  $\beta$ -titanium. Titanium is a low-density element. Density of  $\alpha$ -titanium at 25±2°C is 4.505 gm/cm<sup>3</sup>[1], whereas that of  $\beta$ -titanium at 900°C is 4.32 gm/cm<sup>3</sup>[2]. Young's modulus of titanium generally lies in the range  $(11.0\pm0.4)\times10^{11}$  dyne/cm<sup>2</sup>[3]. It is paramagnetic in nature and shows a relatively lower coefficient of linear thermal expansion and high electrical resistivity. Some important physical properties of titanium are shown in Table 2.1[3,5].

With strength capability most equal to that of low carbon steels and density nearly half (56 %) of them, titanium alloys can be strengthened to achieve a specific strength (strength per unit weight) equal to that of ultra high strength steels. Table 2.2[4] shows typical room temperature tensile strength of some commercial titanium alloys. Titanium approaches the high hardness value possessed by some of the heat-treated alloy steels[29].

Titanium and its alloys have exceptionally high fatigue strength, if the surface is carefully prepared. It is 0.82 and 0.31 of tensile strength for unnotched and notched samples, respectively and thus lies in the same range as the steels[3,6]. Fatigue crack growth rates of annealed Ti-6Al-4V alloy in distilled

**Table 2.1 : Physical Properties of Elemental Titanium**

Atomic Number	22
Atomic Weight	47.90
Atomic Volume	10.6 W/D
Covalent Radius	1.32 Å
First Ionisation Energy	158 K-cal/gm-mole
Thermal Neutron Absorption Cross Section	5.6 barns/atom
Colour	Dark Gray
Density	$\alpha$ - 4.505 gms/cm <sup>3</sup> at 25±2°C $\beta$ - 4.32 gms/cm <sup>3</sup> at 900°C
Melting Point	1941±10 K
Solidus/Liquidus	1998±10 K
Boiling Point	3533 K
Specific Heat(at 25°C)	0.518 J/kg K
Thermal Conductivity	9.0 BTU/hr ft <sup>2</sup> °F
Heat of Fusion	440 kJ/kg
Heat of Evaporation	9.83 MJ/kg
Heat of Transformation	678 cal/mole
Yong's Modulus	$10.7 \times 10^{11}$ dyne/cm <sup>2</sup>
Temp. Coeffn. Of Young's Modulus	$6.28 \times 10^8$ dyne/cm <sup>2</sup> °C
Modulus of Rigidity	$(3.87 \pm 0.1) \times 10^{11}$ dyne/cm <sup>2</sup>
Poisson's Ratio	0.36
Coefficient of Friction	0.8 at 40 m/min
Coefficient of Linear Expansion	$(8.35 \pm 0.15) \times 10^{-6}$ /°C at 15°C
Electrical Resistivity	$(42.05 \pm 0.5) \times 10^{-6}$ ohm-cm
Magnetic Susceptibility	3.2±0.4 emu/gm
Work Function	4.05±0.1 eV
Electronic Specific Heat	$8.0 \times 10^{-4}$ cal/°C mol

**Table 2.2 : Typical Room Temperature Tensile Strengths Of Some Commercial Titanium-base Alloys**

Alloy Name	Nominal Composition	Condition	UTS $10^8 \text{ Nm}^{-2}$	YS $10^8 \text{ Nm}^{-2}$	Elong. %
5-2.5	Ti-5Al-2.5Sn	A,.25-4h,1300-1600°F	8.3-9.0	7.9-8.3	13-18
3-2.5	Ti-3Al-2.5Sn	A,1-3h,1200-1400°F	6.5	6.2	22
6-2-1-1	Ti-6Al-2Nb-1Ta-1Mo	A,.25-2h,1300-1700°F	8.6	7.6	14
8-1-1	Ti-8Al-1Mo-1V	A,8h,1450°F	10.0	9.3	12
Corona 5	Ti-4.5Al-5Mo-1.5Cr	$\alpha$ - $\beta$ A, after $\beta$ processing	9.7-11.0	9.3-10.3	12-15
Ti-17	Ti-5Al-2Sn-2Zr-4Mo-4Cr	$\alpha$ - $\beta$ or $\beta$ processed + Ag.	1.4	10.7	8
6-4	Ti-6Al-4V	A,2h,1300-1600°F Ag.	9.6 11.7	9.0 11.0	17 12
6-6-2	Ti-6Al-6V-2Sn	A,3h,1300-1550°F Ag.	10.7 12.8	10.0 12.1	14 10
6-2-4-2	Ti-6Al-2Sn-4Zr-2Mo	A,4h,1300-1550°F	10.0	9.3	15
6-2-4-6	Ti-6Al-2Sn-4Zr-6Mo	A,2h,1500-1600°F Ag.	10.3 12.1	9.7 11.4	11 8
6-22-22	Ti-6Al-2Sn-2Zr-2Mo-2Cr-.25Si	$\alpha$ - $\beta$ processed+Ag.	10.0	10.1	14
10-2-3	Ti-10V-2Fe-3Al	A,1h,1400°F Ag.	9.7 12.4-13.4	9.0 11.4-12.4	9 7
15-3-3-3	Ti-15V-3Cr-3Sn-3Al	A,.25h,1450°F Ag.	7.9 11.4	7.7 10.7	20-25 8
13-11-3	Ti-13V-11Cr-3Al	A,.5h,1400-1500°F Ag.	9.3-9.7 12.1	8.6 11.4	18 7
38-6-44	Ti-3Al-8V-6Cr-4Mo-4Zr	A,.5h,1500-1700°F Ag.	8.3-9.0 12.4	7.8-8.3 11.7	10-15 7
$\beta$ -III	Ti-4.5Sn-6Zr-11.5Mo	A,.5h,1300-1600°F Ag.	6.9-7.6 12.4	6.5 11.7	23 7

A → Annealed Ag. → Aged

water are enhanced as compared with that in air; the growth rates are found to decrease with increasing temperature and frequency[7]. These alloys showed creep at room temperature; creep strength of titanium normally decreases at first, but at 120°C begins to increase again, reaching a maximum at 200°C, thereafter falls gradually with increase in temperature. Cold working of titanium increases its creep resistance at room temperature[3,6]. The Charpy impact strength dropped from an average of 15 ft-lb at room temperature to about 6 ft-lb at liquid nitrogen temperature[6]. The specific fracture toughness (fracture toughness,  $K_{IC}$ , per unit weight) of titanium alloys is superior to most of the structural materials. Table 2.3 and 2.4 compares some mechanical properties of Ti and its alloys with some other metals and alloys.

Titanium and its alloys are resistant to corrosion by most reactive substances, their resistance is better than that of stainless steel. It is attacked by hydrofluoric acid and acids containing fluorides, at room temperature[8], but resistant to almost all other corroding media. They also show excellent stress corrosion behaviour except in red fuming nitric acid[3]. They show excellent atmospheric and marine corrosion resistance. Cavitation resistance of Ti-6Al-4V in water is superior to stainless steel[9].

Titanium reacts with oxygen, nitrogen, hydrogen and most gaseous compounds like CO, CO<sub>2</sub>, H<sub>2</sub>O, NH<sub>3</sub> etc. at elevated temperature. Nitrogen is a strong  $\alpha$  stabilizer and not it only forms nitride scale, also goes into the lattice. The reaction is irreversible, though kinetics of this reaction is very slow[16]. Oxygen is also a strong  $\alpha$  stabilizer, which forms oxide scales and goes into the solid solution, increasing the  $\alpha/\beta$  transition temperature and increasing the hardness of the oxygen enriched zone near the surface. This reaction is also irreversible. In the oxidation of titanium, the following reaction may be expected to occur at the metal/oxygen interface[17].

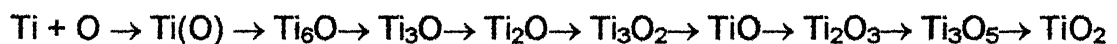


**Table 2.3 : Comparative Mechanical Properties of Some Metals**

<b>Metal</b>	<b>UTS (10<sup>3</sup> psi)</b>	<b>YS (10<sup>3</sup> psi)</b>	<b>Elong. (%)</b>	<b>R.A. (%)</b>	<b>Modulus Elastic. (10<sup>6</sup> psi)</b>	<b>Modulus Rigid. (10<sup>6</sup> psi)</b>	<b>BHN *</b>	<b>Charpy Impact (ft lb)</b>
Al	9	3	60	70	10	3.87	15	19
Cu	37	14	15	52	16	6	47	16
Fe (pure)	40	20	40	80	29.7	10	90	—
Mg	27	10	15	50	6.25	2.4	37	—
Fe (ingot)	44.3	22.7	47	75	29.1	11.6	120	19
Ti (pure)	35	20	55	80	15	5	85	100
Ti (ingot)	75	55	25	50	16	5	180	30

\* Ferrous and titanium metals measured with 3000-kg load and a 10-mm ball, other metal measured with a 500-kg load and a 10-mm ball.

**Table 2.4 : Comparative Mechanical Properties of Some Alloys**

<b>Metal</b>	<b>UTS (10<sup>3</sup> psi)</b>	<b>YS (10<sup>3</sup> psi)</b>	<b>Elong. (%)</b>	<b>R.A. (%)</b>	<b>Modulus Elastic. (10<sup>6</sup> psi)</b>	<b>Modulus Rigid. (10<sup>6</sup> psi)</b>	<b>BHN *</b>	<b>Charpy Impact (ft lb)</b>
Ti (3Al-5Cr)	150	135	18	45	17	6	290	24
Steel (4340)	145	135	20	58	28.7	12	285	52
Stainless Steel (18-8)	89.4	28	61	75	29	—	140	—
Al (4S-O)	26	10	25	50	10	3.9	45	—
Al (75S-T6)	82	72	11	40	10.4	3.9	150	—
Mg (AZ 31)	37	22	21	25	6.5	2.4	56	3.2

\* Ferrous and titanium metals measured with 3000-kg load and a 10-mm ball,  
other metal measured with a 500-kg load and a 10-mm ball.



Hydrogen is one of the most dangerous contaminants in Ti, though its reaction with Ti being reversible, vacuum annealing can cause dehydrogenation. The effects of hydrogen are :

- a) causing strain aging
- b) increasing notch sensitivity, specially below 0°C
- c) causing strain rate sensitivity, tensile strength and elongation to be lower at lower strain rates
- d) stabilizing  $\beta$  phase
- e) forming hydrides and causing embrittlement.

Ti alloys containing hydrogen above 150 ppm. become brittle under stress at high temperature[8].

In air titanium is most readily attacked by water vapour, which is dissociated by titanium at high temperature into hydrogen and oxygen. Hence, care should be taken starting from melting to heat treatment of titanium and its alloys.

All the customary techniques used in joining metals have been successfully applied to titanium and its alloys, except for soft soldering. But care should be taken during joining to prevent  $\alpha \rightarrow \beta$  transformation to get a metallurgically sound structure.

Most of the dual phase titanium alloys of the family represented by Ti-6Al-4V can show a high value of strain rate sensitivity of stress approaching to unity which puts them among the most desirable candidate materials for isothermal forging and superplastic forming-diffusion bonding.

Interest in the properties of Ti and its alloys began to accelerate during the late 1940s and early 1950s as their potential as high temperature, high strength/weight material with aeronautical applications becoming more and more widely recognized. Ti and its alloys have, by now, found widespread use in the aerospace industry and in the chemical and related industries. Figure 2.1[12]

shows some aircraft applications of titanium. Main fields of application of Ti and its different alloys along with their important properties are listed in Table 2.5, which gives an idea about the vast field of usage of Ti and its alloys.

Though strength efficiency is the prime consideration for structural applications and in aerospace industries, which have majority of demand for titanium alloys, other requirements like fatigue life, fracture toughness, creep, microstructural stability at high temperature may also have to be met depending on the nature of application. To meet these multifarious requirements, different alloys have been developed.

### **2.1.2 Classification of Ti-Alloys**

Pure titanium has two allotropic modifications,  $\alpha$ -titanium and  $\beta$ -titanium, as mentioned earlier. The allotropic transformation temperature is 882.5°C (1155.5 K)[19,20]. Table 2.6 lists lattice parameters of the two phases[1,2,21].

Alloy additions to titanium except tin and zirconium tend to stabilize either the  $\alpha$  or the  $\beta$  phase. Sn and Zr are interesting alloying elements in that they have extensive solid solubility in both the  $\alpha$  and  $\beta$  phases. They only slow down reaction kinetics and are useful strengthening agents.

Elements which when dissolved in Ti produce little change in the transformation temperature or cause it to increase are known as " $\alpha$  stabilizers". They are simple metals or interstitial elements, eg., Al, C, N, O etc. Rosenberg[22] has suggested an expression for the aluminium equivalent  $Al^*$  of the alloy :

$$Al^* = [Al] + [Zr]/6 + [Sn]/3 + 10[O + C + N] \quad \text{wt \%}$$

Alloying additions, which decrease the phase-transformation temperature, are referred to as " $\beta$  stabilizers". They are generally transition metals or noble metals, eg., Mo, V, Ni, Mn, Cu, Cr, Fe, H, Si etc. Molchanova[19] has suggested an expression for Mo equivalent  $Mo^*$  of the alloy :

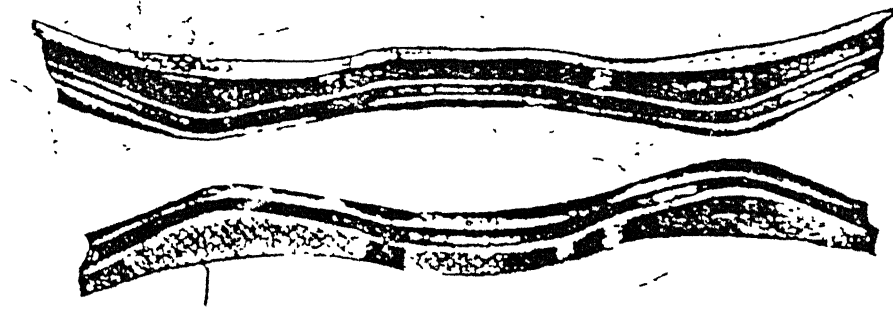


**Figure 2.1(a) Titanium Aircraft Channel Sections**

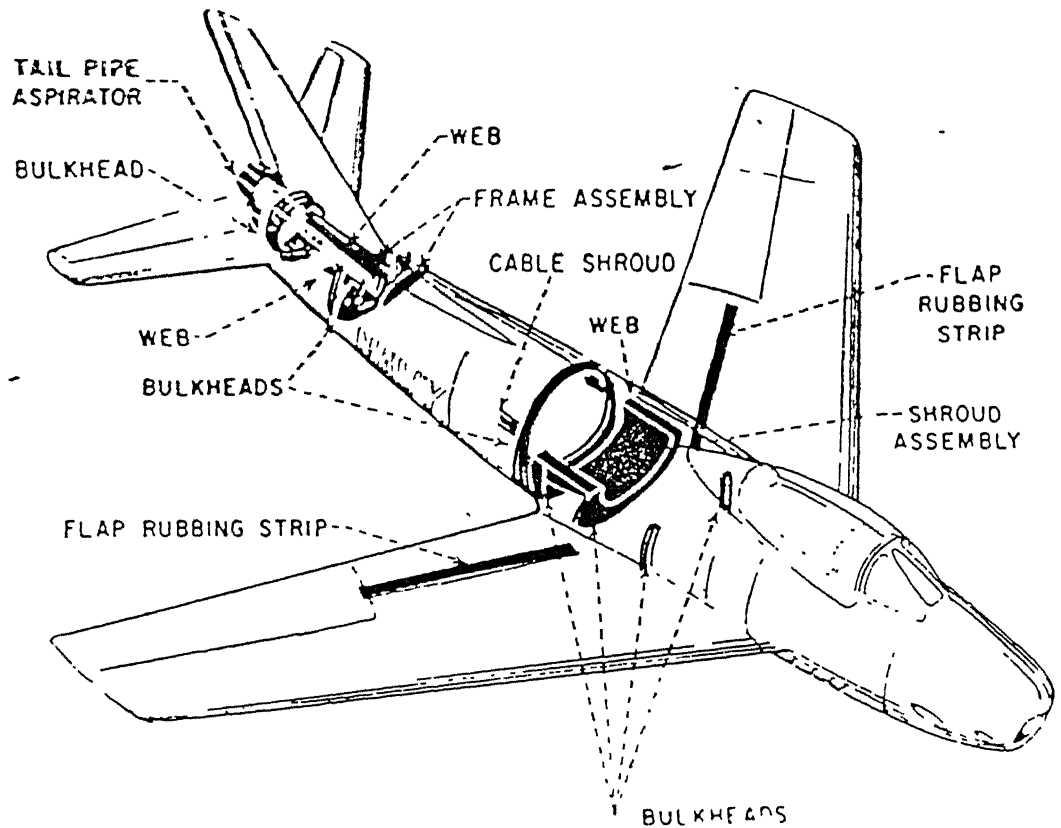


**Figure 2.1(b) Major Fabricated Titanium Parts of The North American FJ-2 Jet Fighter**

**Table 2.5 : Applications of Titanium and its Alloys**

<b>Material</b>	<b>Area of Application</b>	<b>Important Properties</b>	<b>Ref. No.</b>
Several Ti alloys	Low temperature structural application	High strength/weight ratio and corrosion resistance, low thermal conductivity	4
Ti-6242	Structural application up to 480-510°C	Good heat resistance	4
Ti-11	Aircraft gas turbine engine	Heat resistance, surface stability, improved creep strength	4
Ti alloy forgings and sheets	Landing gear components, compressor blades and discs, turbine liners, baffles, skin assembly, tail cones in aircrafts	Heat resistance, surface stability, good creep resistance, high strength/weight ratio	6
Ti-6Al-4V and other Ti alloys	Different parts in Boeing 777	Weight saving, high operating temperature, electrical compatibility with CFRP composites, corrosion resistance	10
Many Ti alloys	Firewalls, nacelles and compressor blades in supersonic aircrafts	Good hot strength, low thermal conductivity	6,8
Ti-6Al-4V	Steam turbine blading	High static and fatigue strength, reasonable ductility, corrosion and pitting resistance, better fatigue property	11
Ti-6Al-4V	Wheel hubs, centrifuges in Airbus A320 etc.	—	12
Ti-6Al-4V	Turbo-fan engines	High strength, good fatigue property, superplasticity	13
Ti-6Al-4V	Under water structures	High strength/weight ratio, excellent corrosion resistance, good fabricability, weldability, shock resistance	14
Ti alloys	Flash suppressors for artillery, guns, missiles, armour plates etc.	Good shock resistance, high weight saving, formability, strength	6,29

( Continued to next page)

<b>Material</b>	<b>Area of Application</b>	<b>Important Properties</b>	<b>Ref. No.</b>
Ti alloys	Piston rods in Formula 1 racing cars	Decreased fuel consumption, better fatigue strength	29, 30
Ti and its alloys	Cable armour material in electrical industry	High electrical resistance, non-magnetic property	29
Several Ti alloys	Seamless tubings in aircrafts, tennis racket, bicycle frame, wheel chairs	—	31
Ti-6Al-4V	Different parts in offshore petroleum hostile environment exploitation	Good strength, pitting, stress and crevice corrosion resistance, resistance against local destruction of passive films	32
Ti and its alloys	Heat exchangers, reactor vessels, condenser tubes in chemical, marine, petrochemical, offshore and power generation industries	Excellent corrosion resistance	32
Ti and its alloys	Prosthetic devices	Non-toxicity, excellent corrosion resistance under body condition, bio-compatibility	15,33

**Table 2.6 : Lattice Paramater(mean) Values of  $\alpha$ - and  $\beta$ -Titanium**

	a	c	c/a
$\alpha$	2.9503 $\pm$ 0.0004 A	4.6831 $\pm$ 0.0004 A	1.5873 $\pm$ 0.0004
$\beta$	3.283 $\pm$ 0.003 A		

$$Mo^* = [Mo] + [Ta]/5 + [Nb]/3.6 + [W]/2.5 + [V]/1.5 + 1.25[Cr] + 1.25[Ni] + 1.7[Mn] + 1.7[Co] + 2.5[Fe]$$

$\beta$ -stabilized systems can be of two types :  $\beta$  isomorphous and  $\beta$  eutectoid, depending upon whether decomposition of  $\beta$  to  $\alpha$  plus eutectoid products occur under equilibrium condition. Figure 2.2 to 2.4 shows some typical phase diagrams of  $\alpha$  and  $\beta$  stabilized systems[23]. Figure 2.5 shows a simple classification scheme for binary Ti-alloy phase diagrams[4]. The type and concentration of alloying elements determine the equilibrium condition, which forms the basis for classification of titanium alloys. Depending on the type of alloying additions made, technical alloys of Ti are classified as “ $\alpha$ ”, “ $\alpha+\beta$ ” and “ $\beta$ ”. Table 2.7 lists some examples of commercial Ti-alloys with their classes[4].

#### 2.1.2.1 $\alpha$ -alloys

These alloys contain no or only  $\alpha$  stabilizers as alloying additions and at ordinary temperature these have hcp  $\alpha$  phase only. Due to single phase nature of these alloys, no microstructural strengthening can be achieved in them. Solid solution strengthening [22] of them is also limited because an aluminium equivalent of more than 9.0 promotes the formation of the brittle phase  $\alpha_2$ . These alloys, according to Wood[24], are characterized by satisfactory strength, toughness, creep resistance and weldability. Furthermore, the absence of a ductile-brittle transformation, a property of the bcc structure, renders  $\alpha$  alloys suitable for cryogenic applications[25]. These alloys have poor workability. Examples are unalloyed Ti and Ti-5Al-2.5Sn.

#### 2.1.2.2 $(\alpha + \beta)$ alloys

These alloys have a mixture of  $\alpha$  and  $\beta$  phase at room temperature and in practice, they usually contain mixtures of both  $\alpha$  and  $\beta$  stabilizers. The simplest of such alloys and undoubtedly the most important is Ti-6Al-4V, which is difficult to form even in the annealed condition[25]. But  $(\alpha+\beta)$  alloys generally exhibit good fabricability, high room temperature strength and moderate elevated temperature strength. Alloys containing more than 20 %  $\beta$  phase at room

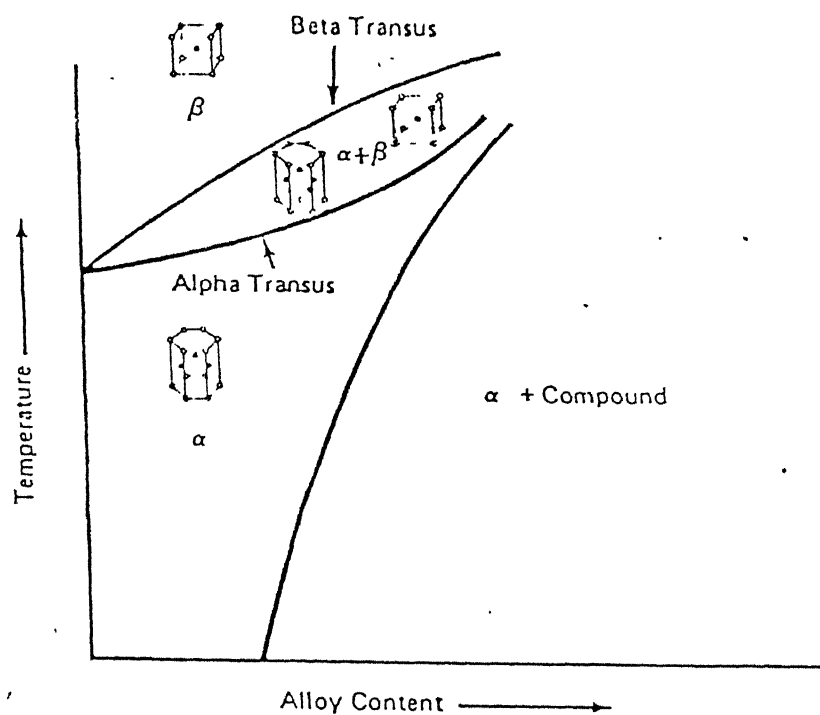


**Figure 2.2 Phase Diagram of  $\alpha$ -Stabilized Systems**



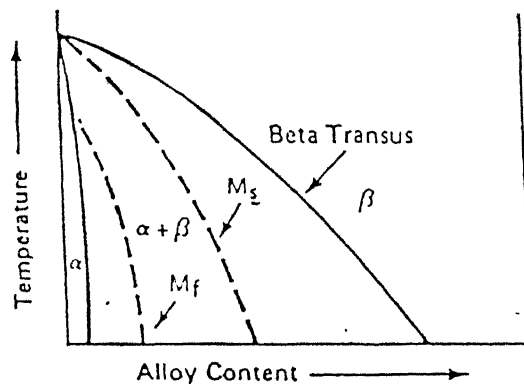


**Figure 2.3 Phase Diagram of  $\beta$ -Isomorphous Systems**

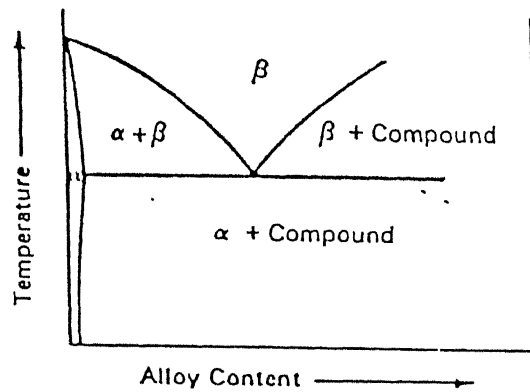


**Figure 2.4 Phase Diagram of  $\beta$ -Eutectoid Systems**

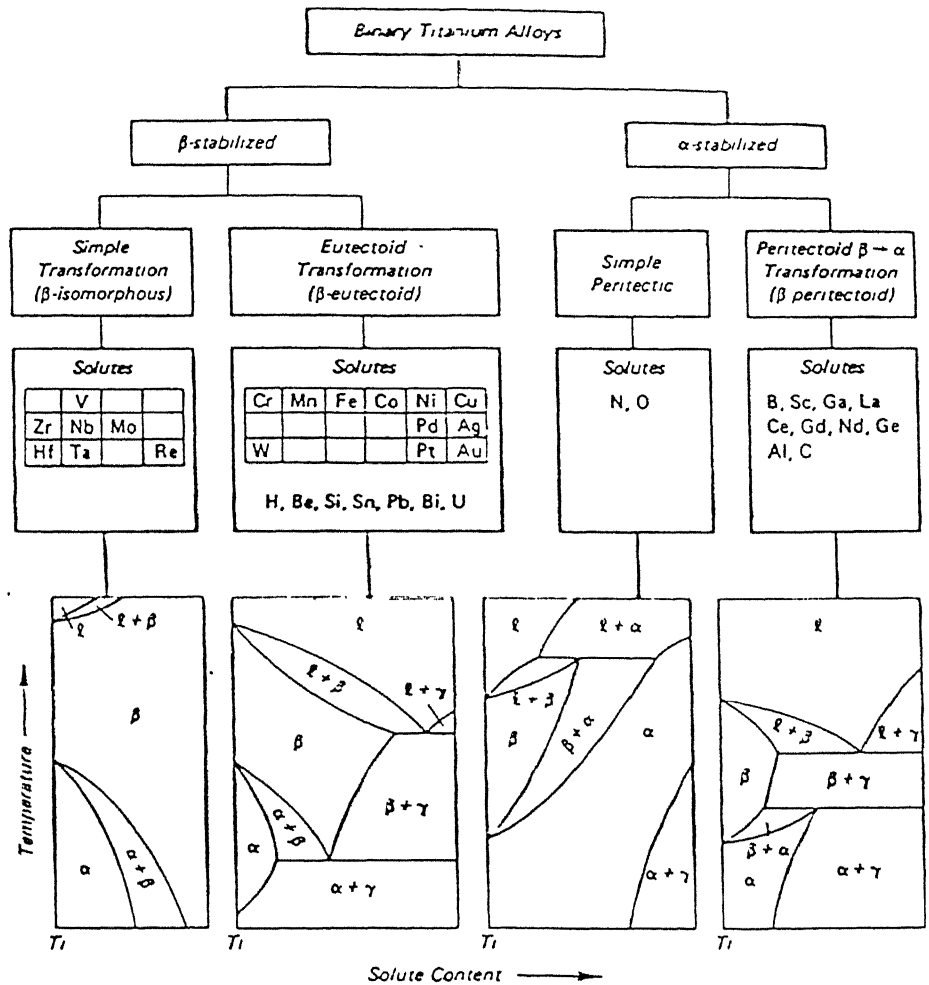


**Figure 2.5 A Simple Classification Scheme for Binary Ti-Alloy Phase Diagrams**

$\alpha$  and  $\beta$  are solid solution alloys,  $\gamma$  is an intermetallic compound.

**Table 2.7 :      Some Commercial Titanium-base Alloys with their Structural Classes**

<b>Alloy</b>	<b>Classification</b>
Ti-5Al-2.5Sn	$\alpha$
Ti-8Al-1Mo-1V Ti-6Al-2Sn-4Zr-2Mo Ti-6Al-4V Ti-6Al-2Sn-6V Ti-3Al-2.5V Ti-6Al-2Sn-4Zr-4Mo Ti-5Al-2Sn-2Zr-4Cr-4Mo Ti-3Al-10V-2Fe	$\alpha+\beta$
Ti-13V-11Cr-3Al Ti-15V-3Cr-3Al-3Sn Ti-4Mo-8V-6Cr-4Zr-3Al Ti-8Mo-8V-2Fe-3Al Ti-11.5Mo-6Zr-4.5Sn	$\beta$

temperature are not weldable. The properties of ( $\alpha+\beta$ ) alloys can be controlled by heat treatment, which is used to adjust the microstructural and precipitational states of the  $\beta$  component. Figure 2.6 and 2.7 show vertical and horizontal sections of Ti-Al-V system, respectively[4].

### **2.1.2.3 $\beta$ alloys**

Generally transition metal solutes are stabilizers of the bcc,  $\beta$  phase and hence, the  $\beta$  alloys contain one or more of them. Typical examples of  $\beta$  alloys, which have  $\beta$  phase at room temperature, are Ti-15Mo-5Zr and Ti-15Mo-5Zr-3Al. The  $\beta$  alloys have high density, poor ductility, poor oxidation resistance and hence, of less commercial importance. They are extremely formable[24], prone to ductile-brittle transformation[26] and unsuitable for low temperature applications[25].

Since the present investigation is concerned with the titanium alloy, Ti-6Al-4V, an ( $\alpha+\beta$ ) alloy, the discussion henceforth will only be confined to the family of ( $\alpha+\beta$ ) alloys.

### **2.1.3 Importance of ( $\alpha+\beta$ ) Alloys**

As a class, ( $\alpha+\beta$ ) alloys account for more than 75 % of all titanium used[27] and Ti-6Al-4V accounted for 56 % of the total output in 1972[24]. ( $\alpha+\beta$ ) alloys have been designed to combine the better properties of both  $\alpha$  and  $\beta$  alloys. Because of its dual phase nature, a wide range of microstructural features, varying in size and morphology of the constituent phases, can be obtained in them. Since the rule of mixture is not followed by them[28], a considerable amount of microstructural strengthening can be imparted to them. Thus, for the same alloy, it is possible to have a wide range of property levels by altering the morphology and size of its microstructural constituents. Yield strength, tensile strength and ductility are not influenced much by a change in microstructure, where as fracture toughness, fatigue strength, fatigue crack propagation rate, creep resistance, creep rupture strength and the

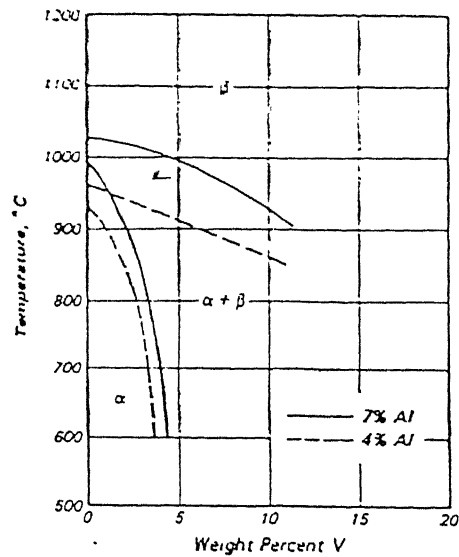


**Figure 2.6(a) Vertical section of The Ti-Al-V Vs T Equilibrium Phase Prism at 4 and 7 wt% Al**

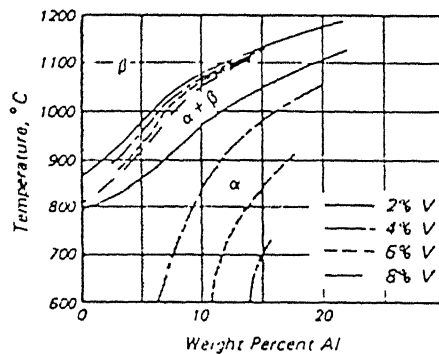


**Figure 2.6(b) Vertical section of The Ti-Al-V Vs T Equilibrium Phase Prism at 2,4,6 and 8 wt% V**

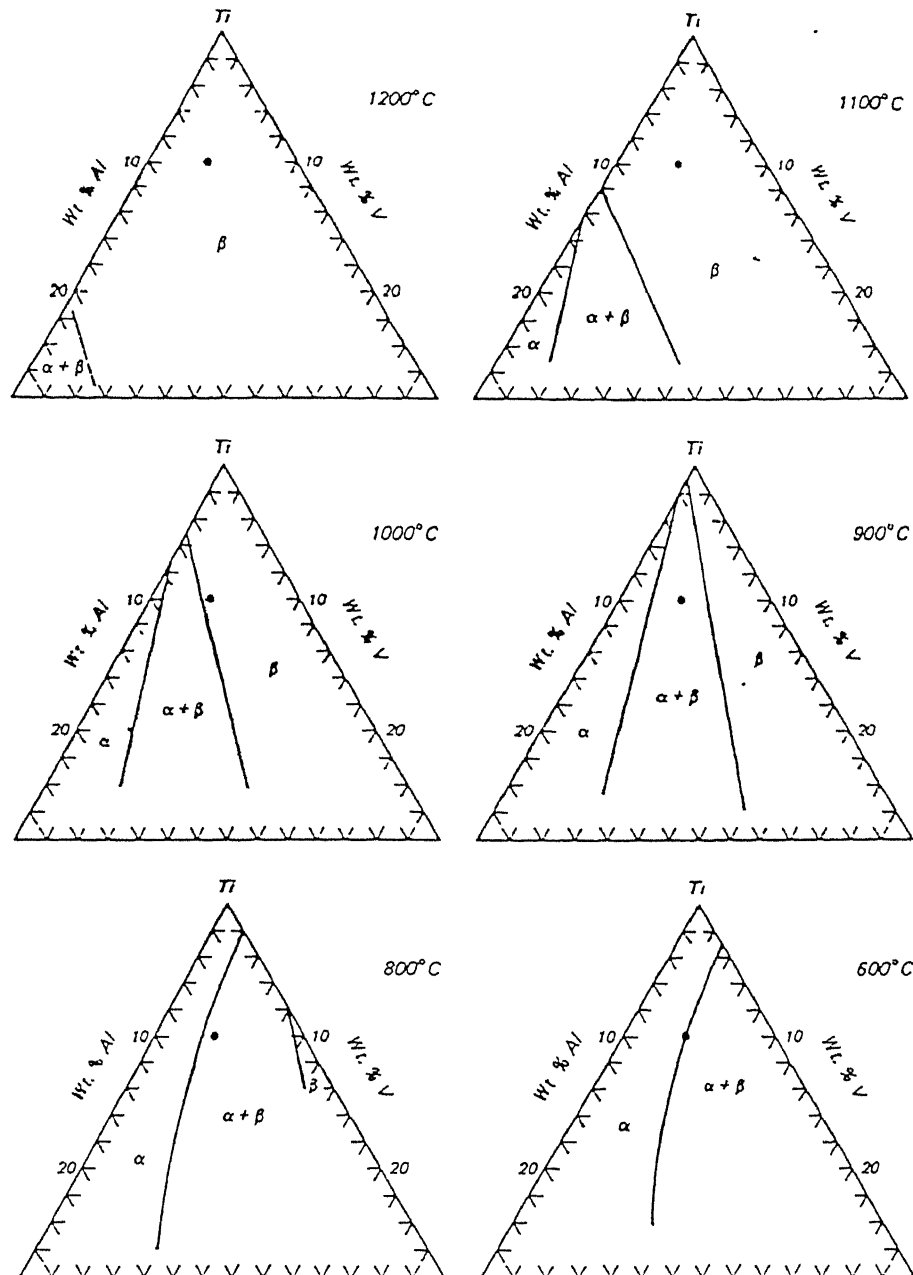


**Figure 2.7 Isothermal (Horizontal) Sections of The Ti-Al-V Vs T Equilibrium Phase Prism at The Temperatures Indicated**

The solid circle represents the alloy Ti-6Al-4V.

superplastic behaviour vary drastically with the microstructural states of the material.

#### **2.1.4 Microstructural Features of Ti-Alloys [42,43,44]**

Microstructures are characterized by nature of phases present, their shape, size, morphology, which, in turn, are functions of heat treatment and working schedule. Before going to the details of microstructure and property control, hence, it is necessary to have a look at common microstructural features in Ti-alloys.

##### **a) Primary $\alpha$ ( $\alpha_p$ ) :**

It refers to the  $\alpha$  phase in crystallographic structure which is retained from the last high temperature ( $\alpha+\beta$ ) working or heat treatment. The morphology of  $\alpha_p$  is influenced by the prior thermo-mechanical treatment and can be lamellar, equiaxed or mixed.

##### **b) Secondary $\alpha$ or transformed $\beta$ :**

A local or continuous structure, comprised of decomposition products arising by nucleation and growth during cooling through the subtransus region. Primary and regrowth  $\alpha$  may be present, it typically consists of  $\alpha$  platelets, which may or may not be separated by  $\beta$  phase.

##### **c) Blocky $\alpha$ :**

$\alpha$  phase, which is considerably larger and more polygonal than the  $\alpha_p$ . It may arise from long exposure high in the ( $\alpha+\beta$ ) field or by slow cooling through the  $\beta$  transus.

##### **d) Elongated $\alpha$ :**

A fibrous type of  $\alpha$  structure brought about by unidirectional metalworking. It may be enhanced by the prior presence of blocky and/or grain boundary  $\alpha$ .

e) Widmanstätten structure :

A structure of  $\alpha$  platelets or  $\alpha$  and  $\beta$  platelets resulting from cooling from a temperature above the  $\beta$  transus. The platelets often produce a basket-weave appearance.

f) Grain boundary  $\alpha$  :

Primary  $\alpha$  outlining prior  $\beta$  grain boundaries. It occurs by slow cooling from the  $\beta$  field into ( $\alpha+\beta$ ) field and may be continuous, unless broken up by subsequent work.

g) Acicular  $\alpha$  :

This is a product of nucleation and growth from  $\beta$  to the lower temperature allotrope  $\alpha$ . It may have a needle-like appearance.

h) Alpha case :

The oxygen, nitrogen or carbon enriched alpha stabilized surface, which results from elevated temperature exposure.

i) Hexagonal martensite ( $\alpha'$ ) :

A supersaturated, non-equilibrium hexagonal phase formed by a diffusionless transformation of the  $\beta$  phase.

j) Orthorhombic martensite ( $\alpha''$ ) :

A supersaturated, non-equilibrium orthorhombic phase formed either by transformation of metastable  $\beta$  during quenching ( $M_o$ , the maximum temperature at which  $\alpha''$  begins to form on cooling) or by stress-induced transformation of retained metastable  $\beta$ .

k) FCC and FCO martensites :

Face-centered cubic and face-centered orthogonal martensites found during TEM analysis of some binary Ti alloys, produced probably as a result of hydrogen contamination.



l)  $\alpha_2$  structure :

A structure consisting of the ordered  $\alpha$  phase,  $\text{Ti}_3\text{Al}$ .

m) Equilibrium  $\beta$  :

Some equilibrium  $\beta$  phase present at room temperature due to partitioning of  $\beta$  stabilizers, in  $(\alpha+\beta)$  and  $\beta$  alloys.

n) Beta flecks :

Regions enriched in a  $\beta$ -stabilized element due to segregation during ingot solidification, present in, generally,  $\beta$  alloys having high amount of  $\beta$ -stabilizer.

o) Metastable  $\beta$  :

$\beta$  phase composition that can be partially or fully transformed to martensites,  $\alpha$  or eutectoid decomposition products with thermal or strain energy activation during subsequent processing or service exposure.

p) Intergranular  $\beta$  :

$\beta$  phase situated between  $\alpha$  grains.

q) Omega phase ( $\omega$ ) :

A non-equilibrium, submicroscopic phase formed either isothermally during aging at about  $475^\circ\text{C}$  or athermally during quenching, often thought to be a transition phase during the formation of  $\alpha$  from  $\beta$ .

r) Gamma phase ( $\gamma$ ) :

An ordered structure of Ti-Al compound.

s) Hydride phase :

The phase  $\text{TiH}_x$  formed in titanium when the hydrogen content exceeds the solubility limit.

t) Silicides :

In high silicon bearing alloys, Si combines with Ti and other alloying elements to form complex compounds as precipitates known as silicates, eg.,  $Ti_5Si_3$ , Ti-Mo-Si etc.

u) Interface phase :

It is a reaction product that forms at the interface between  $\alpha$  and  $\beta$  phases of alloys like Ti-6Al-4V, probably due to hydrogen absorption. It has both fcc and hcp forms.

Different microstructural standards for ( $\alpha+\beta$ ) titanium alloys are given in [42]. Some very common microstructural features observed in titanium alloys are shown in Figure 2.8.

### **2.1.5 Microstructure and Property Control**

The microstructure of  $\alpha+\beta$  titanium alloys strongly depends on both processing and heat-treatments, varying which a wide range of microstructural varieties are produced and these result in the widest range of properties. It has been observed that the percentage, size and distribution of the  $\alpha$  phase as well as prior and/or the recrystallized  $\beta$  grain size plays a key role in determining fatigue, fracture toughness and tensile properties. Especially morphology of primary  $\alpha$  phase in  $\alpha+\beta$  titanium alloys is of considerable importance from the point of view of controlling their static and dynamic mechanical properties. The presence of equiaxed primary  $\alpha$  phase in microstructure promotes ductility at low temperatures, fatigue crack initiation resistance and elevated temperature flow characteristics. Similarly, improved fracture toughness, fatigue crack propagation resistance, creep and stress rupture strengths are obtained in microstructure possessing lamellar primary  $\alpha$  phase. A bimodal microstructure with the smallest amount of primary equiaxed  $\alpha$  phase - embedded into a fine lamellar  $\alpha-\beta$  structure - called 'quasi-lamellar',



**Figure 2.8** **Different Microstructural Conditions in Ti-6Al-4V Alloy**

combines the creep rupture properties and fatigue behaviour almost same as lamellar structure and also high temperature tensile strength and ductility comparable to equiaxed structure. It has been found out by Margolin et.al.[75] that in the microstructure containing equiaxed  $\alpha$  in an aged  $\beta$ -matrix, the mean free path,  $\lambda$ , between  $\alpha$  particles appears to play an important role in determining tensile RA. They observed that voids form at the equiaxed  $\alpha$ -aged  $\beta$  interfaces at low tensile strains. As the strain is increased, these voids readily grow along the interfaces before they, by necessity, grow through the matrix. They proposed that their ease of growth depends upon the spacing of the  $\alpha$ -particles, which act as obstacle to growth. As  $\lambda$  decreases, a growing void encounters more obstacles and growth is impeded. This results in greater strain to fracture and higher attainable ductility. It has also been shown that refinement of the prior  $\beta$  grain-size creates a more tortuous path for fracture, the net result being more difficult void growth and hence higher achievable tensile ductility.

Greenfield and Margolin [75] have shown the effect of prior  $\beta$ -grain size and grain-boundary  $\alpha$  thickness on fracture toughness of acicular  $\alpha$  morphologies. Fracture toughness increases in both equiaxed and acicular  $\alpha$ -structure as the prior  $\beta$  grain size decreases, presumably due to more tortuous crack propagation path encountered. High fracture toughness is also a result of shape characteristics of the acicular  $\alpha$  phase.

Work by Ho and Margolin [75] shows that fatigue crack initiation at low stress occurs more readily in structures with coarser  $\alpha$ , both in acicular and equiaxed. Again in strain controlled low cycle fatigue tests it has been found that number of cycles to pin-point crack initially was significantly lower with an acicular structure as compared to an equiaxed microstructure [75-77].

### **2.1.5.1. Effect of Heat-Treatment**

The microstructural changes that can be brought about through thermal treatments are numerous. Generally lamellar microstructures are obtained by only heat treatments without any mechanical working.

When quenched from above  $\beta$ -transus temperature it is difficult to form a fully martensitic structure in Ti-6Al-4V alloy which is leaner in  $\beta$ -stabilizers, since the kinetics of  $\alpha$ -phase nucleation and growth reaction are more rapid. Thus in thick sections of Ti-6Al-4V, it is unlikely that fully martensitic structure will be produced during quenching. As a result of nucleation and growth of  $\alpha$ -phase, it is frequently present at preferred nucleation sites such as prior  $\beta$ -phase grain boundaries.

Lamellar microstructures require only thermal treatments. The martensitic structure ( $\alpha'$ ) established by water quenching from above the  $\beta$ -transus is very unstable. Short annealing in the  $\alpha+\beta$  phase field are sufficient to precipitate the  $\beta$  phase at boundaries of martensitic needles which results in a fine lamellar  $\alpha+\beta$  microstructure. Remarkable coarsening of the lamella takes place only at high annealing temperatures in the two-phase field near the phase boundary. This coarsening process demands a relatively long time due to long diffusion paths. Coarse lamellar structures are achieved by slow cooling from above the  $\beta$ -transus into the two-phase field. In this case,  $\alpha$  phase precipitates from the  $\beta$  phase. Length of the lamella is restricted by the former  $\beta$  grain size, whereas the width is diffusion controlled and can be coarsened by decreasing the cooling rate. Duplex heat treatment mode has also been developed to synthesize a microstructure with the high toughness characteristics of acicular structure and high ductility of equiaxed morphologies. A volume fraction of 10 - 25 % globular or nearly equiaxed  $\alpha$  is developed by processing or heat treating high in the two-phase region. Subsequent thermal treatment at a lower temperature results in the formation of acicular  $\alpha$  phase termed secondary  $\alpha$ . The final step involves ageing the remaining  $\beta$  to the desired strength level [23,72,74,75].

### **2.1.5.2 Effect of Working**

Microstructural changes brought about through processing are numerous and varied, and are dependant on alloy content and working history. If

working is initiated and completed at temperatures in the  $\beta$ -field, the resulting microstructure will be entirely transformed. The transformation product will consist of acicular or plate-like  $\alpha$ , depending on section size and cooling rate. The structure will also show evidence of coarse equiaxed prior  $\beta$  grains. Structures developed in this manner are not changed significantly through the use of subsequent thermal treatments. Fine acicular structure can be coarsened somewhat by heating in the  $\alpha$  -  $\beta$  field, but the coarse prior  $\beta$  structure can be altered only by further working at a temperature below the  $\beta$  transus.

If the work is initiated in the  $\beta$  field and finished in the  $\alpha+\beta$  field, the resulting microstructure will be predominantly transformed  $\beta$ . The prior  $\beta$  grain boundaries will be distorted and partially broken up due to lower finishing temperature. Work carried out entirely in the  $\alpha+\beta$  field generally yields a fine grain structure with little or no evidence of transformation product.

When total strain is kept same and strain ratios in  $\alpha+\beta$  and  $\beta$  phase field are varied, material deformed more in  $\beta$  phase field has been observed to have microstructure with coarser  $\alpha$  lamella in comparison to those observed in samples given a higher deformation in the  $\alpha+\beta$  phase field [23,76].

### **2.1.5.3. Effect of Thermo-Mechanical Treatment**

Thermo - mechanical processing, both in single phase  $\beta$  as well as two phase  $\alpha+\beta$  field, is the most effective method of modifying and controlling the morphology of the primary  $\alpha$ -phase. While the lamellar  $\alpha$ -morphology arises during slow cooling of the alloy through the  $\alpha+\beta$  two phase field, equiaxed morphology generally results from the recrystallization/ mill annealing of the structure which is obtained by imparting sufficient deformation in the alloy below its  $\beta$ -transus temperature. Thermo-mechanical processing is strongly influenced by the factors:

- 1) The degree of prior deformation in the  $\beta$ -phase field.
- 2) Working temperature and,

---

3) The mode of deformation.

The first two influence the morphology of primary  $\alpha$  as well as the texture, and the third one primarily influence the texture which, in turn, affects the  $\alpha$ -phase morphology during recrystallization annealing.

When the material is warm-worked below the recrystallization temperature, equiaxed  $\alpha$ -grains are nucleated at the  $\alpha/\beta$  interface upon subsequent annealing. The rate at which lamellar  $\alpha$  transform to equiaxed  $\alpha$  is a function of annealing temperature, time and the amount of work  $\alpha$  phase has received.

It has been observed that keeping the deformation temperature and annealing procedure constant, the percentage of equiaxed morphology in resulting microstructure depends on the degree of deformation, i.e. with increasing degree of deformation, percentage of equiaxed morphology increases in the microstructure.

Degree of hot deformation, if exceeds a critical value, may also lead to fracturing of deforming  $\alpha$  lamella and may give rise to primary  $\alpha$  lamella of smaller aspect ratio. Subsequent break-up of  $\alpha$  lamella to equiaxed morphology occurs during subsequent recrystallization annealing when  $\beta$ -phase penetrates across the lamellar widths along the sub-boundaries [76].

In alloys which are  $\alpha$ - $\beta$  finish worked, air cooled and then solution treated at a temperature lower than the finishing temperature, a low density of smaller elongated  $\alpha$ -phase particles develop in addition to primary  $\alpha$ . This phase often occurs at  $\beta$ -phase grain boundaries. This  $\alpha$ -phase develops as a result of coarsening unsolutionized widmanstatten  $\alpha$  during the solution treatment. The resulting microstructure is actually triplex, since it consists of tempered  $\alpha'$ , small elongated  $\alpha$  and much coarser equiaxed or elongated primary  $\alpha$ .

The increasing fineness of equiaxed microstructure with the aging effect resulting from the thermo-mechanical treatment yields an improvement in

tensile properties also. This helps in improvement in superplastic behaviour of the material.

In order to combine good creep rupture behaviour with high tensile ductility at room temperature, it is favourable to produce the quasi-lamellar microstructure by thermo-mechanical treatment. Because it exhibits the same creep rupture strength as the lamellar one without suffering from extreme drop in tensile ductility related to the complete transformation into the  $\beta$ -phase when exceeding the transus during solution treatment. Also the quasi-lamellar structure possesses good fatigue strength at room temperature which is significantly superior to that of the as received condition. Even its drop at very high number of cycles is smaller than that of the lamellar or bimodal structure. Anyway the thermo-mechanical treatment has a strong potential to achieve a significant improvement in static and dynamic mechanical properties at room temperature combined with good elevated temperature strength[72,76,77,78].

#### **2.1.6 Importance of $\beta$ -Processing**

Very fine equiaxed structure for Ti-6Al-4V alloys are required to have good superplastic properties. Now, it has been observed that for a given amount of deformation, thin  $\alpha$ -lamella material is more easily converted into fine equiaxed morphology than thick lamella material. The morphology changes from  $\alpha$ -lamella to lower aspect ratio grains was identified to be a breaking of the  $\alpha$ -lamella essentially by two step process: fraction of low and high angle  $\alpha$ - $\alpha$  boundaries or shear bands across the  $\alpha$ -plates followed by penetration of  $\beta$ -phase to complete the separation. This break-up takes place during hot deformation and subsequent annealing. The separation by  $\beta$ -phase penetration is easier in thin  $\alpha$ -lamella. In thick lamella structure  $\beta$ -phase penetration is incomplete leading to aggregates of needle-like structure. When the plates are thinner and finer they break-up to form fine grains of equiaxed  $\alpha$ -phase. Now, these plates are formed from martensitic needles, when they are heated in the two phase  $\alpha$ - $\beta$  region. So, to get finer equiaxed grains, the needles also are



required to be finer. When the material is solutionized above  $\beta$ -transus and water quenched, the martensitic needles are obtained in the quenched microstructure. So, if some deformation is given in the  $\beta$ -phase field before quenching, the fineness of the martensitic needles in the quenched structure increases. Thus,  $\beta$ -processing helps in getting the finer equiaxed structure with very good superplastic behaviour. There is another advantage of  $\beta$ -processing also. When the material is only solutionized above  $\beta$ -transus and water quenched from there, coarser martensitic needles are obtained. When these are taken in  $\alpha$ - $\beta$  phase field for giving thermo-mechanical treatment, those martensitic needles transform into  $\alpha$ -plates and with increase in temperature the  $\alpha$ -plates become coarser. So, to get fine structure the hot deformation is required to be given in the lower temperature range in the  $\alpha$ - $\beta$  phase field. But in this lower temperature range it is difficult to give heavy deformation as the resistance to plastic flow is higher. And so it is difficult to get fine equiaxed microstructure. But, when the material is  $\beta$ -worked, finer martensitic needles are obtained through water-quenching, which, on heating in the  $\alpha$ - $\beta$  phase field yields finer  $\alpha$ -plates. So, this structure can be given thermo-mechanical treatment at the higher range of temperature in the  $\alpha$ - $\beta$  phase field without hampering the fineness of the equiaxed structure. And also heavy amount of deformation can be given as resistance to plastic-flow is less at higher range of temperature. So, to establish a fine equiaxed microstructure, working in  $\beta$ -phase field is quite useful[72,78].

## **2.2 TEXTURE IN ( $\alpha$ + $\beta$ ) Ti-ALLOYS**

Ti and its alloys show texture which produce pronounced anisotropy in mechanical properties due to lower crystallographic symmetry of hcp  $\alpha$  Ti. By proper control of the variables, texture, as a measure of strengthening can be utilized to fabricate components having higher strength along a particular direction. The main feature of cold-rolled texture of pure Ti is that the  $[10\bar{1}0]$  direction is parallel to the rolling direction and (0002) or basal

poles are concentrated in regions  $\pm 30^\circ$  to  $\pm 40^\circ$  in the transverse direction away from the sheet normal[3,45]. Such a texture is supposed to be produced from a competition between  $\{0001\}\langle 11\bar{2}0 \rangle$  slip and  $\{11\bar{2}2\}$  twinning[4]. Inagaki[46] proposed a three dimensional mechanism of development of cold rolling texture. Below 30 % reduction, initial textures are weakened by twinning and slip rotations, between 30 and 50 % reductions  $\{0001\}\langle 01\bar{1}0 \rangle$  texture is developed mainly through slip rotations and above 50 % reductions  $\{\bar{2}115\}\langle 01\bar{1}0 \rangle$  orientation is developed which is stable end orientation of cold-rolling texture of Ti. It is observed that annealing at low temperatures( $\sim 540^\circ\text{C}$ ) results in the sharpening of the cold-rolled texture, though true recrystallization does not take place at that temperature[3].

Textures observed in titanium, hot rolled at temperatures below  $800^\circ\text{C}$  are essentially same as the cold rolling texture,  $\{\bar{2}115\}\langle 010 \rangle$ . Hot rolling between  $800$  and  $850^\circ\text{C}$  enhances the development of  $\{\bar{2}110\}\langle 01\bar{1}0 \rangle$  and  $\{\bar{2}118\}\langle 84\bar{4}3 \rangle$ , formed by the recrystallization which occurs during and after hot rolling. Hot rolling above  $880^\circ\text{C}$  results in the formation of a strong transformation texture  $\{\bar{2}110\}\langle 01\bar{1}0 \rangle$ , derived from the  $\{100\}\langle 011 \rangle$  of the bcc  $\beta$  phase rolling texture via Burgers' orientation relationship[47].

In the Ti-alloy specimens, hot rolled at temperature above the  $\beta$  transus, transformation textures inherited from the rolling textures of  $\beta$  phase are observed, main orientations being  $(10\bar{1}0)[0001]$  and  $(21\bar{1}0)[01\bar{1}0]$ . These are much stronger in  $(\alpha+\beta)$  alloys. On hot rolling, at temperatures below the  $\beta$  transus, but above the recrystallization temperature of the  $\alpha$  phase, weak recrystallization textures alongwith transformation textures inherited from rolling textures of  $\beta$  are observed, main orientation being  $(\bar{2}110)[01\bar{1}0]$ . If rolling is done below the recrystallization temperature of  $\alpha$  phase, rolling textures of  $\alpha$  phase,  $(21\bar{1}1)[01\bar{1}0]$  as a main component, are observed, which are much stronger in  $(\alpha+\beta)$  alloys[48,49].

The strong prismatic texture,  $\{1120\}\langle 1100 \rangle$ , present in hot rolled Ti-6Al-4V systems, is associated with high anisotropy of the strength of the sheets. To obtain isotropic properties, a deformation texture of basal or near basal type must be created. Such a basal plane texture would show texture strengthening and very high bi-axial strengths. One way of achieving this is round rolling (with  $45^\circ$  rotation after every pass) and cross rolling (with  $90^\circ$  rotation after every pass). Temperature range of such rollings is 811 to 1089 K for Ti-6Al-4V [50,51,52]. For a prismatic texture to be preserved in the metals, recrystallization annealing should be done at temperatures below the polymorphic transformation point [52]. Figure 2.9 shows the main textural components observed in Ti and its alloys.

There has been considerable interest recently in the use of textured titanium alloy sheet for pressure vessel applications due to the large amount of bi-axial strengthening achieved when the through-thickness strain is minimized by the sheet texture. Ideal texture of this application is found to be (0002) parallel to sheet normal [53]. Different factors that affect texture development are :

- 1) starting microstructure [49],
- 2) temperature of deformation [48],
- 3) heat treatment [48],
- 4) cooling rate [48],
- 5) initial texture [46],
- 6) rolling direction [50],
- 7) degree of deformation [54],
- 8) thickness of the specimen [51],
- 9) annealing texture [52],
- 10) alloy composition [48].
- 11) cooling rate [48],
- 12) initial texture [46],

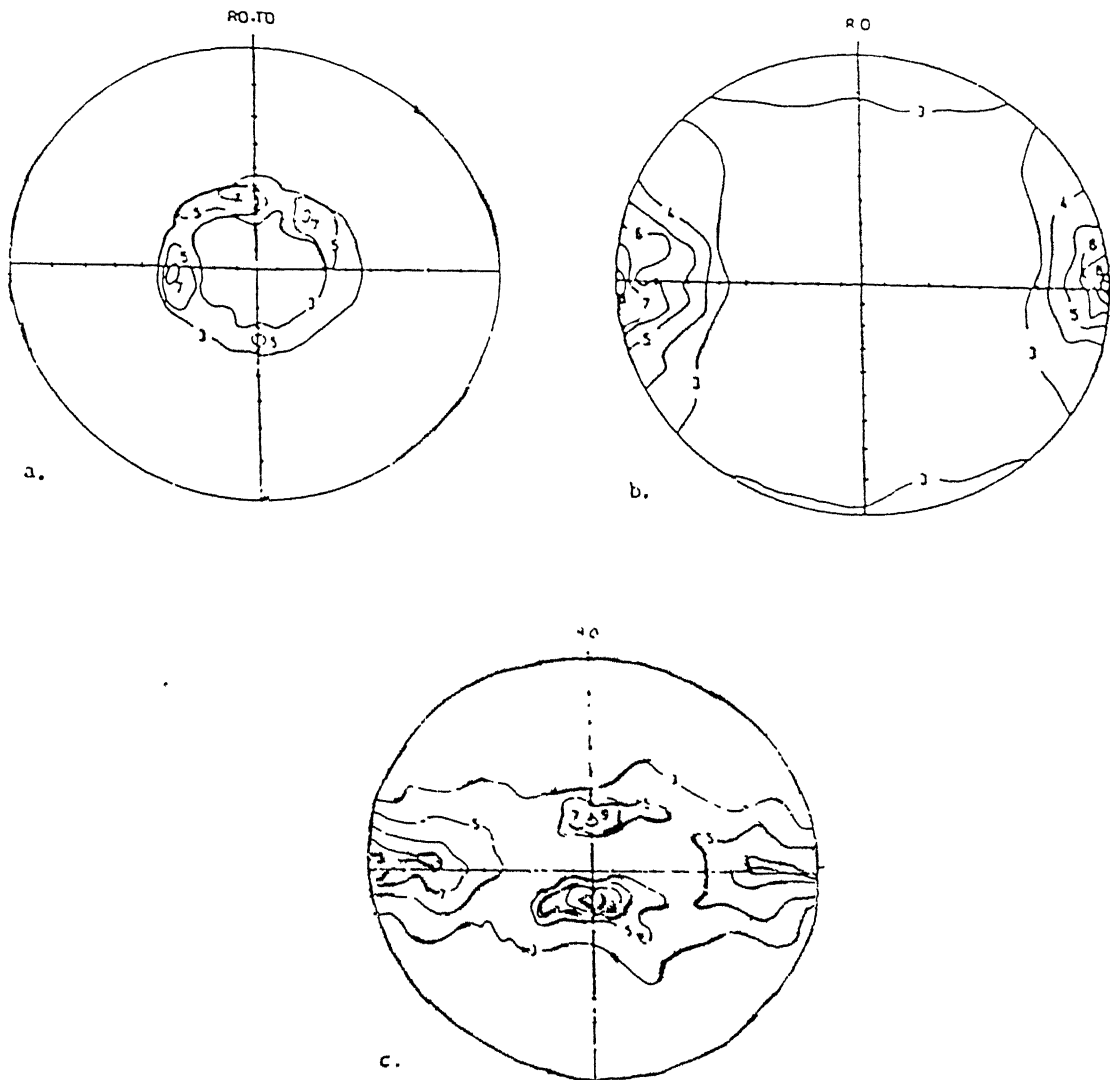


**Figure 2.9 Textures in  $(\alpha+\beta)$  Titanium Alloys**

- (a) Basal Texture**
- (b) Transverse Texture**
- (c) Mixed (Basal+Transverse) Texture**

- 13) cooling rate[48],
- 14) initial texture[46],
- 15) rolling direction[50],
- 16) degree of deformation[54],
- 17) thickness of the specimen[51],
- 18) annealing texture[52],
- 19) composition of the alloy[48].

## **2.2 DEFORMATION CHARACTERISTICS OF Ti AND ITS ALLOYS**

Pure titanium deforms at room temperature both by slip and by twinning. The greater part of the slip observed occurs on the system  $\{10\bar{1}0\}[\bar{1}1\bar{2}0]$ . Slip in the  $\{10\bar{1}1\}[\bar{1}1\bar{2}0]$  system also occurs, but it is less important and occurred in coarse grained specimens of commercial titanium, only when all three  $\{10\bar{1}0\}$  systems are operative[35]. Slip on the basal plane in the  $[\bar{1}1\bar{2}0]$  direction has been reported for the single crystals of commercially pure titanium by Churchman[36], but most of the workers failed to find basal plane slip. Churchman[36] found the CRSS for slip on the basal plane to be greater than that for  $\{10\bar{1}1\}$  slip which, in turn, is greater than that for  $\{10\bar{1}0\}$  slip. The critical shear stresses for slipping and twinning processes occurring in titanium ( $C_s$  and  $C_t$ , respectively) are related by the equation[3] :

$$C_{s\{0001\}} = 1.1 C_{s\{1011\}} = 1.02 C_{s\{1010\}} = C_{t\{1012\}} = C_{t\{1122\}}$$

Twinning occurring in titanium as a result of room temperature deformation takes place on the  $\{10\bar{1}2\}$ ,  $\{11\bar{2}1\}$ ,  $\{11\bar{2}2\}$ ,  $\{11\bar{2}3\}$  and  $\{11\bar{2}4\}$  planes, last two being observed only in single crystal titanium flakes. At liquid nitrogen temperature ( $-196^\circ\text{C}$ ), slip is confined to  $\{10\bar{1}0\}[\bar{1}1\bar{2}0]$  system and greater part of

deformation is due to twinning in the same plane as in room temperature. At higher temperature, eg., at 500°C and 815°C, slip in  $\{10\bar{1}0\}$  planes is the predominant mechanism of slip, though secondary slip of the  $\{10\bar{1}1\}$  type is also present[37,38].

Titanium is reported to have a SFE value of  $300 \text{ MJm}^{-2}$  in the basal planes of the hcp phase, suggesting that it should be characterized as a high SFE metal and hence, dynamic recovery should occur in the  $\alpha$  phase. SFE values of the bcc  $\beta$  phase has not been established. In the alloy Ti-6Al-4V, the influence of Al and V on the SFE values has not been investigated, but the two phase structure, below the transus, appears to modify the hot deformation behaviour, suggesting that differing dynamic restoration mechanisms may be operative. It was observed that the slip in the near- $\alpha$  Ti alloy having a fully martensitic structure is homogeneous in nature. The Widmanstätten  $\alpha$ - $\beta$  structure deforms by planar slip. Slip bands in Widmanstätten  $\alpha$  are not impeded by  $\beta$  films, but the  $\beta$  layers are severely distorted due to deformation[58]. At a glance, the deformation characteristics can be summarized as follows[34] :

- ◆ the hot ductility of the  $(\alpha+\beta)$  alloys is much greater in the  $\beta$  region and decreases fairly rapidly with temperature,
- ◆ the flow stress in the  $(\alpha+\beta)$  regime is very sensitive to strain rate and temperature,
- ◆ in the  $\beta$  region, the activation energy of  $169.962 \text{ kJmol}^{-1}$  is similar to that for self diffusion; in the  $(\alpha+\beta)$  region the activation energy is almost three times that in the  $\beta$  region at  $521.697 \text{ kJmol}^{-1}$ , indicating that deformation is more difficult below the transus,
- ◆ the mode of deformation is dynamic recovery in the  $\beta$  region and dynamic recrystallization in the  $(\alpha+\beta)$  region.

---

## **2.4 FORMING CHARACTERISTICS OF Ti-ALLOYS**

---

Titanium and its alloys can be formed in standard machines to tolerances similar to those obtained in the forming of stainless steel.

Commercially pure titanium and the most ductile titanium alloys (like Ti-8Al-1Mo-1V) can be formed cold to a limited extent, but it generally strain hardens the materials resulting into increase in yield and tensile strengths and a straight drop in ductility. Cold forming of other alloys generally results in excessive springback, requires stress relieving between operations and requires more power. In general, springback in forming Ti and its alloys varies directly with the ratio of bend radius to work-metal thickness and inversely with forming temperature. Springback is generally reduced by increasing the forming pressure. Higher ratios of yield strength to tensile strength generally result in greater springback. However, in order to lessen the effect of springback variation on accuracy and to gain the advantages of increased ductility the great majority of formed titanium parts are made by hot forming or by cold preforming followed by hot sizing[39].

Hot forming does not greatly affect the final properties. Forming at temperatures from 595 to 815°C allows the material to slip more readily and simultaneously stress relieves the deformed material. The commercial conventional hot forging operations should be done at rapid deformation rates (using mechanical press) in order to avoid shear bands and cracks in temperature sensitive alloys, like titanium[40]. Titanium metals also tend to creep at elevated temperature and holding under load at high temperature (creep forming) is another alternative to achieve the desired shape without extensive springback.

In all forming operations, titanium and its alloys are susceptible to the Bauschinger Effect, which is most pronounced at room temperature. Increase in the temperature reduces the Bauschinger Effect, subsequent full thermal stress relieving completely removes it[41].

---

Various methods of forming of ( $\alpha+\beta$ ) titanium alloys include[4,39,41] :

1. Isothermal forging,
2. Hot sizing,
3. Press-brake forming,
4. Deep drawing,
5. Power spinning,
6. Rubber-pad forming,
7. Stretch forming,
8. Roll forming,
9. Creep forming,
10. Vacuum forming,
11. Drop hammer forming,
12. Explosive forming,
13. Superplastic forming.

However, of the above mentioned methods, superplastic forming is replacing all other conventional methods, for it offers some unique advantages over other processes.

## **2.5 SUPERPLASTICITY AND Ti-ALLOYS**

Superplasticity is the deformation process that produces essentially large neck-free elongation (of many hundreds of percent) in metallic materials deformed in tension[57]. Superplastic materials also show high ductility during torsion, compression and indentation hardness testing. The highest elongation, on uniaxial tension, reported, are 4850 % in a Pb-Sn eutectic alloy[58] and greater than 5500 % for an aluminium bronze[59].



Superplasticity can be induced both in materials possessing a stable, ultra-fine grain size ( $< 10\mu\text{m}$ , generally) at the narrow temperature range of deformation ( $\geq 0.5 T_m$ , where  $T_m$  is the absolute melting point) and in those, subjected to special environmental conditions, eg., thermal cycling through a phase change. These two, categories are best described as “structural” and “environmental” superplasticity, respectively. There are two main types of structurally superplastic alloys : pseudo single phase and microduplex. In the former class of materials fine scale distribution of dispersoids are developed to have a small grain size upon recrystallization and to prevent grain growth during superplastic deformation, eg., precipitation strengthened Al alloys, dispersion strengthened Cu alloys etc. The microduplex materials have a fine grain microstructure consisting roughly equal proportions of two or more chemically and structurally different phases to prevent grain growth, eg.,  $\alpha$ - $\beta$  titanium alloys,  $\alpha/\tau$  stainless steels,  $\alpha$ - $\beta$  Cu alloys etc.[63,64].

Many titanium alloys have been investigated successfully for their superplastic behaviour. Maximum of these works were on Ti-6-4 alloy, while some works were on alloys like Ti-6242[62-68]. For the alloy Ti-6-4, it was found that maximum elongation is obtained in the temperature range 880-920°C at a strain rate near about  $10^{-4} \text{ sec}^{-1}$ . It was also observed that the cold formable titanium alloys are not superplastically formable. Many attempts have been made to reduce the superplastic forming temperature by addition of elements like Fe, Co, Ni to the ( $\alpha$ + $\beta$ ) alloys or to the cold formable alloys. These researches have led to the development of new alloys, like  $\beta$ -CEZ[69], which shows superplastic properties at a temperature as low as 725°C and SP-35[70], which shows good cold workability as well as good superplasticity at 700-750°C.

Researches to enhance the superplasticity of the titanium alloys have led to development of new processing routes to obtain an ultra fine ( $\alpha$ + $\beta$ ) structure. Such an attempt has produced a total elongation of 2100% at 850°C even at a high strain rate of  $10^{-2} \text{ sec}^{-1}$ [62] in Ti-6-4 alloy. In a previous work

carried out in this laboratory[5], elongation as large as 900% was found in Ti-6.8Al-3.2Mo-1.8Zr-0.3Si alloy, which is also quite good for this alloy.

## CHAPTER 3

### EXPERIMENTAL PROCEDURE

---

#### 3.1 STARTING MATERIAL

Ti-6Al-4V alloy used in this study (hence after referred to as Ti-6-4 alloy) was supplied by DMSRDE, Kanpur. The supplied material was in the form of a forged bar of square cross section of 150 mm x 150 mm and of thickness of 15 mm. Chemical composition of the supplied material has been shown in Table 3.1.

**Table 3.1      Chemical Composition of the Material**

Alloying Elements	Al	V	O	H	C	N
Composition (Wt%)	5.94	4.07	0.057	0.021	0.014	0.012

#### 3.2 DETERMINATION OF THE $\beta$ -TRANSUS TEMPERATURE

As the main aim of the present study was to observe the effect of  $\beta$ -processing on the structure and recrystallization behaviour of the material, it was very important to know the  $\beta$ -transus temperature of the supplied material. The  $\beta$ -transus temperature of titanium alloys is known to vary with their chemistry including those of interstitial elements present in the material. Thus it is generally necessary to determine the  $\beta$ -transus temperature of every heat separately. The  $\beta$ -transus temperature of Ti-6-4 alloy, with standard interstitial content, is generally found to be about 980°C [55].

The  $\beta$ -transus temperature of the given Ti-6-4 alloy was determined by the metallographic method. For this purpose, six small samples of dimension (4×4×5) mm<sup>3</sup> were taken, which were then heated at different temperatures

### Experimental Procedure

encompassing the likely boundary between ( $\alpha+\beta$ ) and  $\beta$  phase fields, i.e. between 920°C and 1020°C. The six temperatures chosen in this temperature field were 920, 940, 960, 980, 1000 and 1020°C respectively. Samples at these temperatures were soaked for 15 minutes for temperature homogenization and were directly quenched in water to arrest the phases present at these respective temperatures. Optical microscopy was done of these samples to identify the phases present therein and hence, to determine the  $\beta$ -transus temperature of the supplied material.

### **3.3 THERMO-MECHANICAL TREATMENT**

Thermo-mechanical processing in the present investigation was done by hot rolling of the alloy by imparting the known amount of thickness deformation at a given temperature either in the  $\beta$  or the ( $\alpha+\beta$ ) phase field followed by water quenching. Thus, it involved homogenizing and water quenching, followed by with or without hot rolling at different temperatures.

#### **3.3.1 Equipments for Thermo-Mechanical Processing**

Heating and soaking of the samples was done in a specially designed high temperature furnace, kept very close to the rolling mill. Muffle of the furnace consisted of an inconel tube and was closed from one end. Gas was introduced into the furnace through a 4 mm internal diameter stainless steel tube passing through the closed end of the chamber. Thus, the furnace was capable of maintaining a protective atmosphere during heating and soaking of the alloy. Further, the furnace was mounted on wheels so as to bring it very close to the rolling mill. The furnace was heated by silicon carbide rods and had a constant temperature zone of length of about 17.5 cm. To protect the Ti-6-4 alloy from oxygen absorption during its heating and soaking grade I pure Ar gas was continuously passed through the furnace.

Hot rolling of flat specimen of Ti-6-4 alloy was done on a 2-high rolling mill having rolls of 135 mm diameter. Speed of rotation for the rolling mill

was kept constant at 55 rpm in all the experiments. No prior heating of the rolls was done before hot rolling of the specimens and they were maintained at room temperature. Prior to the thermal treatment, the samples were placed on a small, perforated Inconel tray fitted with a long handle and then pushed carefully into the constant temperature zone of the furnace.

Hot rolling was essentially multi-pass in nature. To nullify the temperature drop effect a soaking treatment of two minutes was given in between each pass. Before hot rolling the samples were taken out from the furnace and were quickly fed (within 4-5 seconds) to the feeding end of the rolling mill. Thus, there was a very little temperature drop during rolling. The samples were quickly quenched into water after the last pass of the given hot rolling schedule.

In order to remove the possible  $\alpha$ -casing layer, if any, formed due to oxygen diffusion, the surface of hot rolled samples were ground and subjected to pickling in a pickling solution comprising of 10 %  $\text{HNO}_3$  + 5 % HF for nearly 3 hours at room temperature. These samples were further subjected to belt grinding and emery paper polishing before being investigated further.

### **3.3.2 Working Schedule**

Details of different thermo-mechanical treatment are schematically shown in Figure 3.1. It can be seen from this figure that the thermo-mechanical processing schedule followed in this work could be broadly divided into two stages : Stage I (consisting of the thermo-mechanical treatment in the  $\beta$ -phase region so as to obtain differently conditioned  $\beta$  grains prior to working of the alloy in the  $(\alpha+\beta)$  field) and Stage II (consisting of the thermo-mechanical treatment in the  $(\alpha+\beta)$  region so as to refine the morphology of the  $\alpha$  phase obtained after Stage I of the processing). Samples were ground to different initial thickness values so as to ensure that the thickness of the samples, after Stage I, becomes

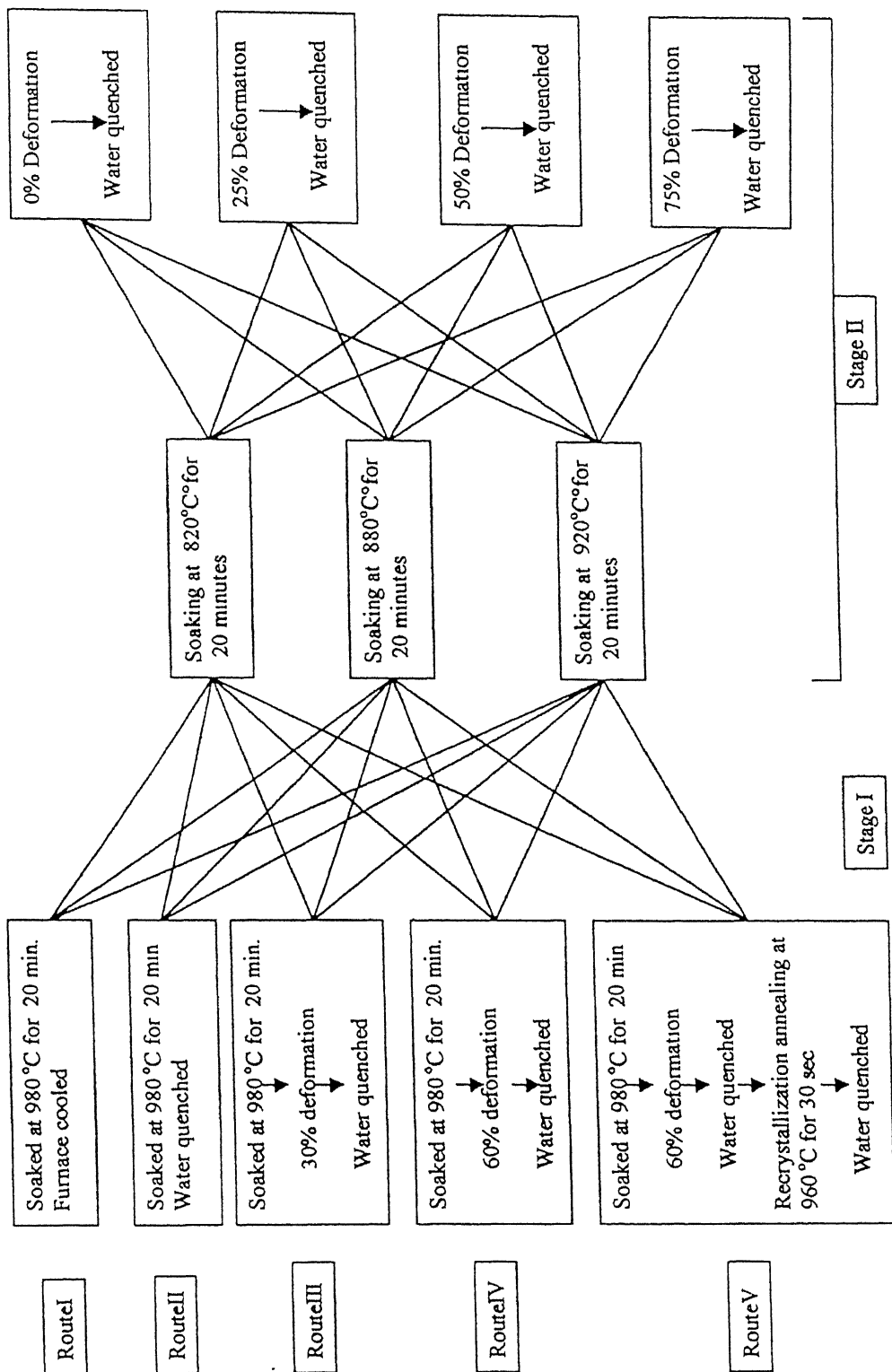


Figure 3.1: Flowsheet of the TMT Studies

6 mm. Conditioning of  $\beta$  grains through working in Stage I was obtained by five different routes. Details of Stage I of different routes adopted are given below.

**Stage I: Route I**

The specimens were heated in the  $\beta$ -phase field. To avoid the grain growth at higher temperature in the  $\beta$ -phase field, the temperature of 980°C, i.e., the temperature 30°C above the  $\beta$ -transus, was selected. The samples were soaked at that temperature for 20 minutes for homogenization of temperature and then furnace cooled to room temperature.

**Stage I: Route II**

The specimens were heated at 980°C, soaked there for 20 minutes followed by direct water quenching.

**Stage I: Route III**

The specimens were heated at 980°C, soaked there for 20 minutes, rolled at that temperature in 2 passes giving 30% deformation and were subjected to water quenching.

**Stage I: Route IV**

The specimens were heated at 980°C, soaked there for 20 minutes, rolled at that temperature in 4 passes giving 60% deformation and were subjected to water quenching.

**Stage I: Route V**

The specimens were heated at 980°C, soaked there for 20 minutes, rolled at that temperature in 4 passes to give 60% deformation and were subjected to water quenching. The samples were then further recrystallized in the  $\beta$ -phase field at 960°C, i.e. just 10°C above the  $\beta$ -transus, soaked there for 30 seconds and were subjected to water quenching.

Small samples for microstructural studies were cut out from each of the specimens.

**Stage II**

---

All the specimens produced through route I to route V were subjected to different degree of deformation at different temperatures in the stage II. At three different soaking temperatures, namely 820°C, 880°C and 920°C the samples were soaked for 20 minutes. At each temperature, the samples were subjected to 25%, 50% and 75% thickness reductions by unidirectional rolling followed by water quenching. The samples quenched in water directly after soaking at the specific temperature were treated as those, which were subjected to 0% thickness reduction. The rolling was done in multi-pass manner and 25%, 50% and 75% thickness reductions were given in 2, 3 and 5 passes respectively.

Samples for microstructural analysis were cut from each of these samples.

**3.4 MICROSTRUCTURAL CHARACTERIZATION**

Microstructures taken from all the specimens were examined by optical and scanning electron microscopes. Prior to the observations, all the samples were mechanically polished on emery papers (0 to 4 grades) followed by wheel polishing with alumina powders of sizes 1  $\mu\text{m.}$ , 0.3  $\mu\text{m.}$  and 0.05  $\mu\text{m.}$ , respectively. The samples were then etched with Kroll's reagent, which comprises of 4% HF + 2% HNO<sub>3</sub> in water. Microstructural observations were, generally, done on transverse cross sections of the specimens, unless otherwise mentioned.

Optical microscopy was done under a Leitz Wetzlar optical microscope.

Scanning electron microscopy was done under a JEOL-JSM 840A Scanning electron microscope. The samples were observed under the scanning electron microscope, operated at 10 kV using secondary electron radiation (SE mode).



### 3.5 QUANTITATIVE METALLOGRAPHIC MEASUREMENTS

The present study involves extensive metallographic measurements. In general, all measurements were done on the  $\alpha$  phase unless otherwise mentioned. As the structure consisted of at least two phases in all the cases, line intercept method was not applicable here for measuring the size and size distributions. Hence, in the present study, measurements were done on individual lamella/grain. In each lamella/grain length as well as thickness measurements were made. In each structure at least 50 such lamella/grain were chosen to have a statistically reliable data. Measurements were done directly under an optical microscope fitted with an eyepiece having a line of specific length drawn on it, at a magnification of 1000X. The length of the line, at a magnification of 200X, was supplied as 720  $\mu\text{m}$  and the line was divided into 100 divisions. Measurements were done randomly throughout the structure to make it statistically more meaningful.

Grain size, wherever mentioned, is taken as the diameter of the circle having same area with the measured structural feature i.e. measured by the projected area diameter method [83]. According to this method, if the length and thickness of the grain were 'l' and 't' respectively, then grain size(d) was calculated as

$$d = 2 \times \sqrt{(l \cdot t / \pi)}$$

### RESULTS AND DISCUSSION

---

The alloy Ti-6Al-4V is an important member of the family of two phase ( $\alpha+\beta$ ) titanium alloys with both the bcc ( $\beta$ ) and hcp ( $\alpha$ ) phases being stabilized at room temperature. Control of  $\alpha$  morphology is essential in this alloy as far as superplastic forming is concerned. An equiaxed primary  $\alpha$  morphology with grain size less than  $10\mu\text{m}$  is generally necessary for such applications. Lamellar or Widmanstätten primary  $\alpha$  transforms to equiaxed primary  $\alpha$  morphology on hot working of the material in ( $\alpha+\beta$ ) phase field. During hot working the lamellar  $\alpha$  breaks down into small parts and finally results into near equiaxed or equiaxed  $\alpha$  structure either during the hot working itself or during post deformation recrystallization annealing.

The conventional thermo-mechanical processing of ( $\alpha+\beta$ ) titanium alloys, therefore, involves forging/rolling/extrusion through the  $\beta$ -transus of the alloy with a minimum specified reduction in the two-phase field. Generally, the conventional processing is carried out by

- (a) giving more than 30-40% reduction at a temperature atleast 50 -  $60^\circ\text{C}$  below the  $\beta$ -transus temperature of the alloy followed by
- (b) post-deformation mill annealing at a temperature lower than the hot working temperature.

Such a processing schedule does transform the lamellar  $\alpha$  structure to the equiaxed  $\alpha$  morphology with grain sizes varying between  $10\text{-}50\mu\text{m}$ , generally.

The  $\alpha$  grain size in the equiaxed structure, however, depends on the thickness of the  $\alpha$  lamellas, which in turn, depends on the morphology and size of the prior  $\beta$  grains from which it transforms. The present investigation was undertaken to study the effect of thermomechanical processing parameters on

- (i) the conditioning of  $\beta$  grains and
- (ii) conditioning of lamellar  $\alpha$  prior to working in the  $(\alpha+\beta)$  phase field and
- (iii) the recrystallization behaviour of Ti-6-4 alloy.

#### **4.1 STRUCTURE OF THE AS RECEIVED ALLOY**

The as received structure of the alloy is given in Figure 4.1. The microstructure consists of equiaxed  $\alpha$  grains in  $\beta$  matrix. The X-ray diffraction pattern of the as received material is given in Figure 4.2. The diffraction pattern clearly shows the presence of  $\alpha$  and  $\beta$  phases only in the microstructure. The  $\alpha$  grain size of the material vary between 11.5-31.7 $\mu\text{m}$  and most of them are equiaxed or near-equiaxed in nature.

#### **4.2 $\beta$ -TRANSUS OF THE ALLOY**

The  $\beta$ -transus of the given alloy was determined by metallographic technique. Microstructures of the samples quenched from different temperatures were observed to identify the phases at that temperature. Sample quenched from 960°C showed full  $\beta$  whereas that from 940°C showed presence of  $\alpha$  grains almost 6% in volume fraction [Fig 4.3]. So, the  $\beta$ -transus of the given alloy was taken to be 950 $\pm$ 5°C. This is somewhat lower than the theoretical  $\beta$ -transus temperature of this alloy [55]. This lower value of  $\beta$ -transus temperature was explained by the lower value of oxygen.

#### **4.3 EFFECT OF TEMPERATURE ON $\beta$ GRAIN SIZE**

Soaking of Ti-6-4 alloy in the  $\beta$  phase field produces recrystallized equiaxed  $\beta$  grains. Soaking temperature affects the  $\beta$  grain size. It was observed that as the soaking temperature was increased from 960°C to

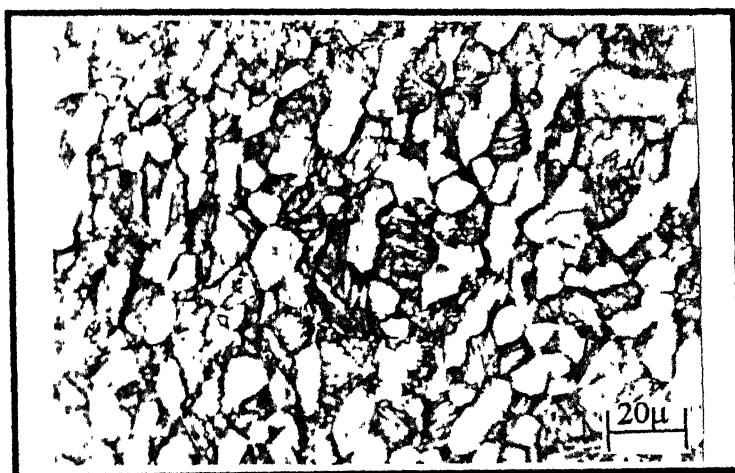


**Figure 4.1**     **Microstructure of The As Received Material**

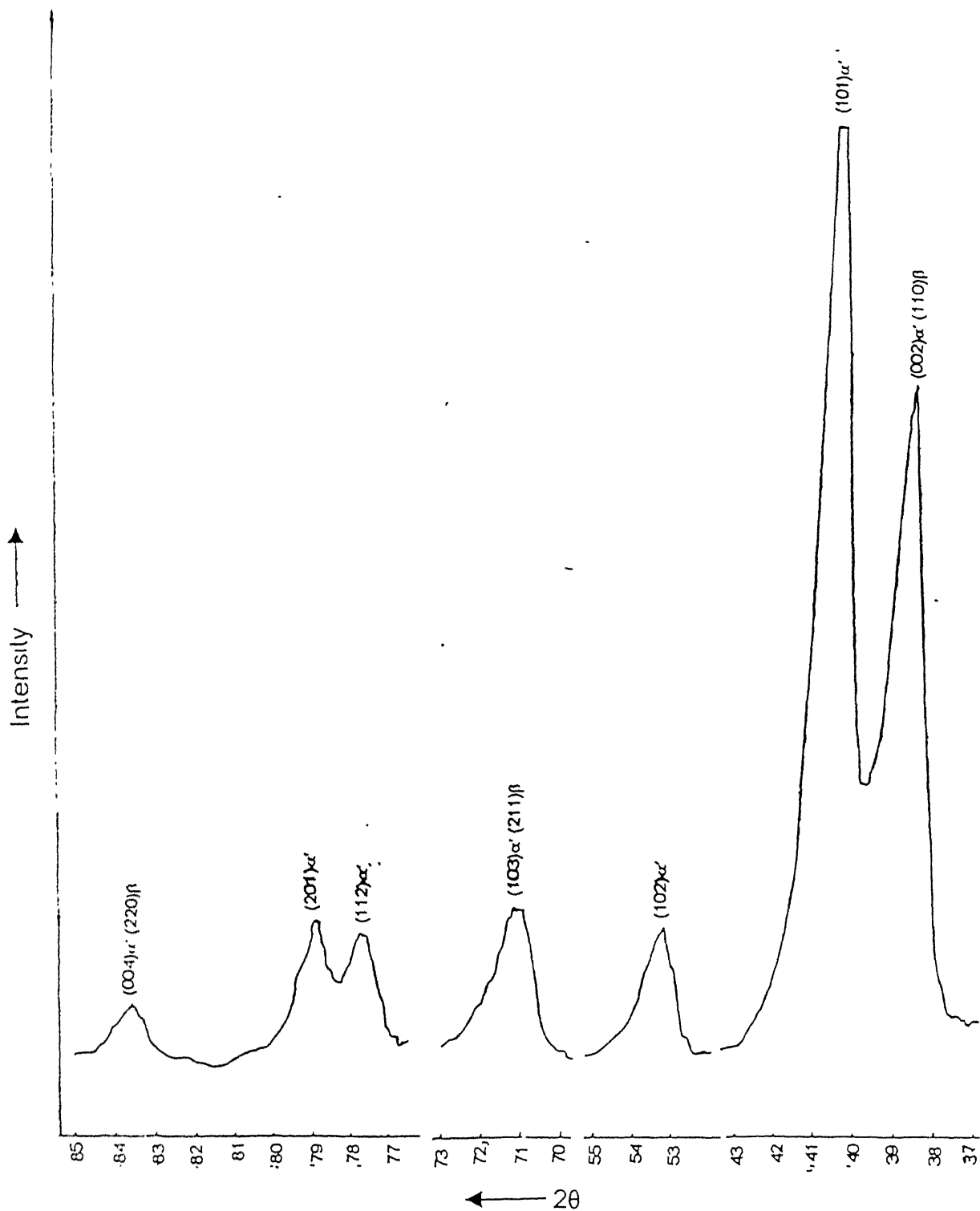
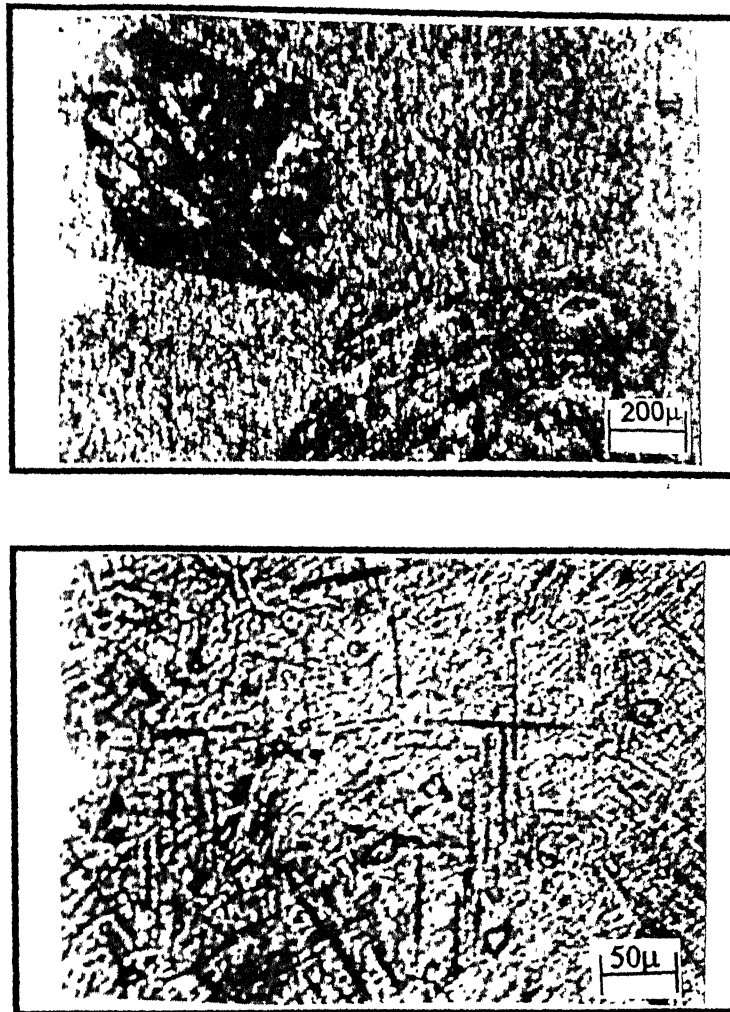


Figure 4.2 XRD Pattern of the As Received Material



**Figure 4.3**     **Microstructure of Samples Water Quenched from**

- (a)     950°C ( consisting of martensite with no trace of  $\alpha$  )
- (b)     940°C ( consisting of small island of  $\alpha$  in martensitic structure )

1020°C with two more intermediate temperature, the average grain size increases from 682 $\mu\text{m}$  to 860 $\mu\text{m}$ [Fig 4.4]. It was thus seen that  $\beta$  grains in Ti-6-4 alloy undergoes rapid grain growth when heated in the single phase  $\beta$  region. This type of behaviour was also observed for other ( $\alpha+\beta$ ) titanium alloys. The martensitic needles become thicker as the soaking temperature increases from 960°C to 1020°C.

#### **4.4 EFFECT OF THERMOMECHANICAL PROCESSING VARIABLES ON CONDITIONING OF $\beta$ GRAINS**

Detailed thermomechanical processing schedule is given in chapter 3. In short, the processing of Ti-6-4 alloy consisted of the following paths:

- (a) preserving equilibrium structure by recrystallization annealing of the material at 980°C followed by furnace cooling;
- (b) obtaining typical martensitic structure by annealing at 980°C followed by water quenching;
- (c) producing pancaked structure of different size and aspect ratio by rolling the alloy with varying deformation at 980°C;
- (d) producing fine recrystallized  $\beta$  grains by subjecting the pancaked structure to recrystallization annealing treatment at 960°C for 30 seconds.

##### **4.4.1 Effect of Cooling Rate on the Structure**

In order to compare the effect of cooling rate from above  $\beta$ -transus, on the structure of the alloy, samples are furnace cooled and water quenched from 980°C after 20 minutes soaking at that temperature. Figure 4.6 shows the microstructures of these samples. Furnace cooling from above  $\beta$ -transus produces the equilibrium  $\alpha+\beta$  structure which is Widmanstätten in nature[Figure 4.5(a)]. The microstructure shows the typical basket-weave



**Figure 4.4** Grain Growth in  $\beta$  Grains as a Function of  $\beta$  Annealing Temperature  
(microstructures were observed in water quenched conditions)

- (a) 980°C
- (b) 1000°C
- (c) 1020°C



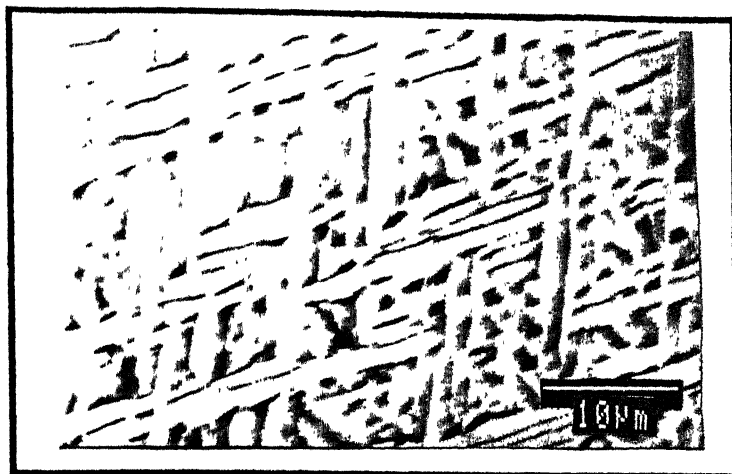


**Figure 4.5(a)**      Equilibrium ( $\alpha+\beta$ ) Widmanstätten Structure as Obtained from Samples Processed Through Route I after Stage I

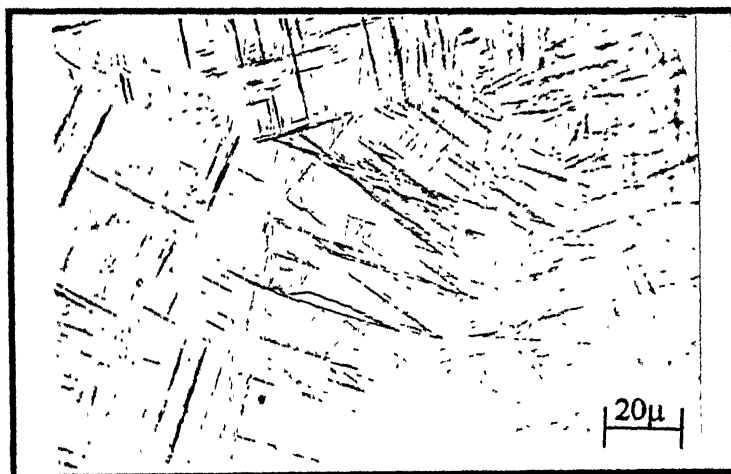


**Figure 4. 5(b)**      Martensitic Microstructure as Obtained from Samples of Ti-6-4 Alloy Processed Through Route II after Stage I

pattern of the Widmanstätten  $\alpha+\beta$  phase. The water quenched structure converts to a full martensitic one [Figure 4.5(b)].

### 4.4.2 Effect of Thickness Reduction on $\beta$ Grain Characteristics

High temperature stress strain curves for its deformation in the  $\beta$  phase field clearly indicate that the  $\beta$  phase during its deformation does not undergo dynamic recrystallization [6]. To study the effect of deformation on the  $\beta$  grain characteristics, samples are soaked at 980°C for 20 minutes followed by 30% and 60% thickness reduction, respectively. The samples are water quenched immediately after rolling. Pancaked grains of  $\beta$  phase are readily seen in both the cases which clearly indicate that like other ( $\alpha+\beta$ ) titanium alloys, Ti-6-4 alloy also does not undergo dynamic recrystallization during its high temperature deformation at a strain rate of  $10^{-1} \text{ sec}^{-1}$  which is typical of rolling conditions prevailing under the present study. The fact that the pancaked grains of  $\beta$  were observed in the material even after 60% thickness reduction supports the above conclusion. With increasing amount of deformation the  $\beta$  grains become increasingly pancaked.

Since the  $\beta$  phase is not stable at room temperature even after water quenching, the development of cell boundaries and substructure can not be directly seen by the examination of the microstructure of the alloy being deformed. The morphology of the transformation product from the  $\beta$  phase i.e.  $\alpha'$ , on the other hand, is expected to be influenced by the substructure of deformed  $\beta$  grains. Though the morphology of  $\alpha'$  was not studied by the transmission electron microscopy, characteristics of those martensitic platelets were studied under high magnification optical microscope. It was seen that the aspect ratio of martensitic platelets continuously decreased with increasing thickness reduction. Since the development of sub-grains in non-recrystallizing structure occurs with increasing strain and the size of the sub-grains decreases with increasing strain, the aspect ratio of martensitic plates seem to be correlated with the development

of sub-grains in the pancaked  $\beta$  grains. Such observations have also been made in case of steels.

### **4.4.3 Effect of Recrystallization Annealing on the Microstructure**

It has already been stated that the objective of changing the condition of  $\beta$  grains, as followed in the present study, was to recrystallize pancaked  $\beta$  grains. The effect of recrystallization annealing on the  $\beta$  grain structure is studied by subjecting one 60% deformed sample to static recrystallization by soaking at 960°C for only 30 seconds. Annealed specimen was then water quenched to retain  $\beta$  grain boundaries for their subsequent microstructural examination. The microstructure is presented in the Figure 4.6. The heavily deformed structure is transformed to a fine equiaxed  $\beta$  structure. The kinetics of recrystallization of pancaked  $\beta$  grains is very fast at as a low temperature as 10°C above the  $\beta$ -transus temperature.

### **4.4.4 Comparison of Different Structures Produced by $\beta$ Processing**

The previous subsections have dealt with the microstructural evolution of  $\beta$  grains during the five  $\beta$  processing routes followed in the present investigation. Considerable refinement of  $\beta$  grains was achieved by the processing route V. The martensitic structure obtained is important in the comparison of the 5 processing route followed. Refinement of martensitic plates occur in the as rolled specimens obtained by route III and 4 by the process as discussed in section 4.4.2. The martensitic plate thickened in the recrystallized grains after annealing the specimens, obtained by route IV. This is also shown in figure 4.7. The refinement of martensitic platelets in the as  $\beta$  rolled and water quenched structure is due to the formation of  $\beta$  sub-grains during the heavy deformation above the  $\beta$ -transus temperature. These fine sub-grains provide a number of nucleation sites during water quenching and so the occurrence of fine martensitic plates.



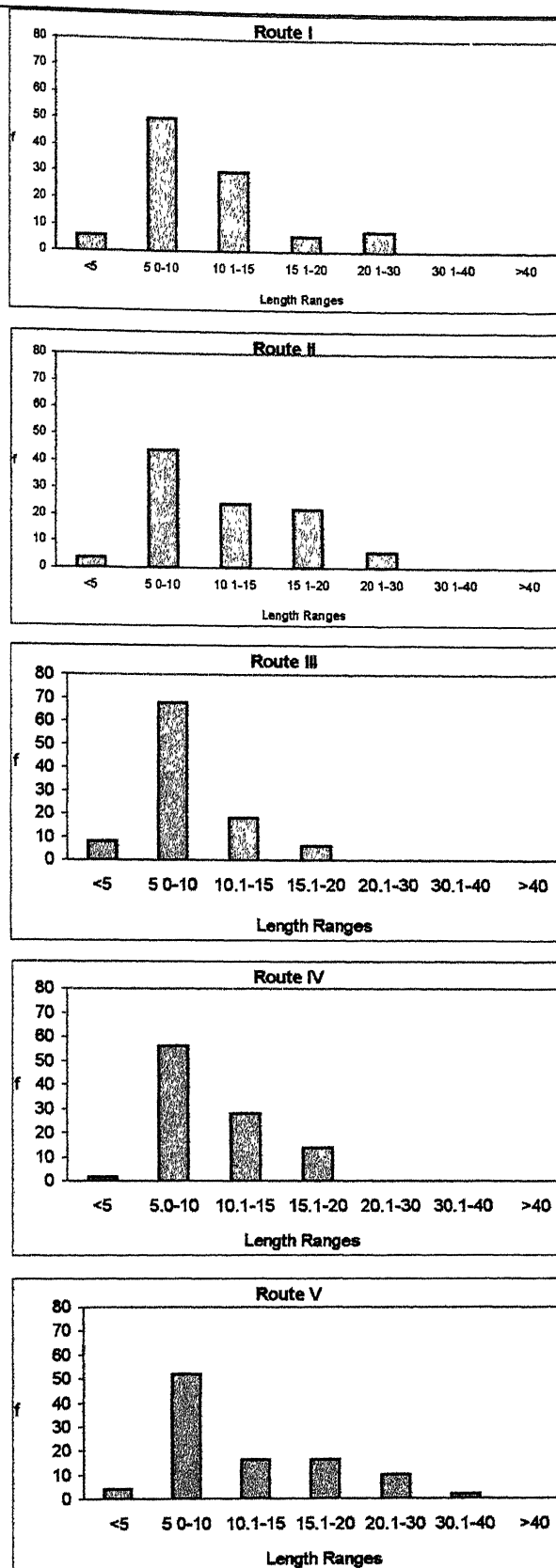
**Figure 4.6**     Microstructure of the Sample 60% Deformed at 980°C Followed by Recrystallization Annealing at 960°C for 30 seconds (in water quenched condition)



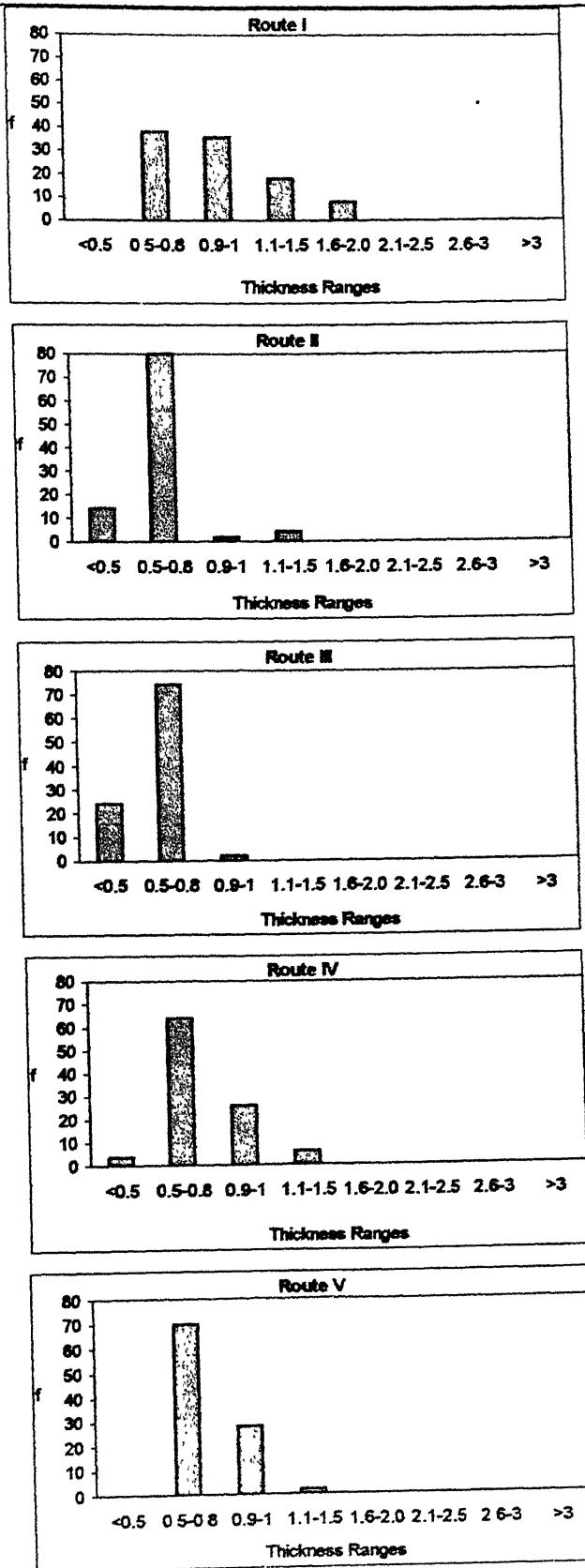
**Figure 4.7(a)**      Details of Typical Martensitic Microstructure Obtained After Stage I, Processed Through Route IV ( SEM Micrograph)



**Figure 4.7(b)**      Details of Typical Martensitic Microstructure Obtained After Stage I, Processed Through Route V ( SEM Micrograph)



Figurew 4.8(a) Length Distribution of Martensitic Needles after  $\beta$  Processing for Different Routes



Figurew 4.8(b)Thickness Distribution of Martensitic Needles after  $\beta$  Processing for Different Routes

#### **4.5 EFFECT OF THERMOMECHANICAL PROCESSING IN ( $\alpha$ + $\beta$ ) PHASE FIELD ON MICROSTRUCTURAL REFINEMENT OF THE ALLOY**

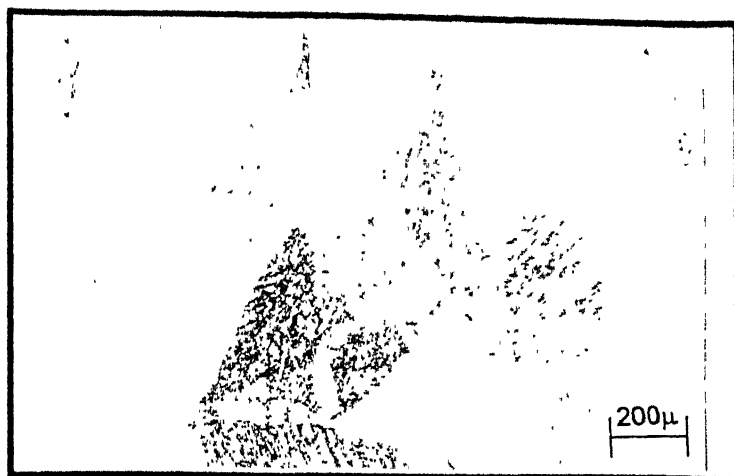
Effect of thermomechanical processing in altering characteristics of  $\beta$  grains has already been described and discussed in the previous section. Conventional thermomechanical processing route for ( $\alpha$ + $\beta$ ) titanium alloys involving deformation in the two phase field transforms  $\beta$  to  $\alpha$  by air cooling which produces thick primary  $\alpha$  plates. On the other hand, acicular morphology of  $\alpha$ , obtained by the transformation of  $\alpha'$  to  $\alpha$  during preheating to hot rolling temperature, is known to be of considerably lower thickness and a higher aspect ratio[56]. However specific morphological features of  $\alpha$  are primarily dependent on conditioning of  $\beta$  grains. Thus, the differently conditioned  $\beta$  grained structures, obtained by processing through route I to V in stage I, were hot rolled in the ( $\alpha$ + $\beta$ ) phase field for different thickness reductions and at different temperatures. All the samples were heated at three different temperatures, namely, 820°C, 880°C and 920°C and at each temperature the samples were hot rolled to different thickness reductions of 0%, 25%, 50% and 75%. The effect of different temperatures and deformations in the ( $\alpha$ + $\beta$ ) phase field on the refinement of the structure is described and discussed in the present section.

##### **4.5.1 Effect of Thermo-mechanical Processing Variables on the Microstructures of the Samples Treated Through Route I**

###### **4.5.1.1 Effect of Temperature**

To observe the effect of temperature on the equilibrium structure obtained from route I in the  $\beta$  phase field, the samples were heated at three different temperatures of 820°C, 880°C and 920°C, soaked there for 15 minutes followed by water quenching. This treatment arrests the structures present at those temperatures by martensitic transformation. The microstructures of the samples are shown in Figure 4.9(a) to (c). The length and thickness ranges of





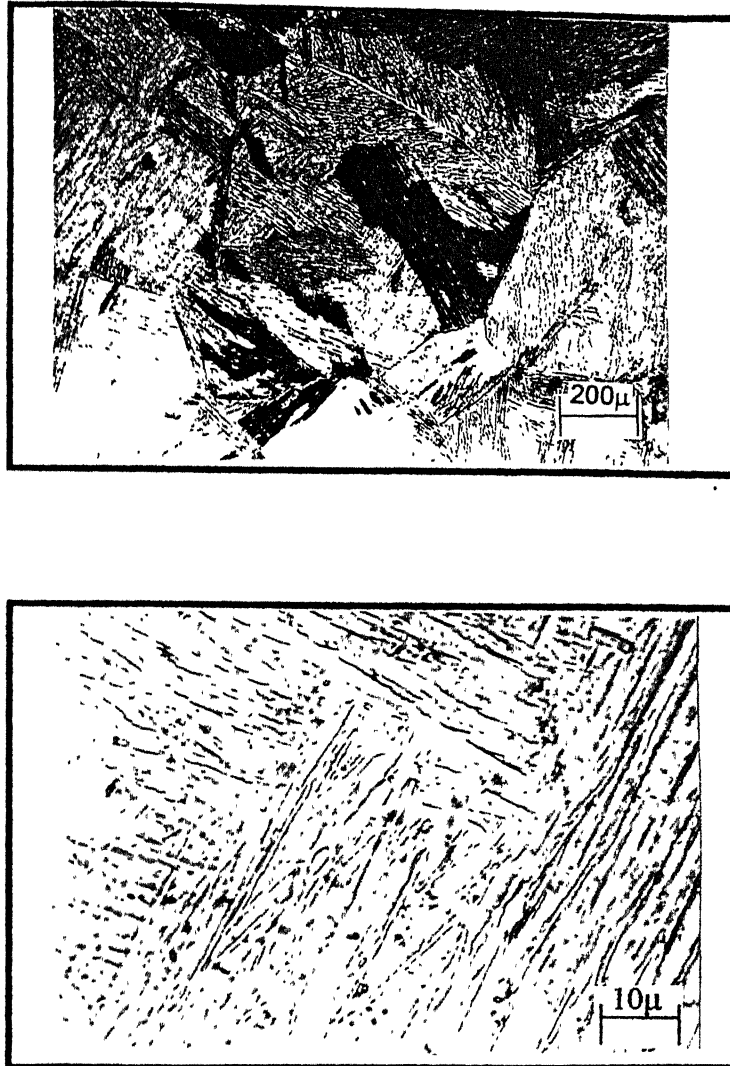


**Figure 4.9** Microstructure of the Samples Processed Through Route I, in Stage I, Followed by Heating at (in water quenched condition)

- (a) 820°C
- (b) 820°C
- (c) 880°C
- (d) 920°C
- (e) 920°C

the  $\alpha$  lamellae treated at these three temperatures are shown in Figure 4.10(a), 4.11(a) and 4.12(a), respectively. It is observed from these figures that with increasing temperature the volume fraction of lamellae having length less than 5  $\mu\text{m}$  is increasing from nil to above 5%. And the volume fraction of lamellae with lengths ranging between 5-20 $\mu\text{m}$  increases drastically with temperature and becomes almost double the amount in 920°C than that was in 820°C. In addition, the volume fraction of  $\alpha$  lamellae with length ranges >20 $\mu\text{m}$  decreases with increasing temperature. This gives an indication that the increasing amount of  $\beta$  present in the samples with increasing temperature, eats away the  $\alpha$  mostly from their length direction. In case of thickness, it decreases first with increasing temperature. But at 920°C again the thickness increases a little bit.

### 4.5.1.2 Effect of Deformation

The length and thickness distribution of  $\alpha$  lamellae after deforming at the above mentioned three temperatures in the ( $\alpha+\beta$ ) field, water quenched, are shown in Figures 4.10, 4.11 and 4.12 (b) to (d). As the samples were given different thickness reductions of 25%, 50% and 75% at 820°C, the population of  $\alpha$  lamellae in the smaller length ranges increases with increasing deformation. The thickness of the  $\alpha$  lamellae also decreases with higher amount of thickness reduction. After 75% deformation major fraction of the lamellae lies in the range of 0.5 - 0.8  $\mu\text{m}$ . Breakage and elongation of  $\alpha$  lamellae with increasing amount of deformation, makes them shorter and thinner, respectively. The elongation of the  $\alpha$  lamellae is clear after 50% deformation, which leads to some increase in the length of  $\alpha$  lamellae. On the other hand, at 880°C length of the  $\alpha$  lamellae decreases first with 25% deformation, but after that with increasing deformation length increases indicating that, at that temperature high deformation results to the elongation of the  $\alpha$  lamellae in preference to the breakage of them. The same trend is almost followed at the temperature of 920°C. The thickness of the  $\alpha$  lamellae, however, first decreases and then increases with increasing deformation at both the temperatures. Microstructures are shown in Figure 4.13.

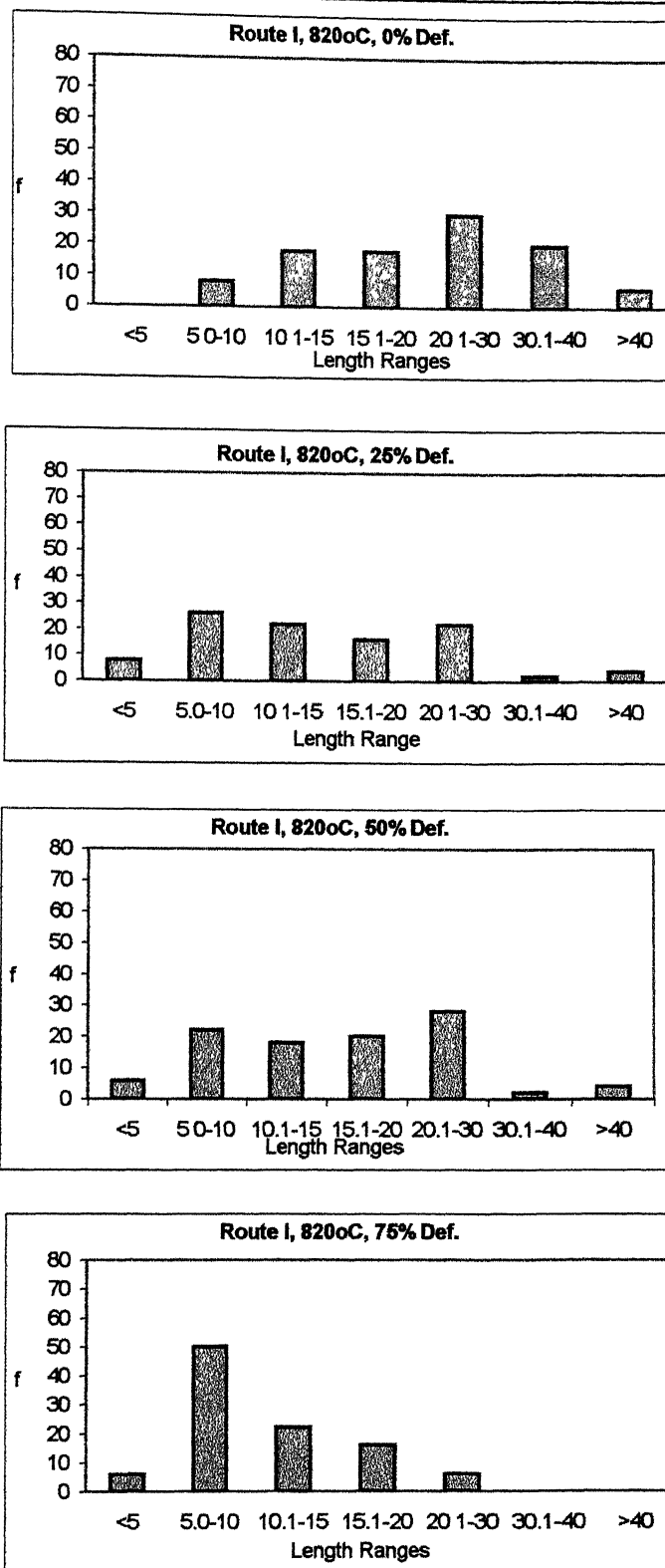


Figure 4.10/1

Length Distribution of  $\alpha$  Lamellae after Stage II

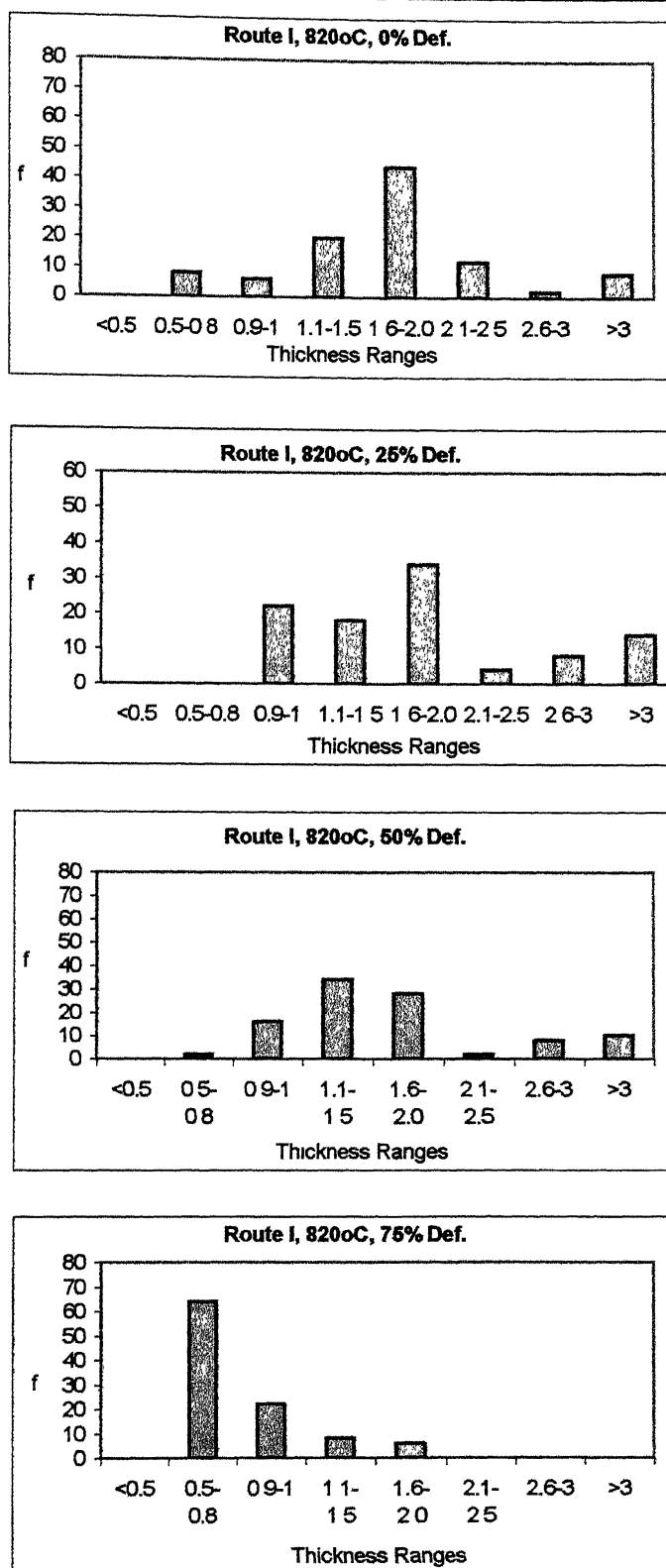


Figure 4.10/2

**Thickness Distribution of  $\alpha$  Lamellae after Stage II**

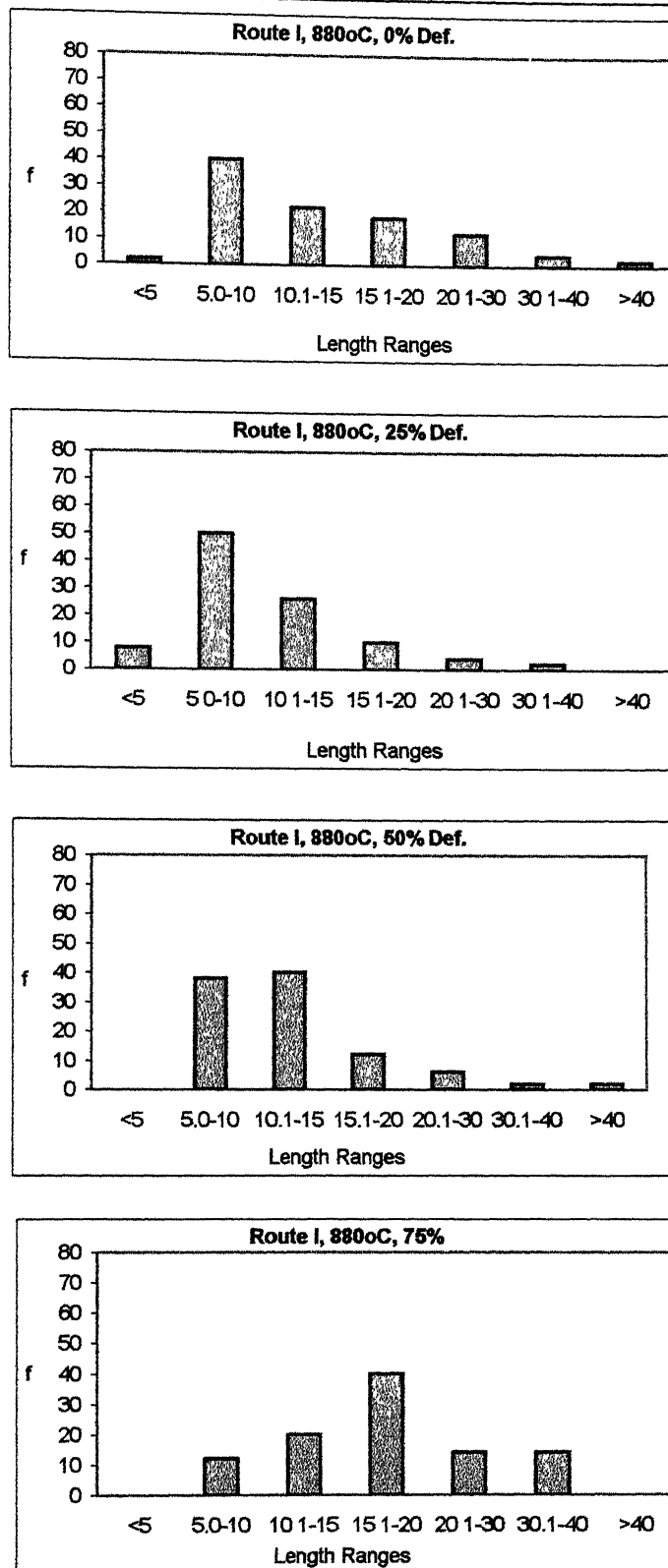


Figure 4.11/1

Length Distribution of  $\alpha$  Lamellae after Stage II

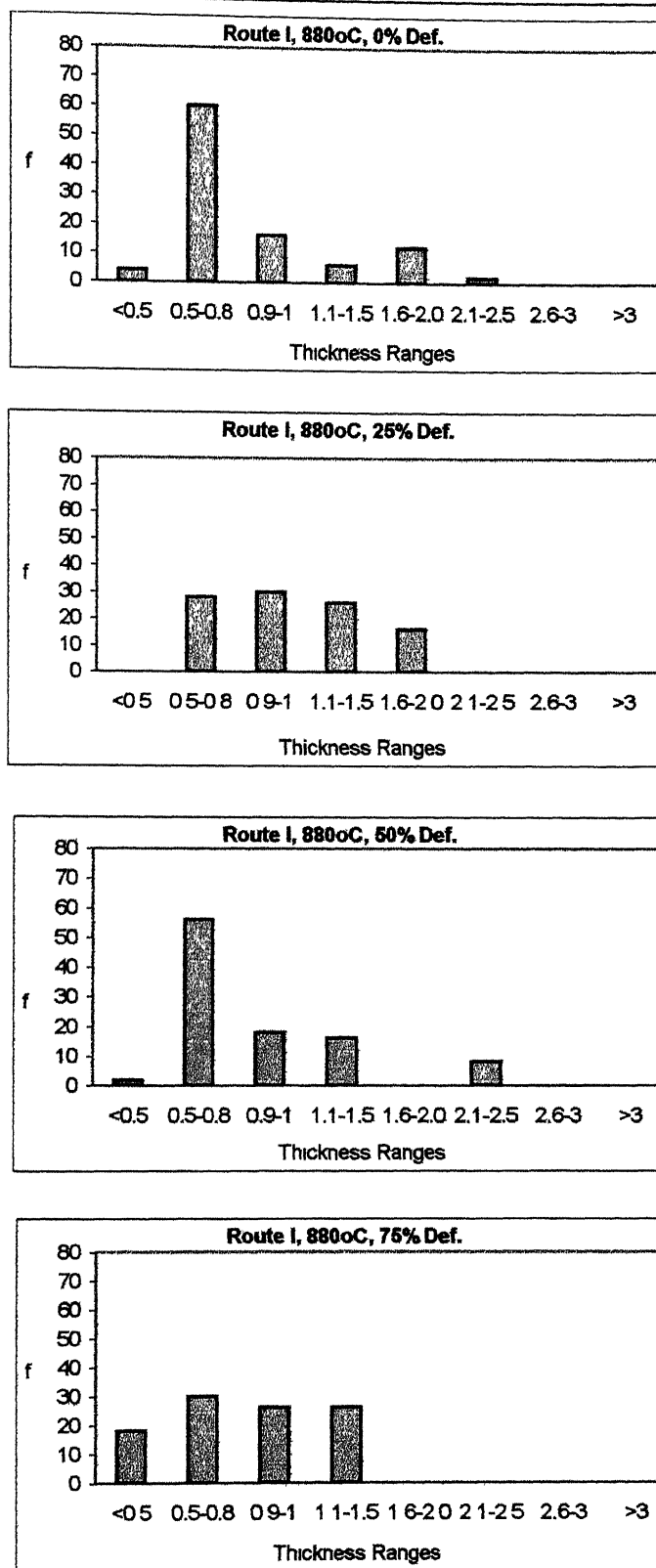


Figure 4.11/2

Thickness Distribution of  $\alpha$  Lamellae after Stage II

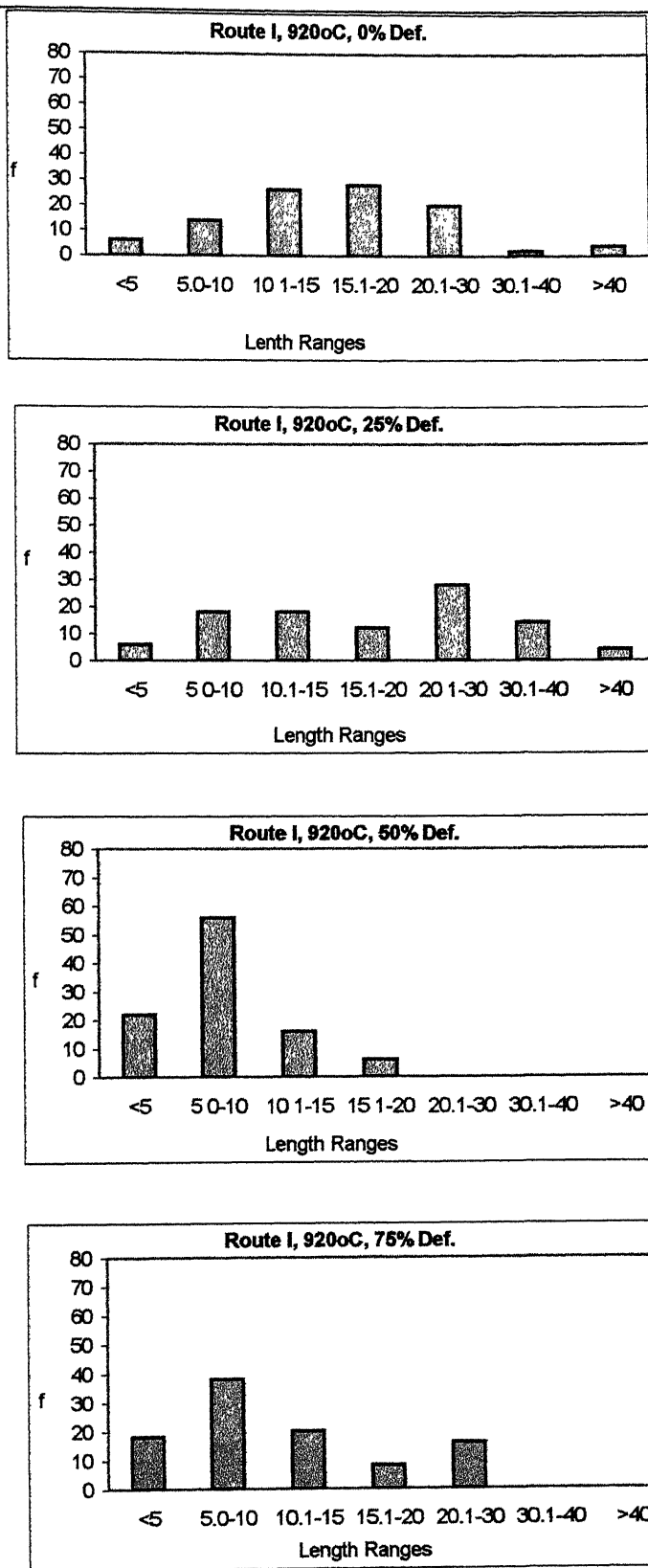


Figure 4.12/1

**Length Distribution of  $\alpha$  Lamellae after Stage II**



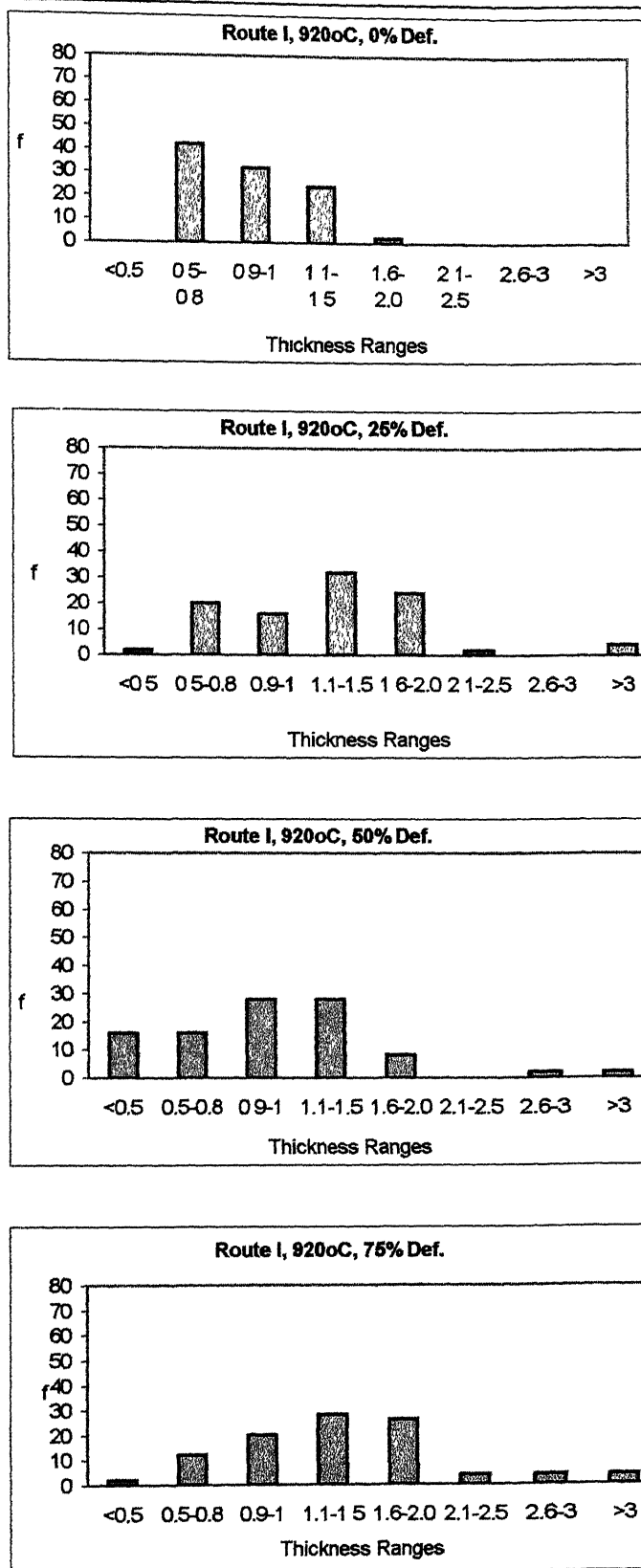
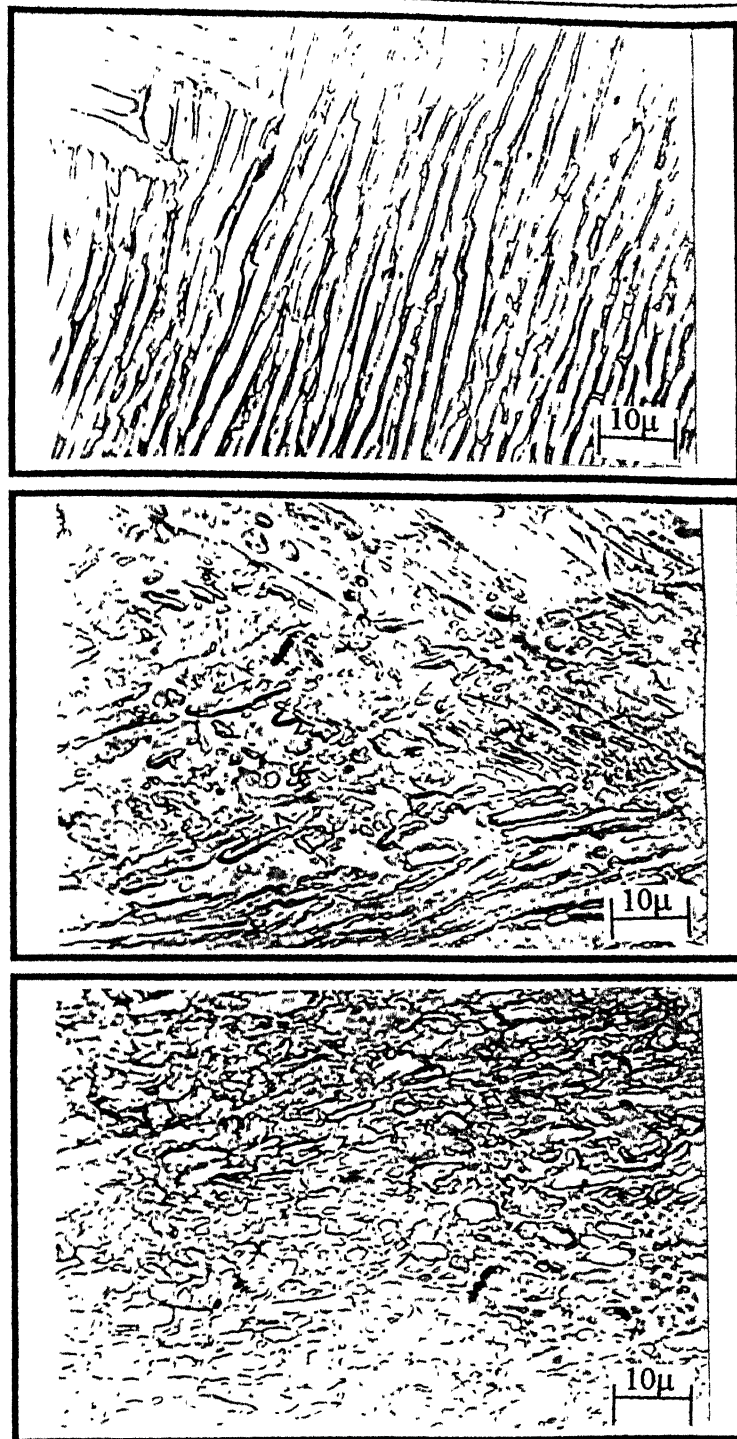


Figure 4.12/2

**Thickness Distribution of  $\alpha$  Lamellae after Stage II**



**Figure 4.13** Microstructure of Samples Processed Through Route I, in Stage I, Followed by Heating at 920°C and Thickness Reduction of (in water quenched conditions)

- (a) 25%
- (b) 50%
- (c) 75%

### **4.5.2 Effect of Thermo-mechanical Processing Variables on The Samples Treated Through Route II**

#### **4.5.2.1 Effect of Temperature**

The length and thickness distribution of  $\alpha$  lamellae, annealed at 820°C, 880°C and 920°C in the ( $\alpha+\beta$ ) phase field and water quenched without deformation, are shown in Figure 4.14(a), 4.15(a) and 4.16(a). Length of the  $\alpha$  lamellae decreases drastically with increasing temperature of annealing in the ( $\alpha+\beta$ ) phase field. Volume fraction of the shorter  $\alpha$  lamellae increases with increasing temperature. Thickness of the  $\alpha$  lamellae also decreases with increasing temperature. This indicates that dissolution of  $\alpha$  plates by increasing amount of equilibrium  $\beta$  phase with increasing temperature occurs from both the length and width portion. Microstructures are shown in Figure 4.17(a) to (c).

#### **4.5.2.2 Effect of Deformation**

The length and thickness distribution of  $\alpha$  lamellae after deforming at the above mentioned three temperatures in the ( $\alpha+\beta$ ) field, water quenched, are shown in Figures 4.14, 4.15 and 4.16 (b) to (d). Some Microstructures are shown in Figure 4.17(d) to (f). At 820°C, with 25% thickness reduction the volume fraction of  $\alpha$  lamellae with length less than 5 $\mu$ m increases to a high value indicating that  $\alpha$  lamellae are breaking at that deformation. But the longer volume fraction of  $\alpha$  lamellae also increases, i.e. elongation of the  $\alpha$  lamellae is also taking simultaneously with their breakage. With higher amount of deformation also this same trend keeps on repeating though breaking of  $\alpha$  lamellae becomes sufficiently high so that the total spectra of length decreases with increasing amount of deformation. Thickness of the  $\alpha$  lamellae first increases up to 50% deformation, but after 75% deformation it decreases drastically.

As the temperature of working was increased to 880°C, with increasing amount of deformation, volume fraction of shorter  $\alpha$  lamellae decreases up to 50% deformation pointing out that elongation is the main

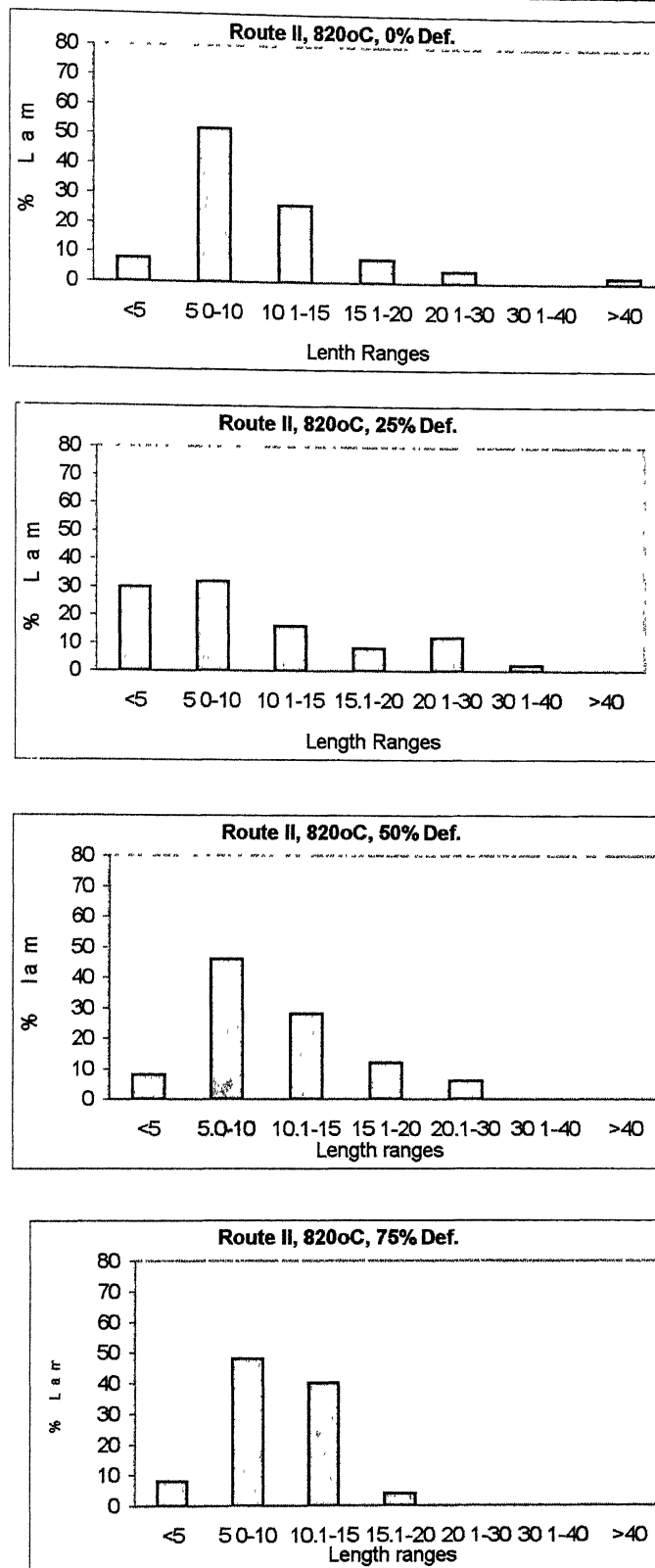


Figure 4.14/1

Length Distribution of  $\alpha$  Lamellae after Stage II

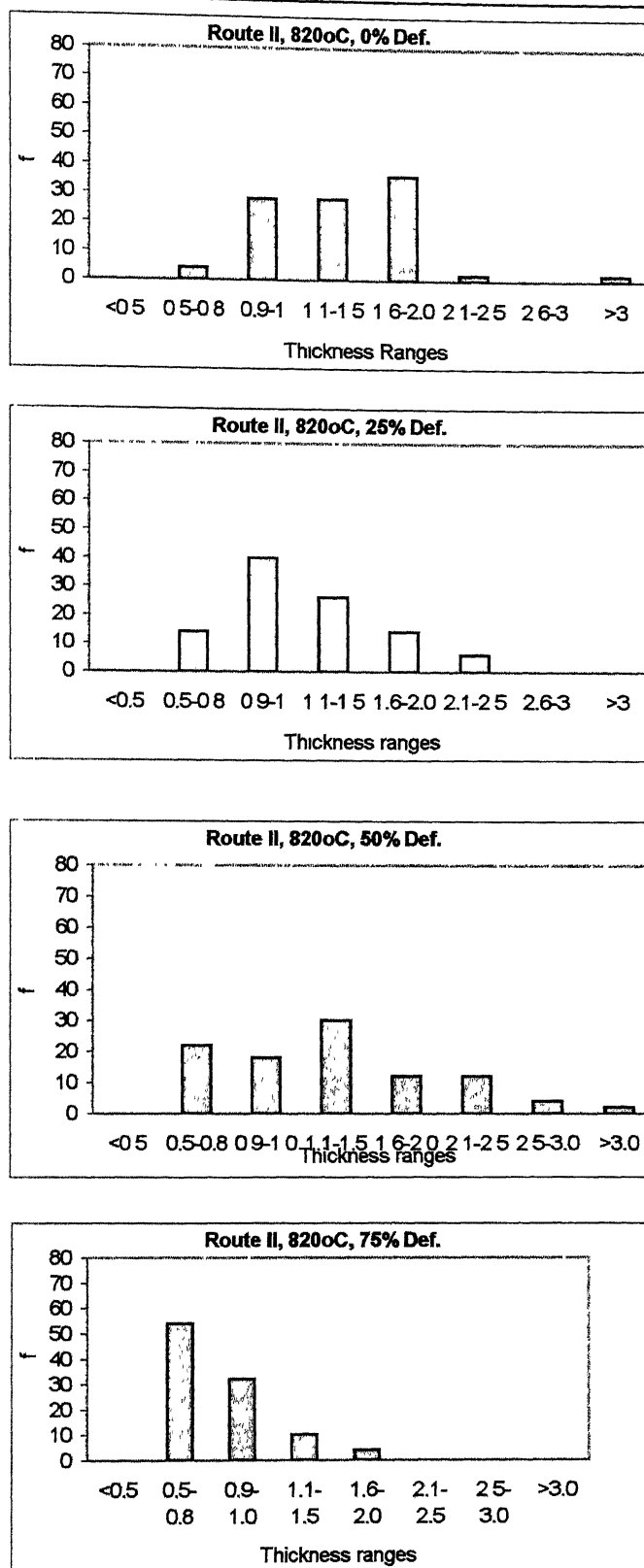


Figure 4.14/2

**Thickness Distribution of  $\alpha$  Lamellae after Stage II**

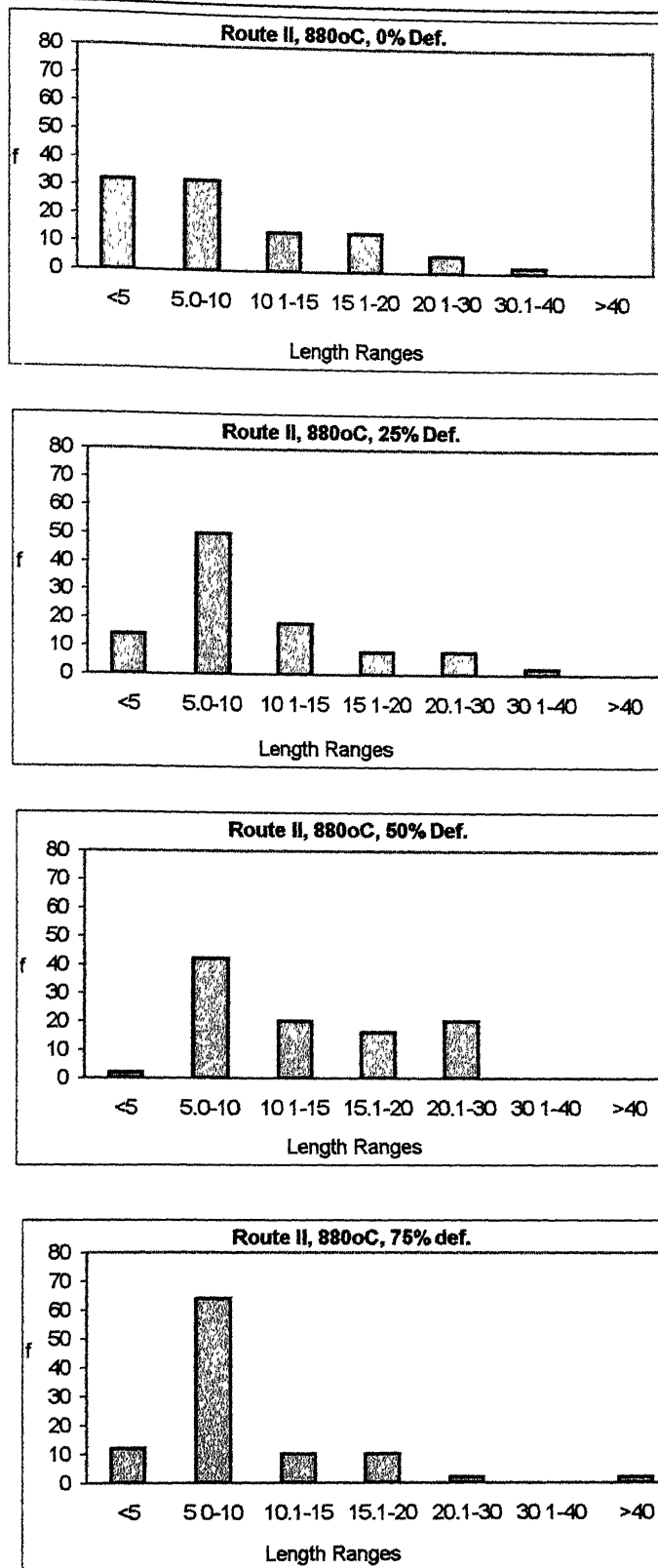


Figure 4.15/1

**Length Distribution of  $\alpha$  Lamellae after Stage II**

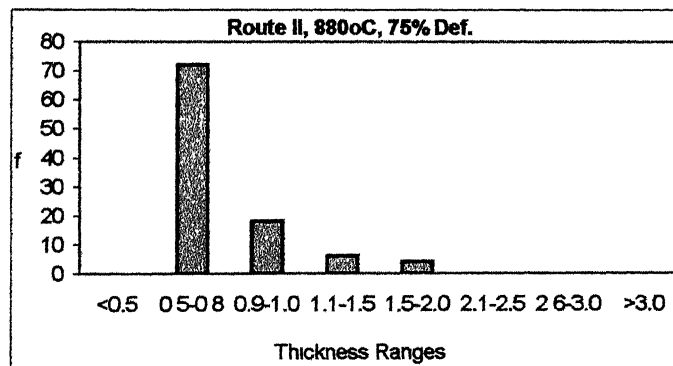
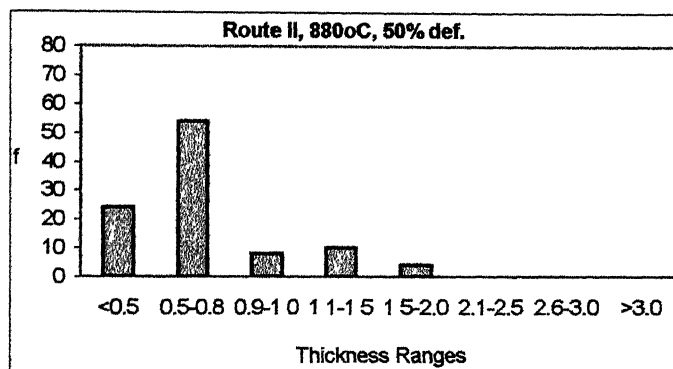
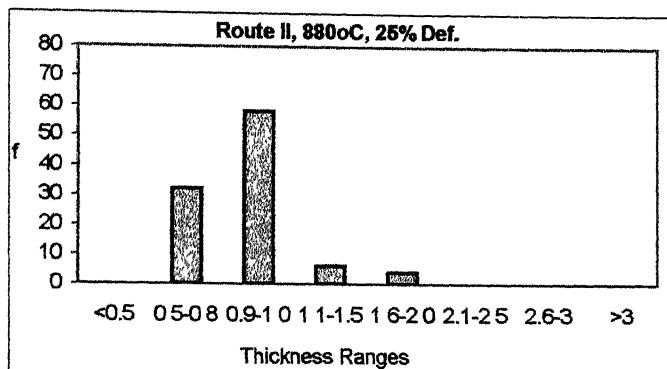
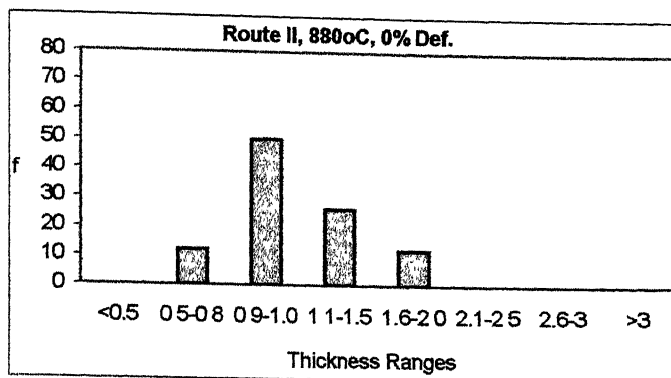


Figure 4.15/2

**Thickness Distribution of  $\alpha$  Lamellae after Stage II**

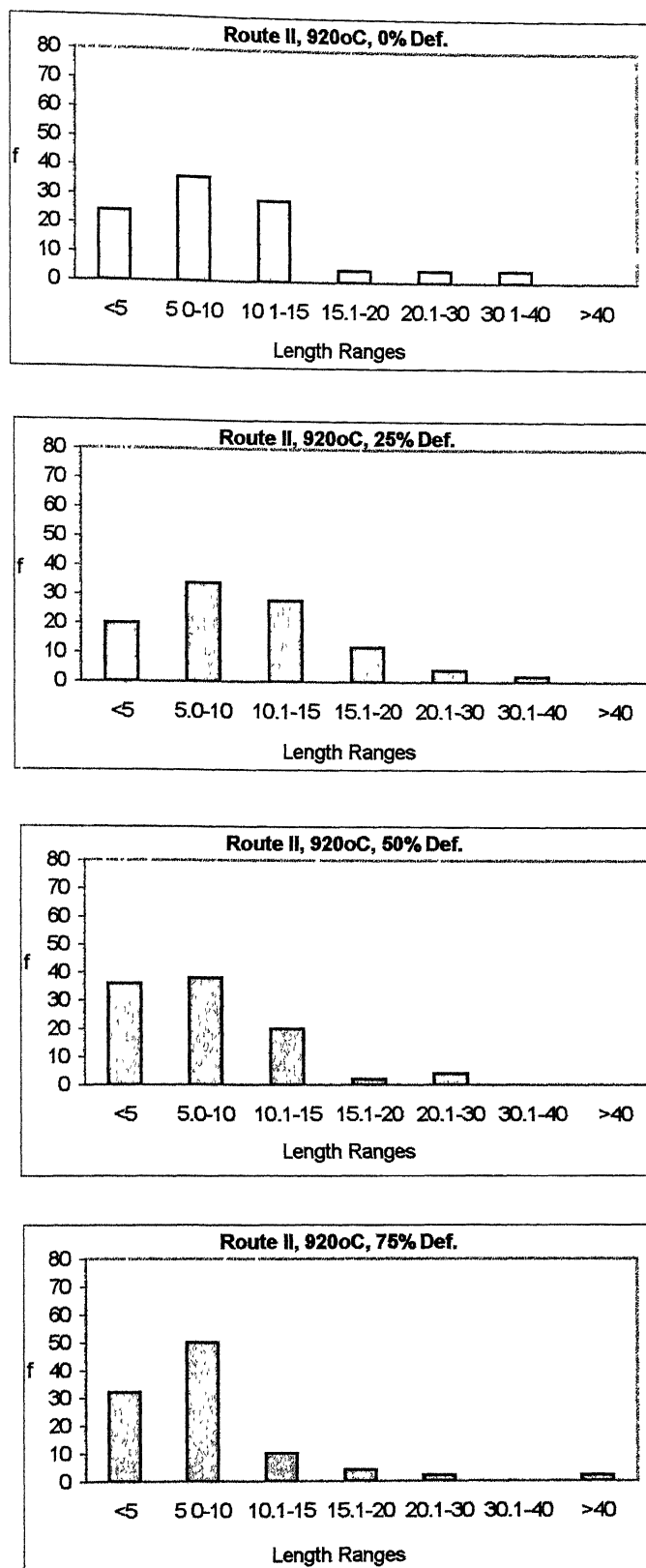


Figure 4.16/1

**Length Distribution of  $\alpha$  Lamellae after Stage II**



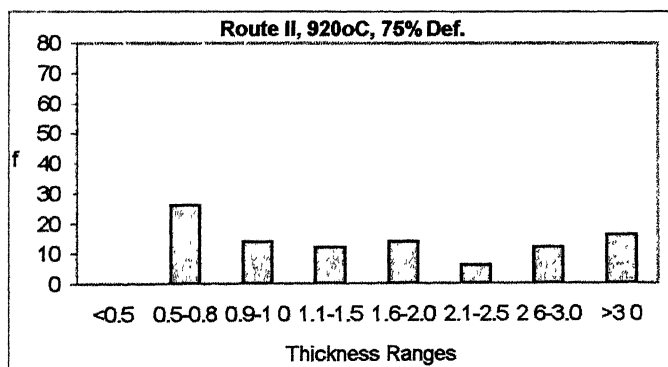
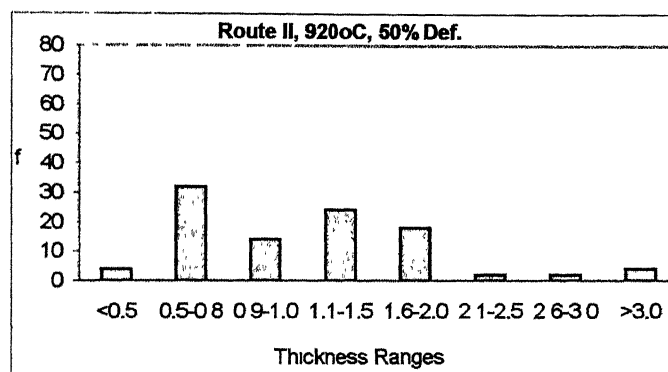
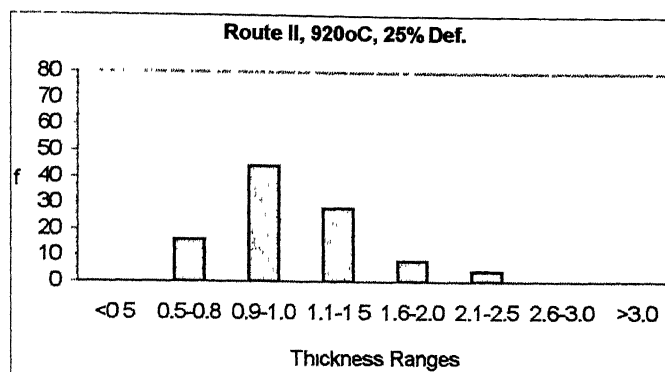
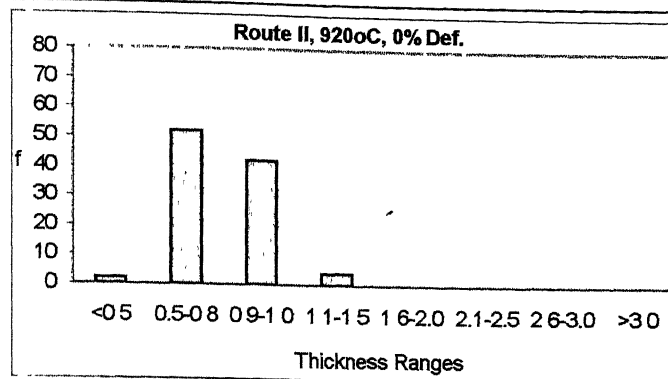
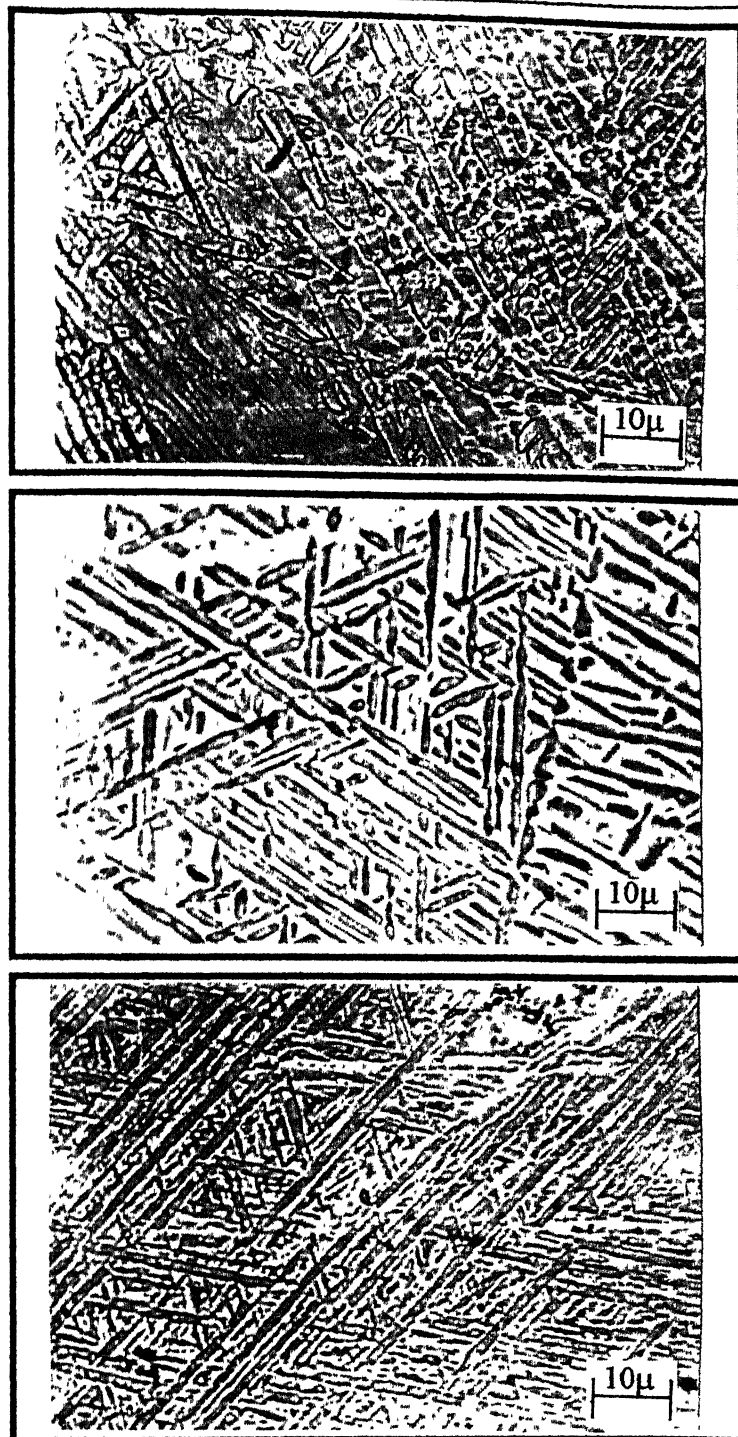


Figure 4.16/2

**Thickness Distribution of  $\alpha$  Lamellae after Stage II**



**Figure 4.17** Microstructure of Samples Processed Through Route II , in Stage I, Followed by Heating at (in water quenched conditions)

- (d) 820°C
- (e) 880°C
- (f) 920°C

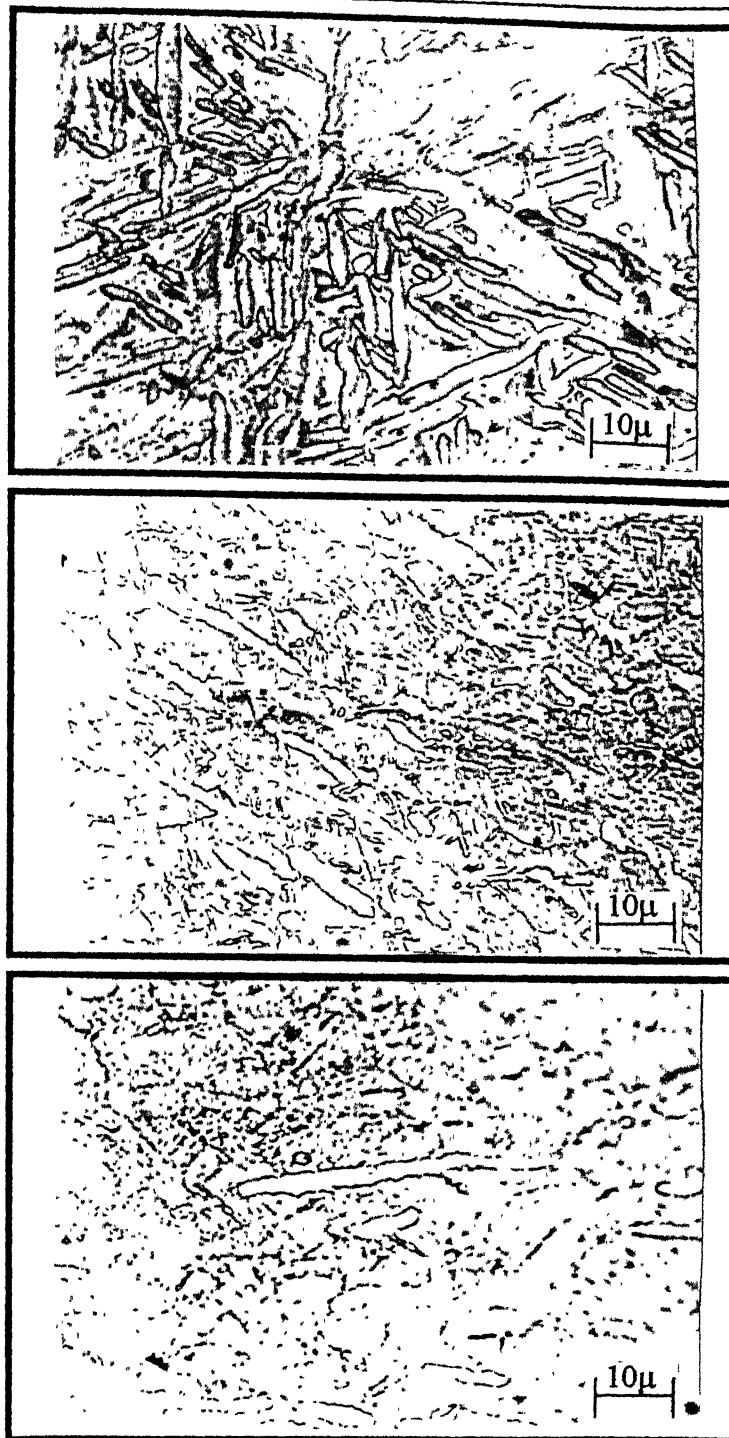


**Figure 4.18** Microstructure of Samples Processed Through Route II , in Stage I, Followed by Heating at 920°C and Thickness Reduction of (in water quenched conditions)

- (a) 25%
- (b) 50%
- (c) 75%

process happening at that temperature up to a sufficiently high amount of deformation. After 75% deformation, however, the shorter volume fraction increases so that breakage of  $\alpha$  lamellae becomes predominant at that high deformation value only. Thickness of the  $\alpha$  lamellae decreases up to 50% deformation, but after 75% deformation it increases. At deforming temperature of 920°C, the same trend is observed in the length of the  $\alpha$  lamellae except that the breakage starts after 50% deformation at this temperature. The thickness of  $\alpha$  lamellae varies in some peculiar manner at this temperature, it first increases, then decreases and finally after 75% deformation it again increases.

### **4.5.3 Effect of Thermo-mechanical Processing Variables on the Morphology of $\alpha$ Lamellae in the Sample Processed Through Route III**

#### **4.5.3.1 Effect of Temperature**

Effect of temperature on the length and thickness distribution of the  $\alpha$  lamellae in the sample processed through route III and reheated at 820°C, 880°C and 920° are shown in Figures 4.18(a), 4.19(a) and 4.20(a). It is observed from these figures there is no fixed trend in the length and thickness values of the  $\alpha$  lamellae. These values change almost randomly in different ranges indicating that dissolution of  $\alpha$  lamellae by the  $\beta$  takes place preferentially on different lamellae in different directions.

#### **4.5.3.2 Effect of Deformation**

The length and thickness distribution of  $\alpha$  lamellae after deforming at the above mentioned three temperatures in the ( $\alpha+\beta$ ) field, water quenched, are shown in Figures 4.18, 4.19 and 4.20 (b) to (d). At 820°C after 25% deformation, the  $\alpha$  lamellae mainly elongate without breaking. But higher amount of deformation causes the  $\alpha$  lamellae to break up. Elongation of the  $\alpha$  lamellae is not very clear in this deformation range, though with further increase in amount of

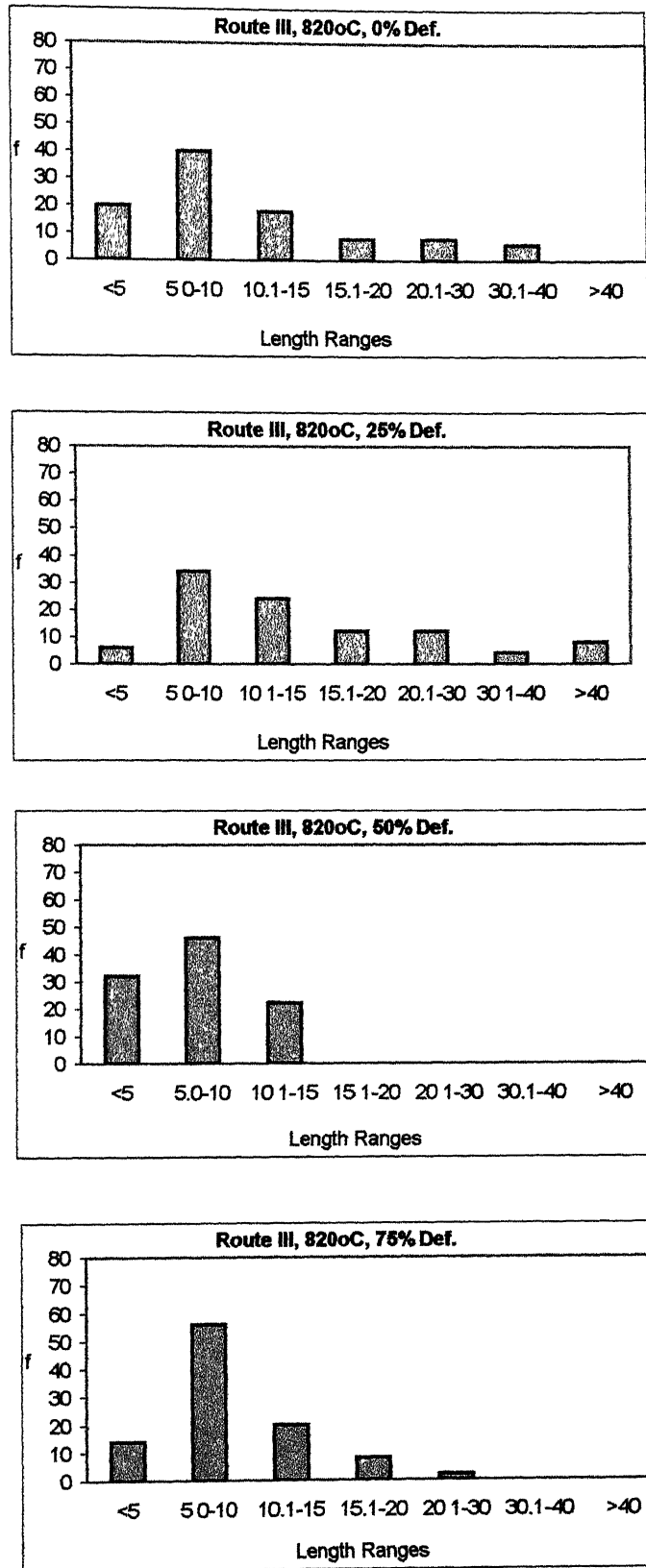


Figure 4.19/1

Length Distribution of  $\alpha$  Lamellae after Stage II

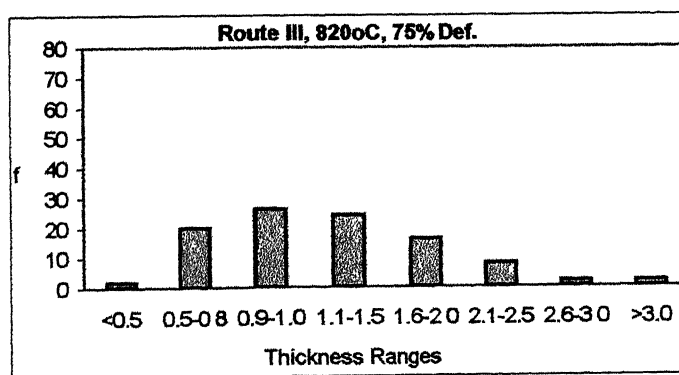
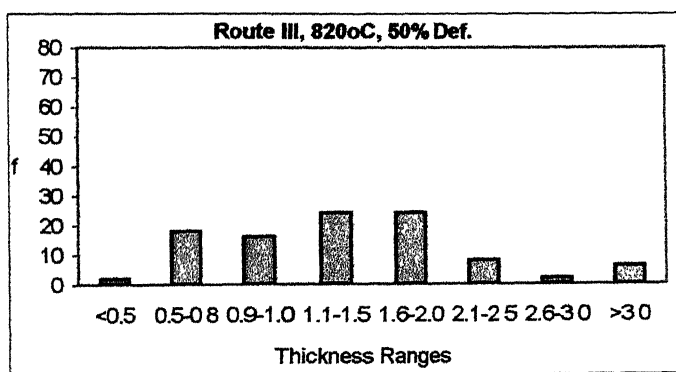
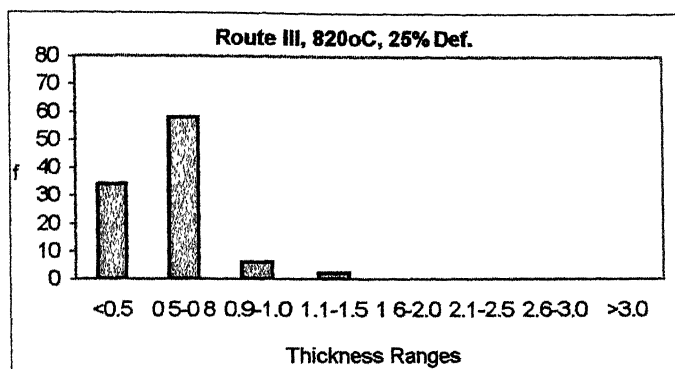
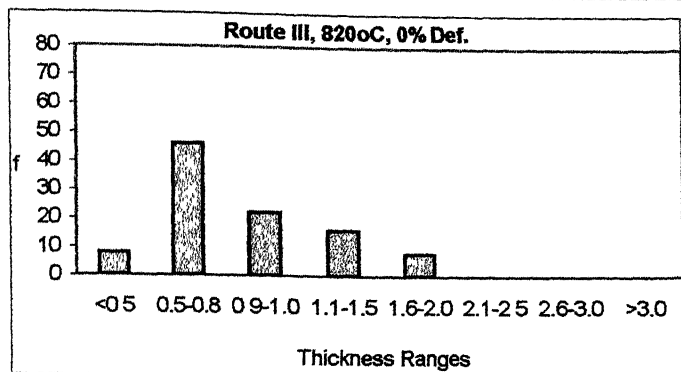
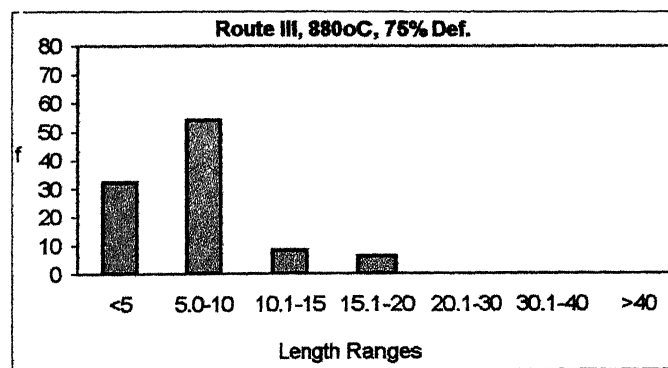
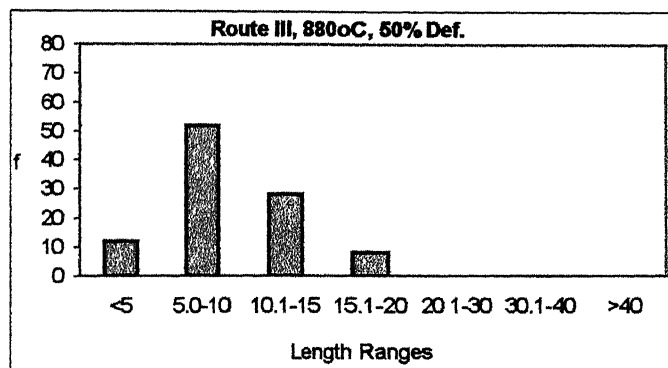
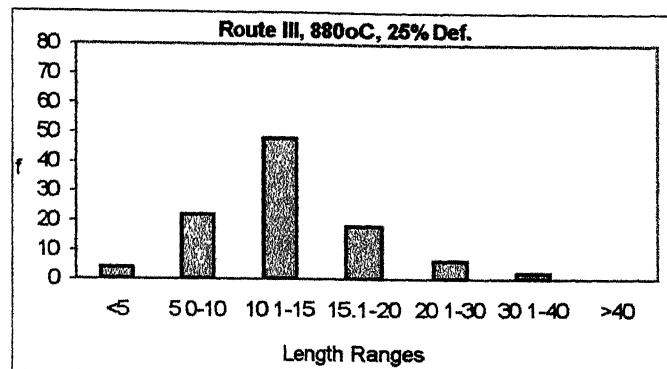
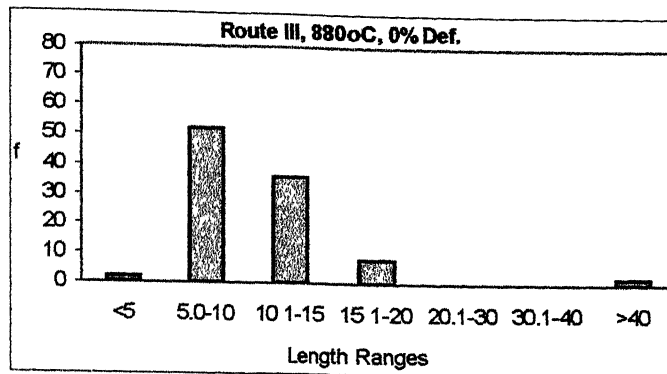
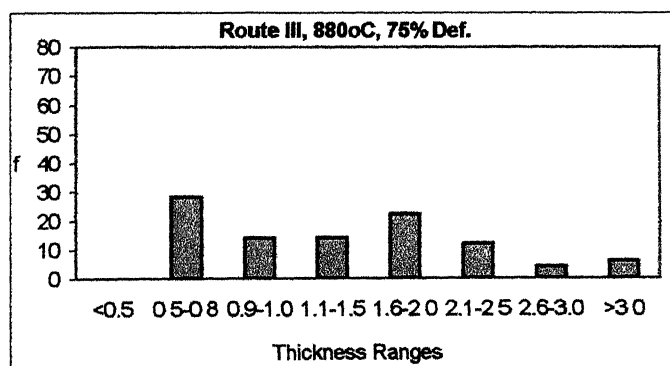
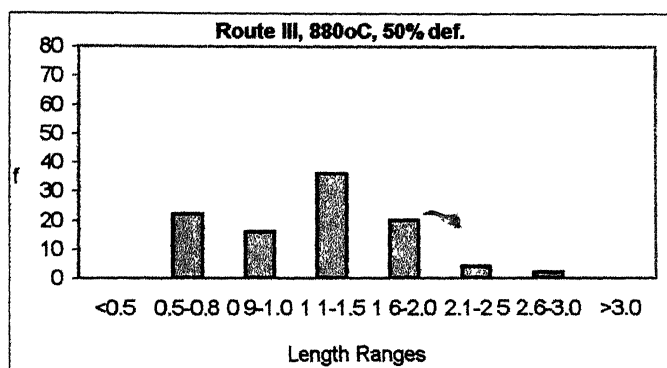
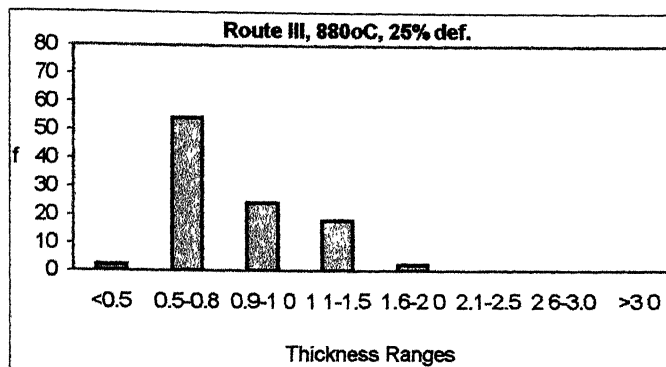
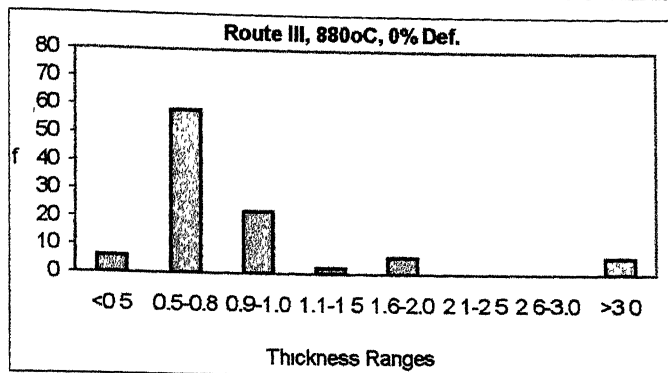


Figure 4.19/2

**Thickness Distribution of  $\alpha$  Lamellae after Stage II**



**Figure 4.20/1 Length Distribution of  $\alpha$  Lamellae after Stage II**



**Figure 4.20/2 Thickness Distribution of  $\alpha$  Lamellae after Stage II**



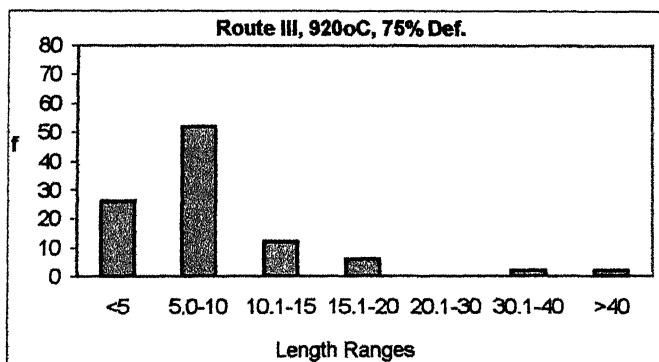
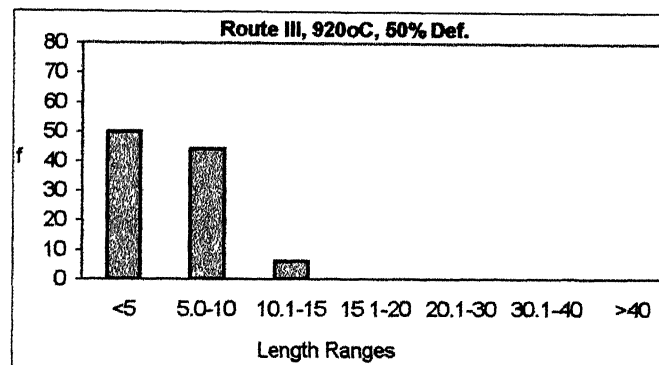
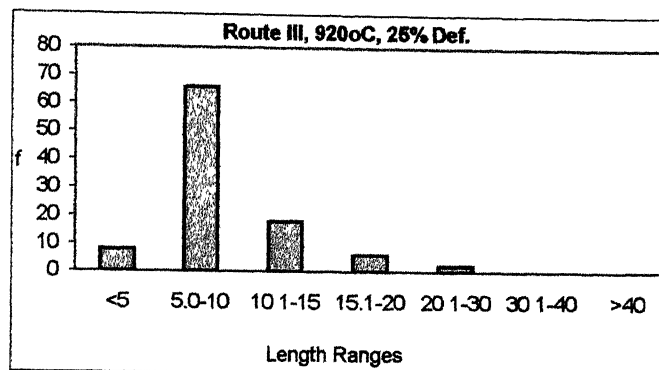
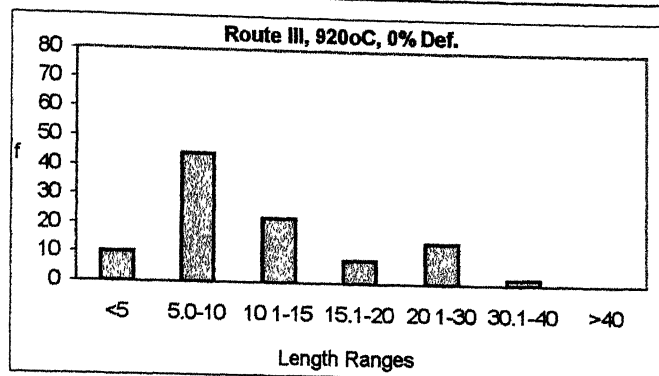


**Figure 4.21/1** **Length Distribution of  $\alpha$  Lamellae after Stage II**

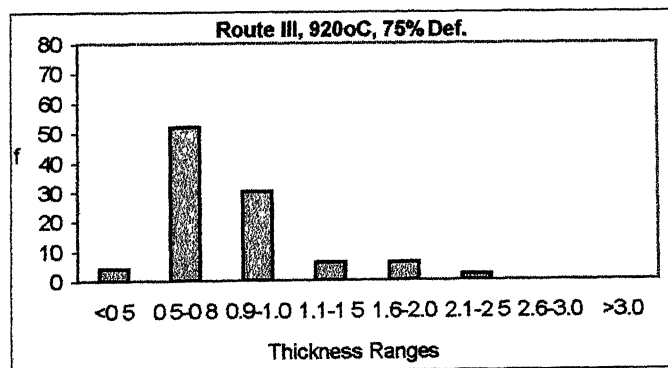
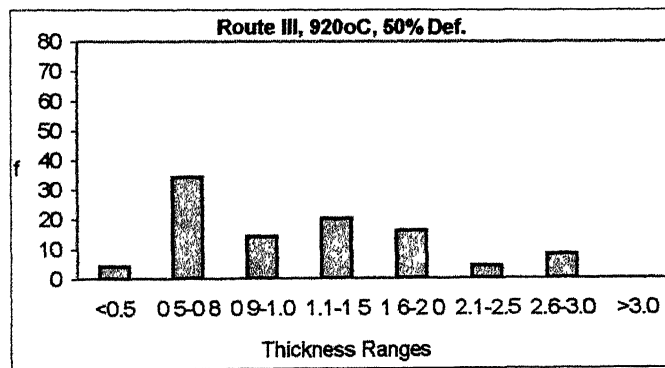
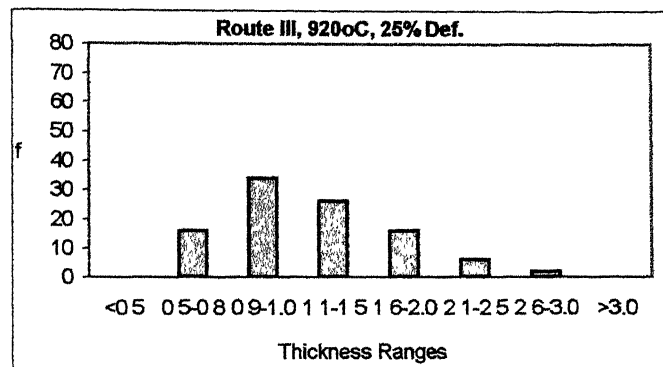
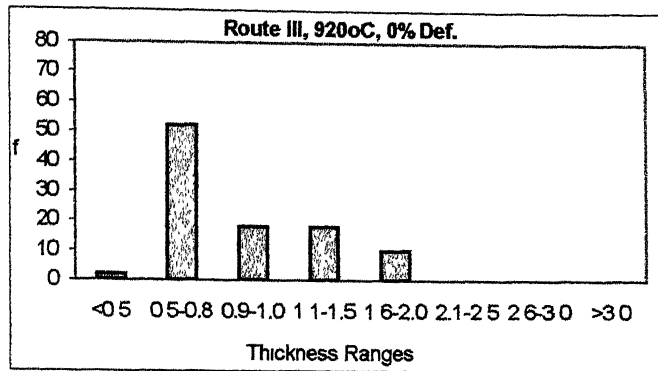


**Figure 4.21/2 Thickness Distribution of  $\alpha$  Lamellae after Stage II**

deformation elongation of the  $\alpha$  lamellae is observed. Thickness of the  $\alpha$  lamellae decreases first to some extent, but with higher deformation it increases.

At 880°C also almost the same trend is followed.  $\alpha$  lamellae first increases in length in preference to breakage up to 25% deformation, though with higher amount of deformation breakage becomes prominent with volume fraction of shorter lamellae increasing. At this temperature,  $\alpha$  lamellae becomes thicker with increasing deformation up to highest level. At 920°C both breakage and elongation of the  $\alpha$  lamellae is observed starting from 25% deformation and it continues till the highest amount of deformation, elongation being mostly predominant at the highest value of deformation. Thickness of the  $\alpha$  lamellae first increases to some extent, then it decreases constantly with increasing amount of deformation.

#### **4.5.4 Effect of Thermo-mechanical Processing Variables on the Morphology of $\alpha$ Lamellae in the Sample Processed Through Route IV**

##### **4.5.4.1 Effect of Temperature**

Effect of temperature on the length and thickness distribution of the  $\alpha$  lamellae in the sample processed through route IV and reheated at 820°C, 880°C and 920°C, are shown in Figures 4.21(a), 4.22(a) and 4.23(a). In this case also, like the last one, it is difficult to point out any specific effect of temperature on the morphology of  $\alpha$  lamellae as both the length and thickness of  $\alpha$  lamellae keep on changing almost randomly with temperature. Probably high amount of deformation induced into the material creates some tendency of preferential dissolution of  $\alpha$  lamellae at some positions due to unstable flow, which results into this type of behaviour.

##### **4.5.4.2 Effect of Deformation**

The length and thickness distribution of  $\alpha$  lamellae after deforming at the above mentioned three temperatures in the ( $\alpha+\beta$ ) field, water quenched, are shown in Figures 4.21, 4.22 and 4.23 (b) to (d). At 820°C after 25%

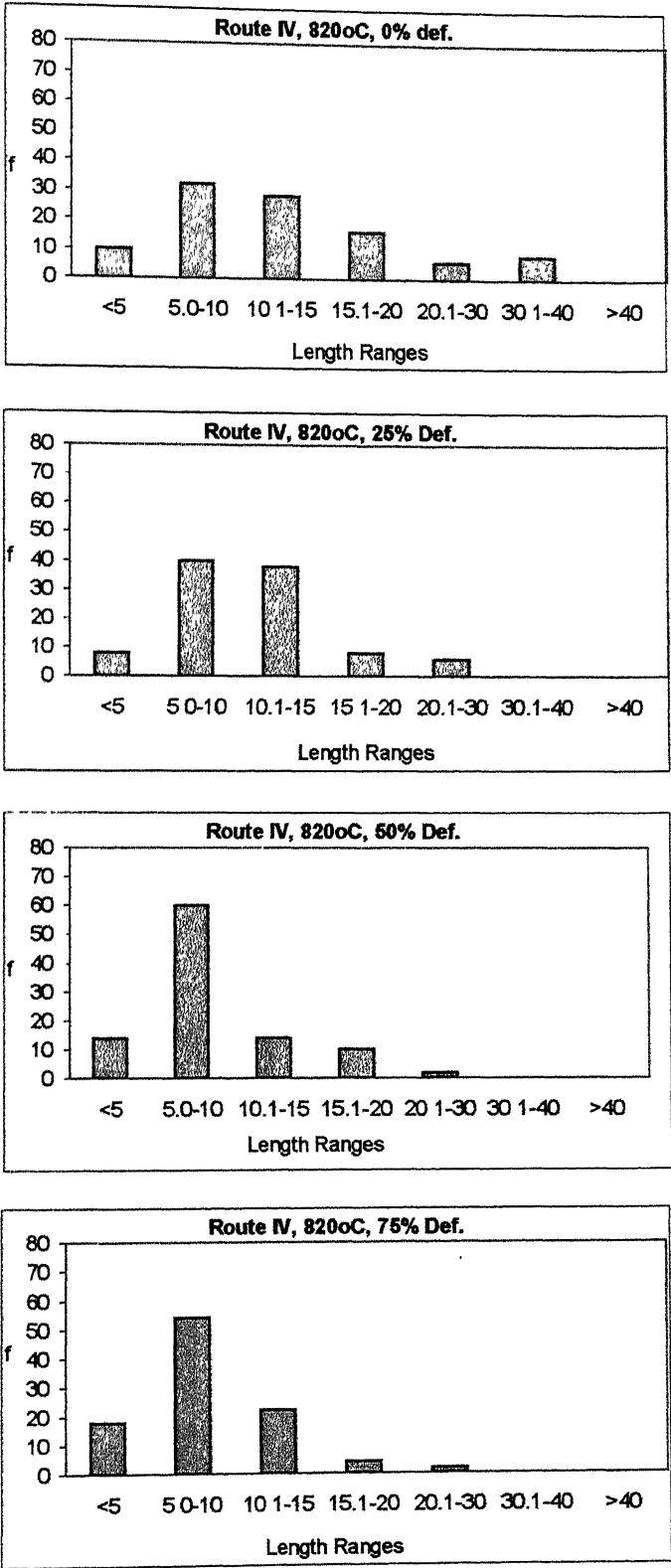


Figure 4.22/1      Length Distribution of  $\alpha$  Lamellae after Stage II

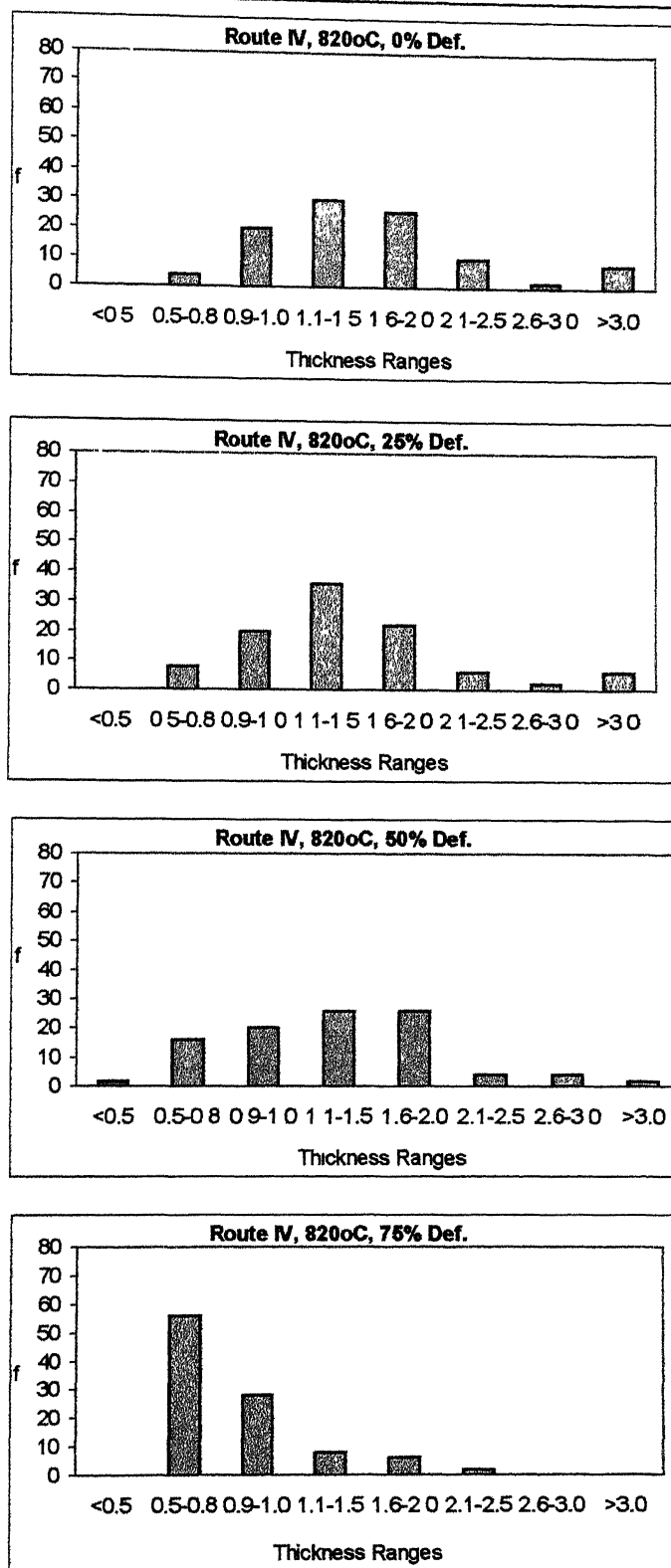


Figure 4.22/2

Thickness Distribution of  $\alpha$  Lamellae after Stage II

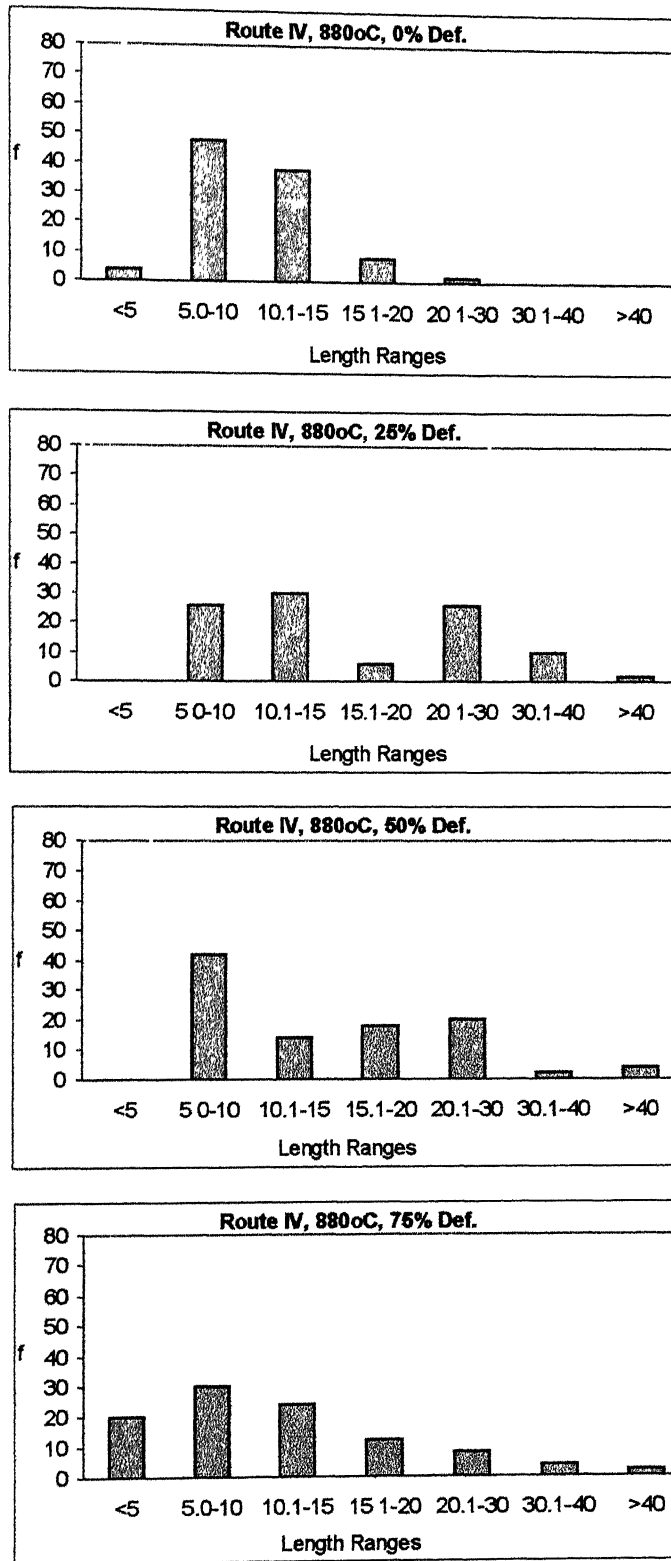


Figure 4.23/1

Length Distribution of  $\alpha$  Lamellae after Stage II

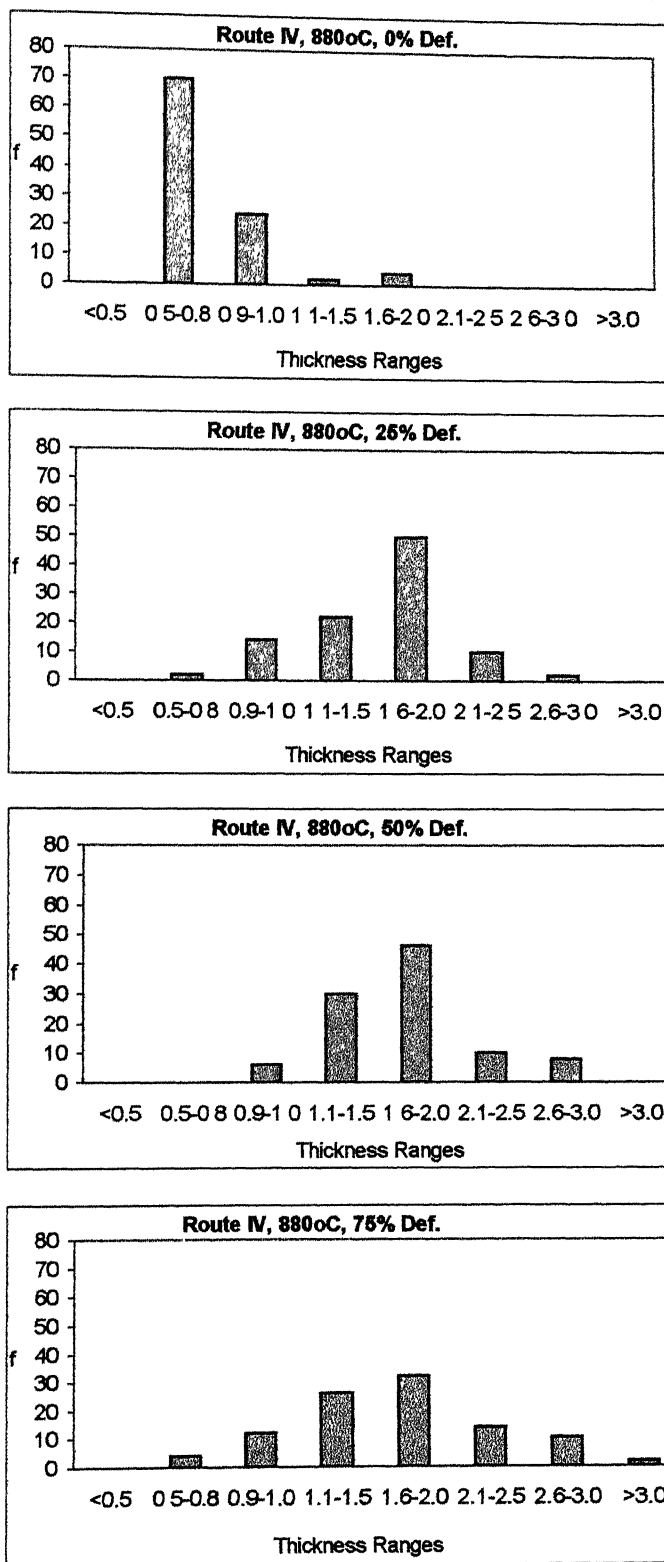


Figure 4.23/2

**Thickness Distribution of  $\alpha$  Lamellae after Stage II**

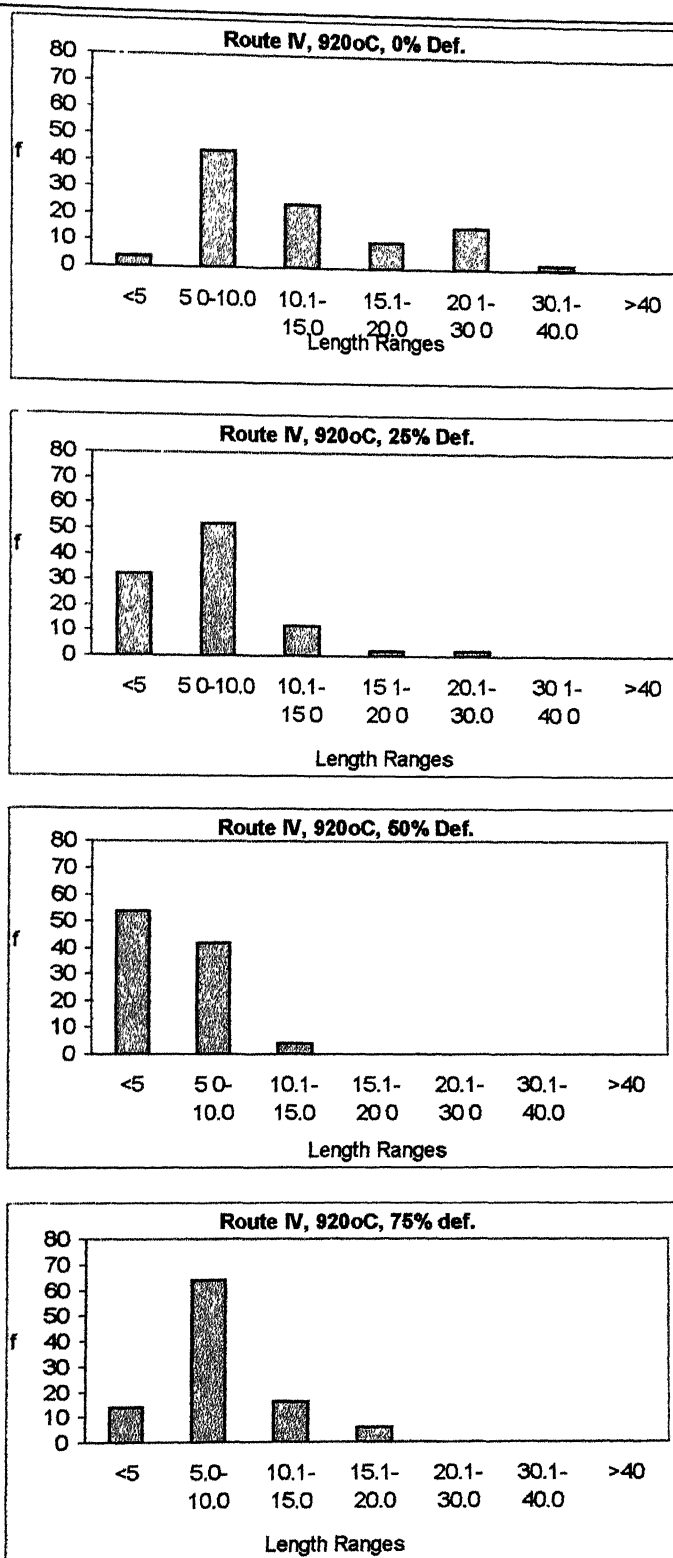


Figure 4.24/1

Length Distribution of  $\alpha$  Lamellae after Stage II



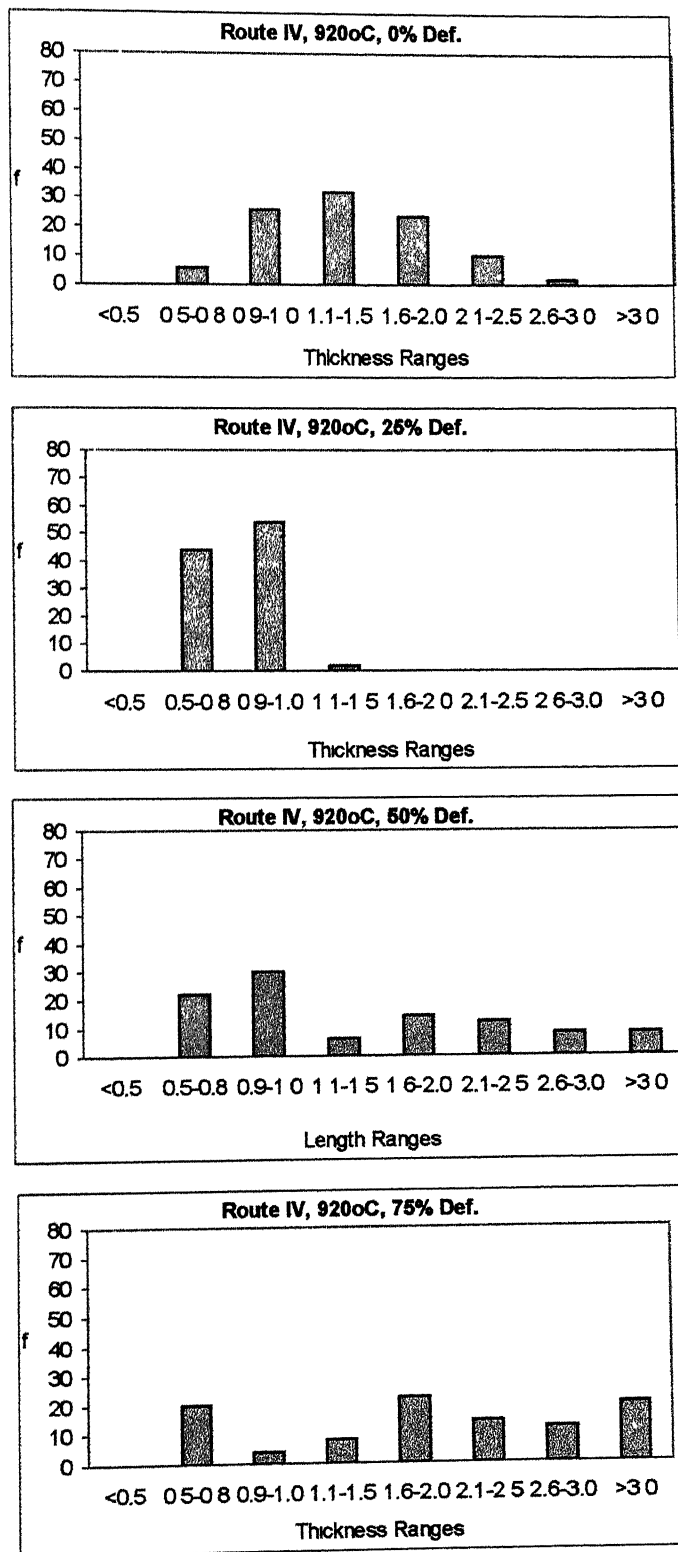


Figure 4.24/2

Thickness Distribution of  $\alpha$  Lamellae after Stage II

deformation, both elongation and breakage of  $\alpha$  lamellae is observed as total spectra of length comes down, indicating that  $\alpha$  lamellae are breaking, along with decrease in the volume fraction of the shortest length of  $\alpha$  lamellae indicating that some elongation is also taking place simultaneously. With increasing amount of deformation, breakage of  $\alpha$  lamellae becomes the predominant feature. Thickness of  $\alpha$  lamellae increases at first to a small extent upon 25% deformation, but then with higher amount of deformation it decreases.

As the temperature of working is increased to 880°C, elongation of  $\alpha$  lamellae is the predominant event, which occurs up to 50% deformation as the volume fraction of longer  $\alpha$  lamellae increases. Breaking up of  $\alpha$  lamellae starts at 50% deformation only as volume fraction of  $\alpha$  lamellae in the length range 5-10 $\mu$ m increases but after 75% deformation only breakage becomes predominant as the shortest  $\alpha$  lamellae increases in volume fraction. Thickness of  $\alpha$  lamellae increases up to 50% deformation and then it decreases to give thinner  $\alpha$  lamellae. On the other hand, at 920°C shorter  $\alpha$  lamellae volume fraction increases with increasing amount of deformation up to 50% deformation above which some elongation takes place which is shown by the broadening of the spectra of  $\alpha$  lamellae and decrease in the volume fraction of the shortest  $\alpha$  lamellae. Thickness of  $\alpha$  lamellae at this temperature first decreases with 25% deformation, but later with higher amount of deformation it increases. Some microstructures are shown in Figure 4.24(a) to (c).

### **4.5.5 Effect of Thermo-mechanical Processing Variables on the Morphology of $\alpha$ Lamellae in the Sample Processed Through Route V**

#### **4.5.5.1 Effect of Temperature**

Effect of temperature on the length and thickness distribution of the  $\alpha$  lamellae in the sample processed through route V and reheated at 820°C, 880°C and 920°C are shown in Figures 4.25(a), 4.26(a) and 4.27(a). When the

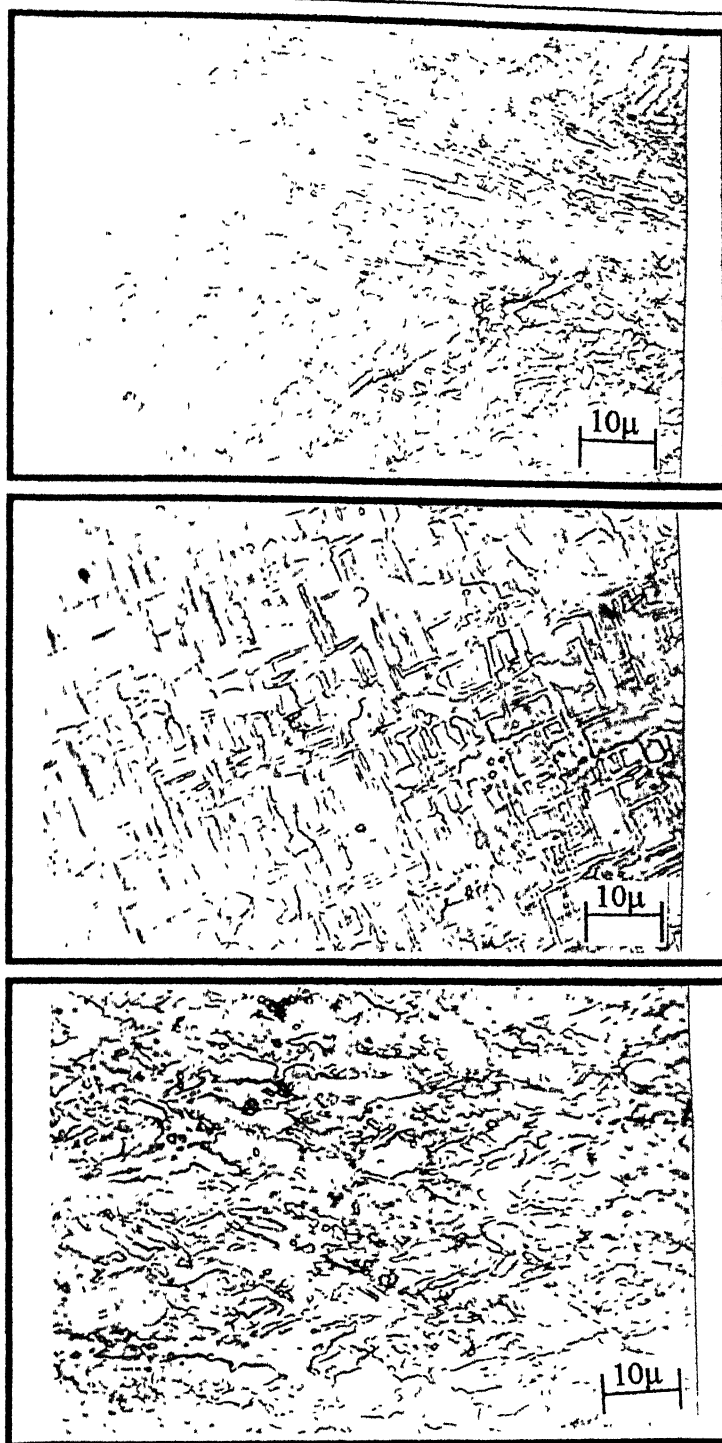


**Figure 4.25** Microstructure of Samples Processed Through Route IV , in Stage I, Followed by Heating at 920°C and Thickness Reduction of(in water quenched conditions)

- (a) 25%
- (b) 50%
- (c) 75%

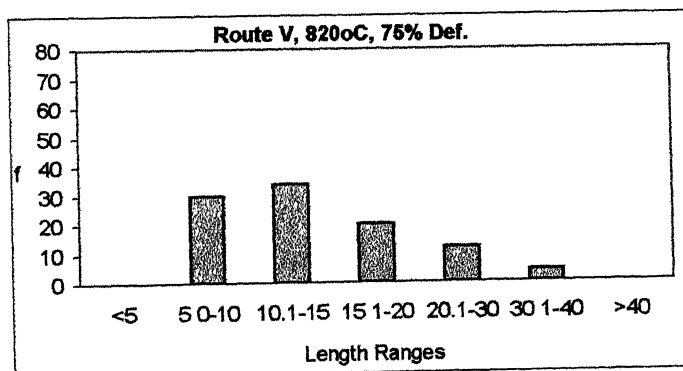
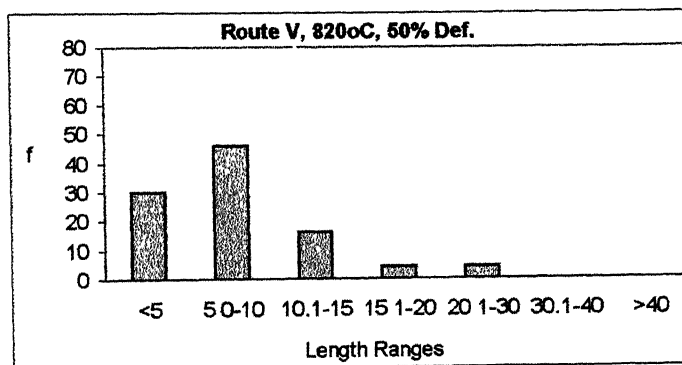
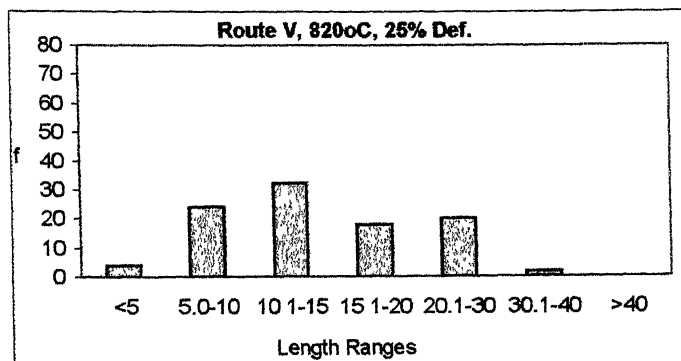
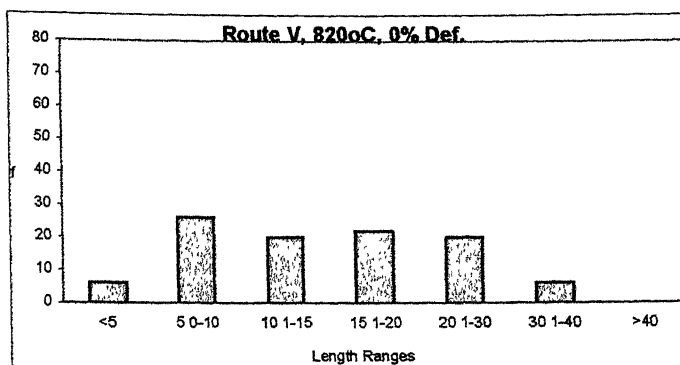


**Figure 4.26/1**

**Length Distribution of  $\alpha$  Lamellae after Stage II**

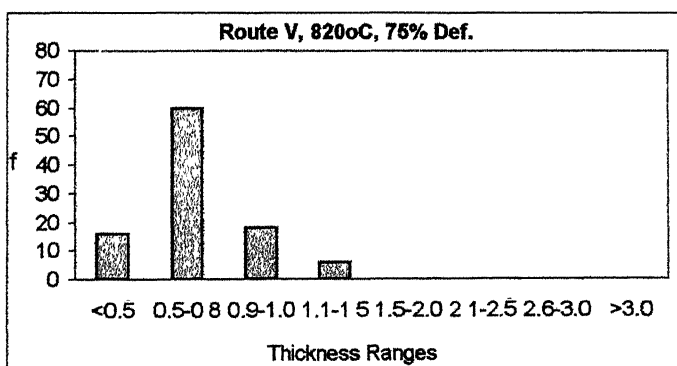
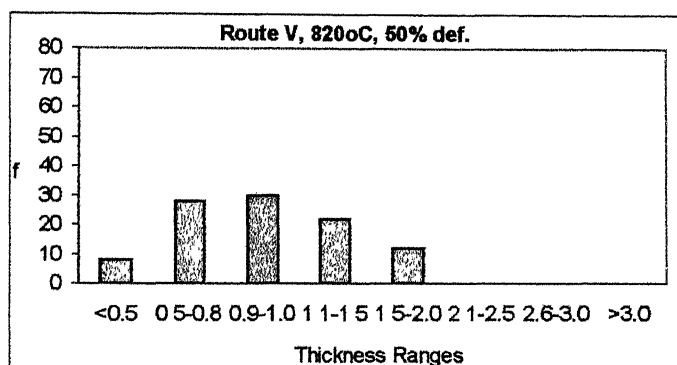
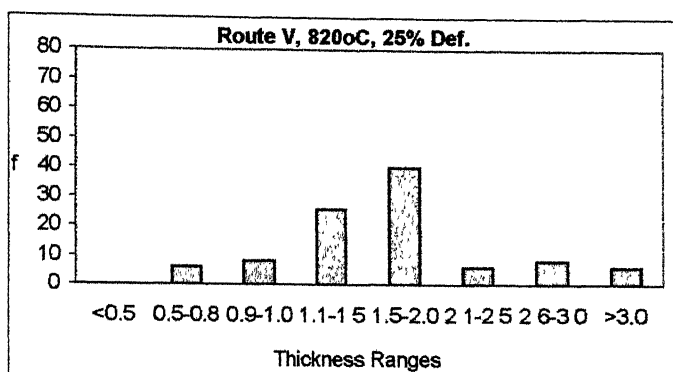
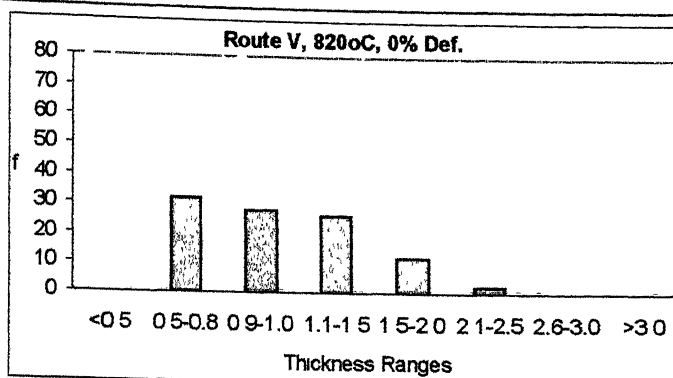


Figure 4.26/2

**Thickness Distribution of  $\alpha$  Lamellae after Stage II**

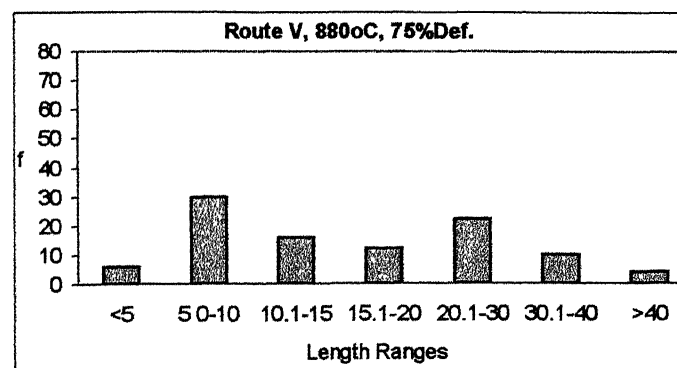
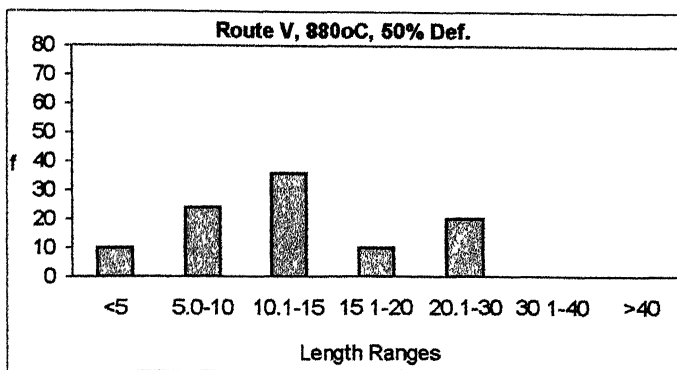
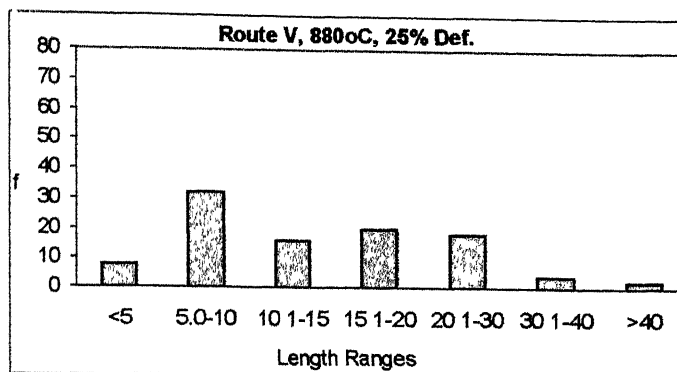
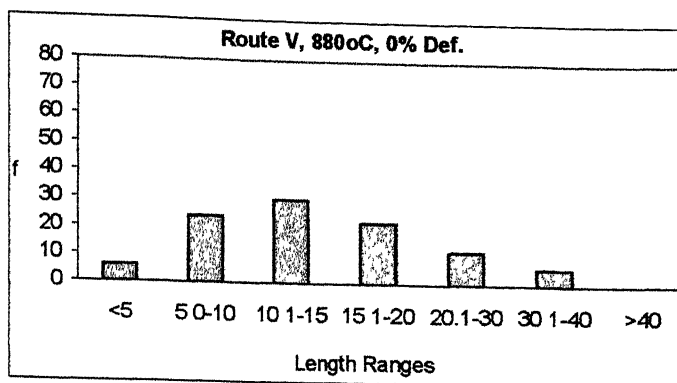


Figure 4.27/1

**Length Distribution of  $\alpha$  Lamellae after Stage II**

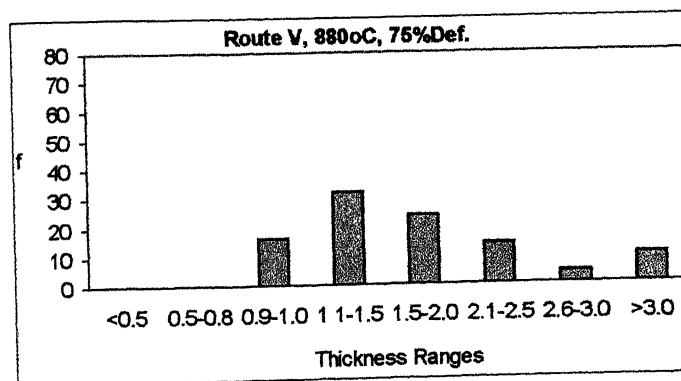
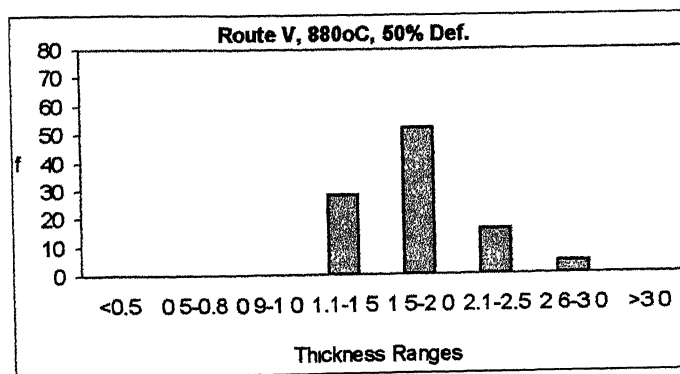
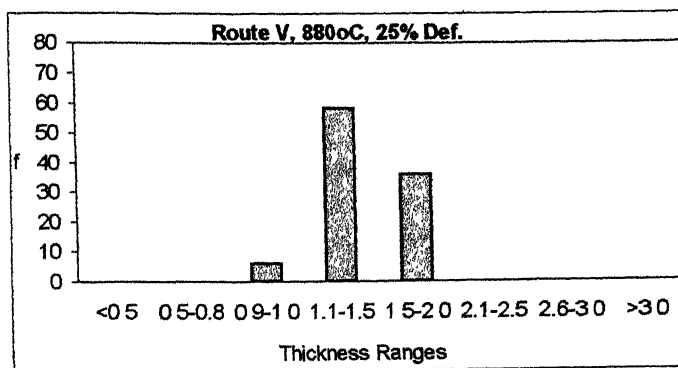
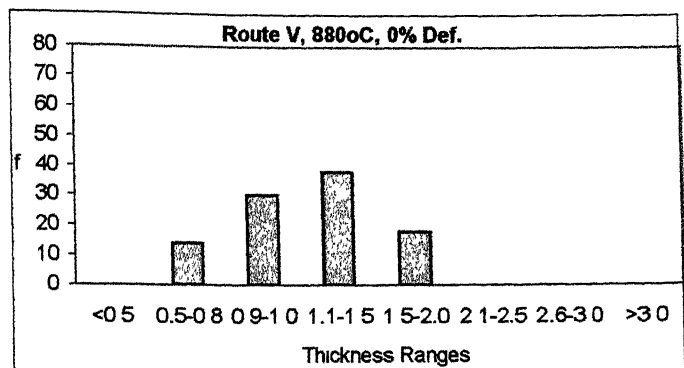


Figure 4.27/2

**Thickness Distribution of  $\alpha$  Lamellae after Stage II**

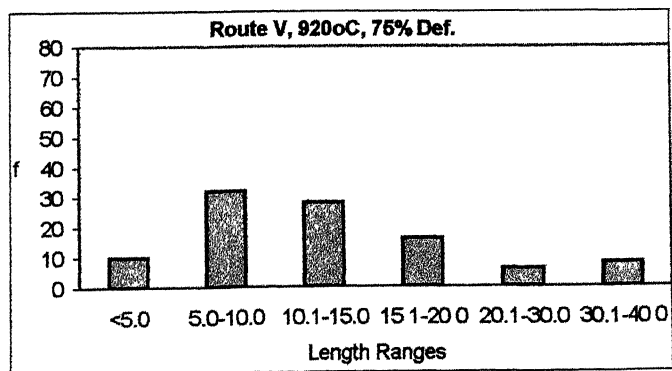
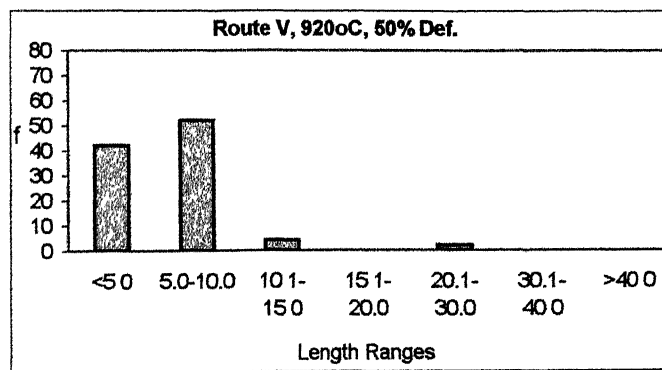
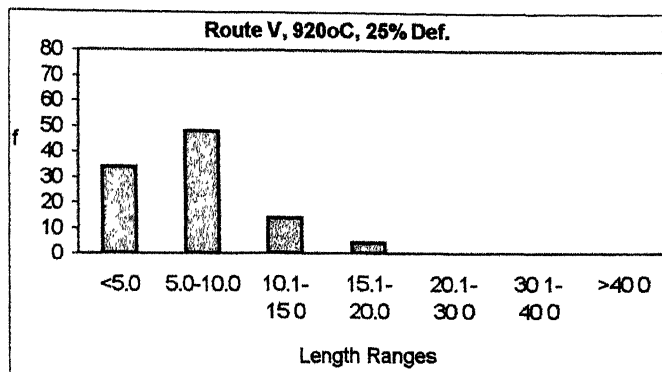
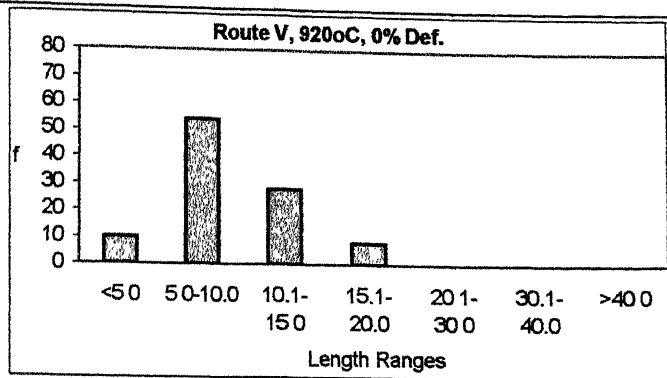
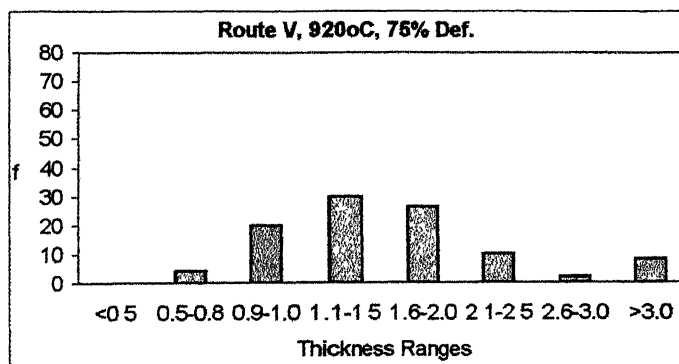
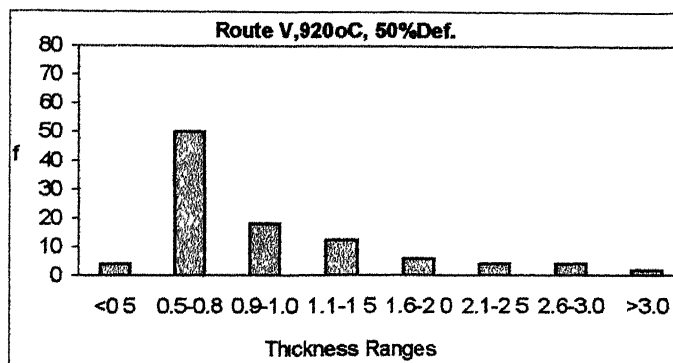
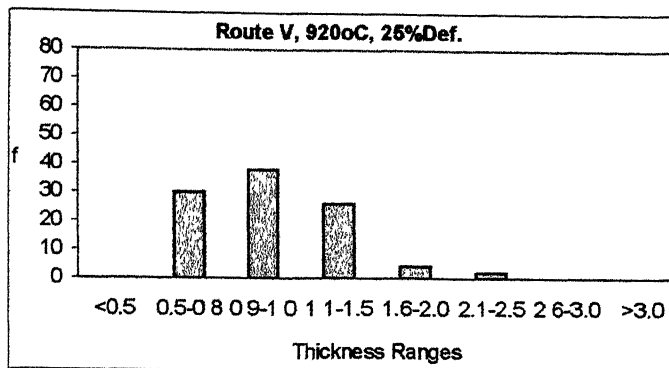
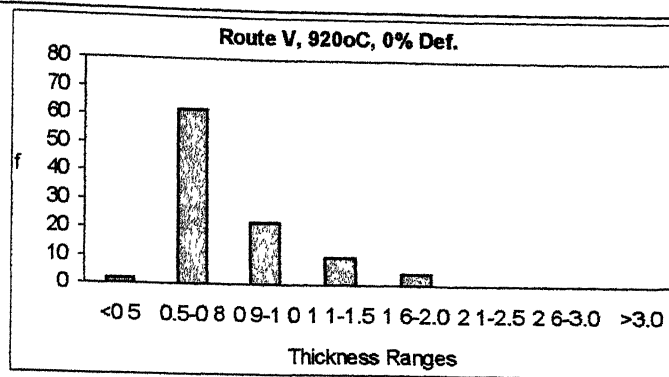


Figure 4.28/1

Length Distribution of  $\alpha$  Lamellae after Stage II





185.14.28/2

**Thickness Distribution of  $\alpha$  Lamellae after Stage II**

recrystallization temperature of the sample is increased from 820°C to 920°C through 880°C, shorter  $\alpha$  lamellae are observed to increase in length, as fraction of  $\alpha$  lamellae in the 5-10 $\mu$ m region decreases and that fraction in 10.1-15  $\mu$ m increases, upon heating at 880°C. But again fraction of  $\alpha$  lamellae in 20.1-30  $\mu$ m region decreases indicating that  $\alpha$  lamellae are being shortened also. At 920°C, however, shortening becomes the main feature as longer fraction of  $\alpha$  lamellae disappears from the structure and shorter fractions increase. Thickness of  $\alpha$  lamellae also first increases and then at further higher temperature it decreases. This type of random behaviour was also observed in the samples treated through routes III and IV.

#### **4.5.5.2 Effect of Deformation**

The length and thickness distribution of  $\alpha$  lamellae after deforming at the above mentioned three temperatures in the ( $\alpha+\beta$ ) field, water quenched, are shown in Figures 4.25, 4.26 and 4.27 (b) to (d). At 820°C after 25% deformation, small increase in length of the  $\alpha$  lamellae is observed though after 50% deformation breaking up of  $\alpha$  lamellae becomes the main feature as fraction of shorter  $\alpha$  lamellae increases and also the maximum length of  $\alpha$  lamellae becomes smaller. But after 75% deformation some increase in length of  $\alpha$  lamellae is observed as fraction of shortest  $\alpha$  lamellae becomes nil and also the maximum size increases. Thickness of  $\alpha$  lamellae first increases on smaller deformation, but with higher thickness reduction it constantly decreases. This same trend in length change is observed at 880°C also though thickness increases rapidly up to 50% deformation and above that it decreases to some extent. On the contrary, breakage of  $\alpha$  lamellae at 920°C is the main feature from the smallest amount of deformation. This trend continues up to 50% deformation above which elongation of  $\alpha$  lamellae is observed. Thickness of  $\alpha$  lamellae, on the other hand, has an almost increasing tendency with increasing deformation. Some microstructures are shown in Figure 4.28 (a) to (c).



**Figure 4.29** Microstructure of Samples Processed Through Route V , in Stage I, Followed by Heating at 880°C and Thickness Reduction of (in water quenched conditions)

- (a) 25%
- (b) 50%
- (c) 75%

#### **4.6 EFFECT OF MILL ANNEALING TREATMENT ON THE EVOLUTION OF THE EQUIAXED $\alpha$ STRUCTURE IN HEAVILY ( $\alpha+\beta$ ) DEFORMED Ti-6-4 ALLOY**

To observe the effect of mill annealing on the deformed structure, samples treated through different routes in the  $\beta$  phase field and deformed at a thickness reduction of 75% at 880°C were recrystallized at three different temperatures in the ( $\alpha+\beta$ ) phase field, namely 700°C, 800°C and 850°C, followed by water quenching. The size of the  $\alpha$  grains was measured by the projected area diameter method, which is explained in chapter 3. The aspect ratio and size distribution of  $\alpha$  grains thus obtained after mill annealing is presented in Figures 4.29 to 4.38. A comparison between these figures point out the fact that with increasing temperature of mill annealing, in all the routes, both aspect ratio and size of the grains decreases. This indicates that with increasing temperature of mill annealing,  $\alpha$  grains are becoming more and more equiaxed and also finer in size. But there is some difference in the nature of distribution of aspect ratio and size of the grains among different routes. In the samples treated through routes II and IV, a mixture of lower and higher aspect ratio grains are observed even at the highest annealing temperature whereas in other samples most of the grains has aspect ratio less than 3.0. Again samples treated through routes II, III and IV show most of the grains having size less than 5.0  $\mu\text{m}$  while samples treated through routes I and V show wide distribution of grain size having almost equal fraction of  $\alpha$  grains in all the ranges. So from these results it can be said that samples treated through routes II and IV and further rolled to give 75% deformation at 880°C show different recrystallization response compared to the others. Some typical microstructures are shown in Figure 4.39(a) to (c). A recrystallization time of 15 minutes and 30 minutes were used and it is observed from the microstructure shown in Figure 4.40 that time of this magnitude has negligible effect on the recrystallization behaviour.

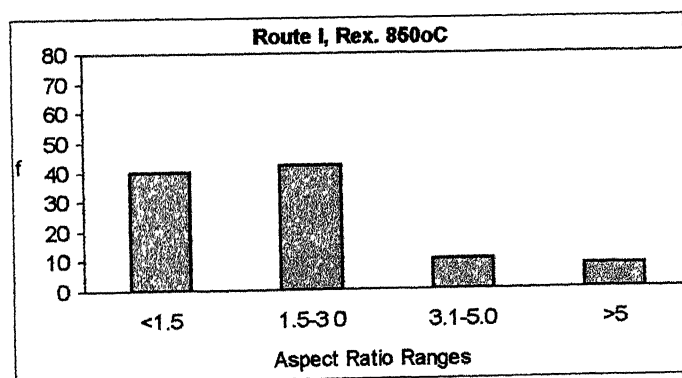
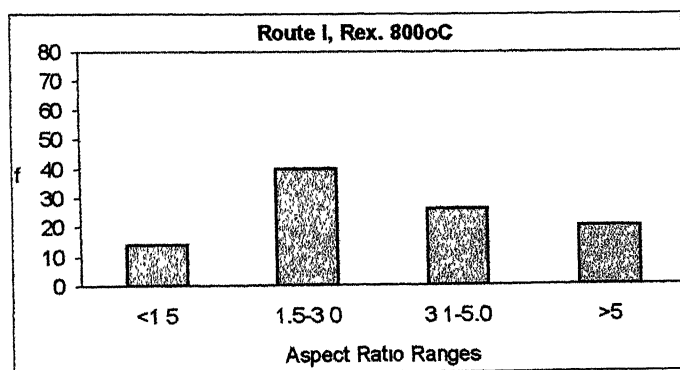
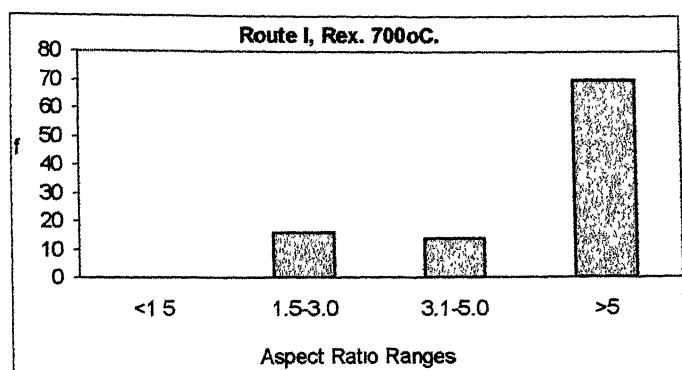
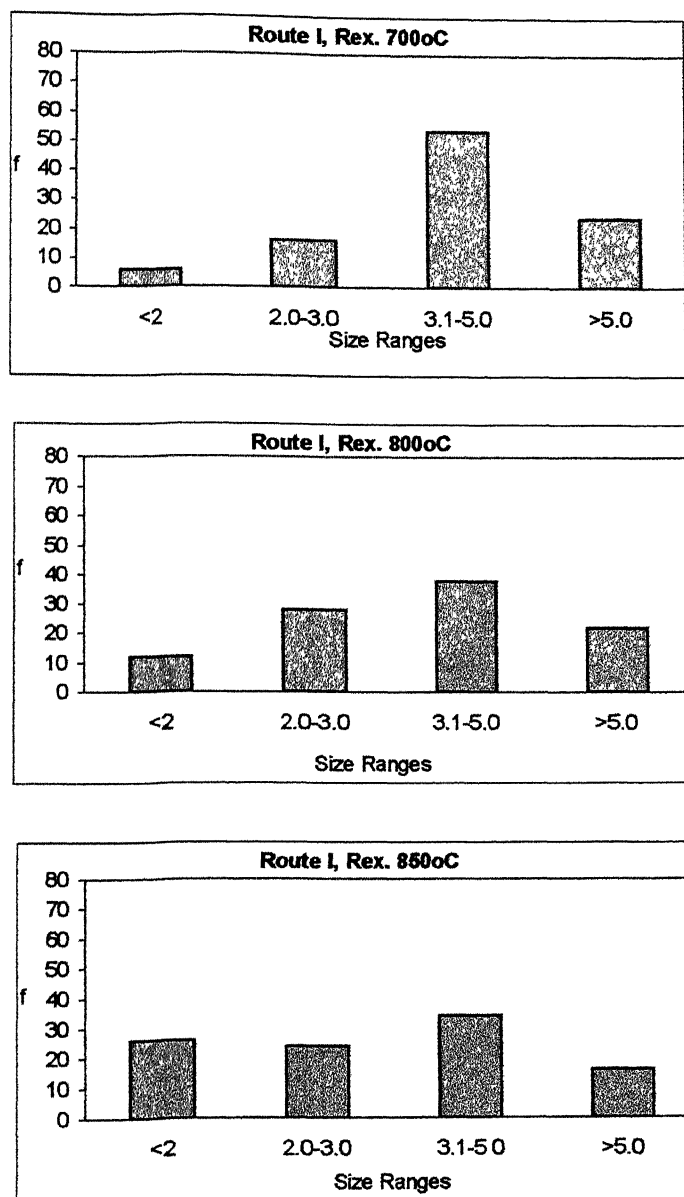


Figure 4.30 Aspect Ratio Distribution of Samples Processed Through Route I and Recrystallized at Different Temperatures



**Figure 4.31** Grain Size Distribution of Samples Processed Through Route I and Recrystallized at Different Temperatures

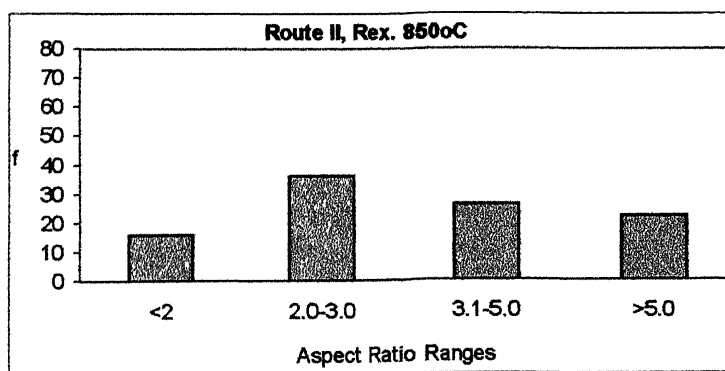
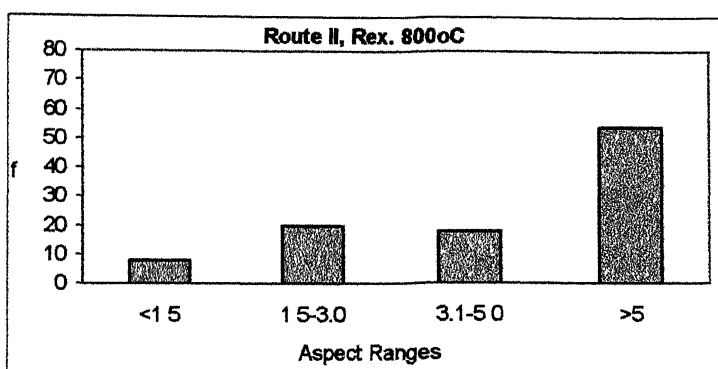
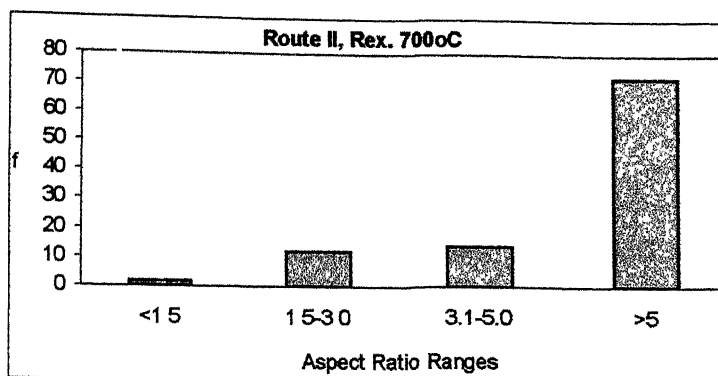
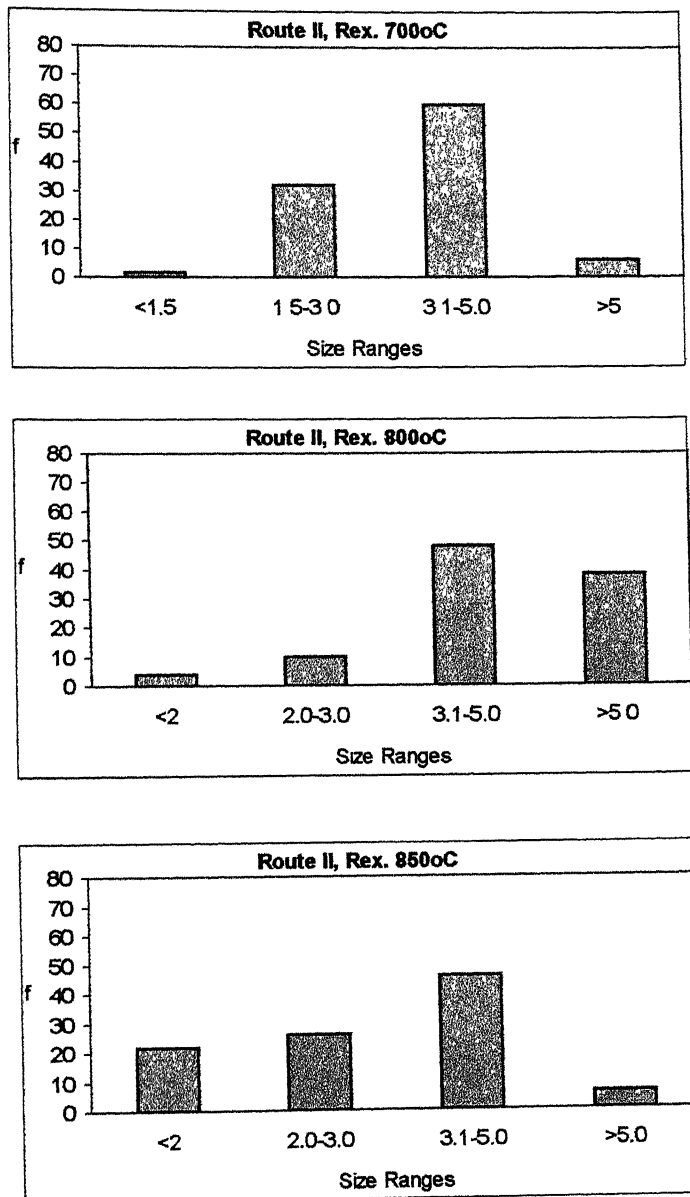


Fig. 4.32

**Aspect Ratio Distribution of Samples Processed Through Route II and Recrystallized at Different Temperatures**



**Figure 4.33** Grain Size Distribution of Samples Processed Through Route II and Recrystallized at Different Temperatures



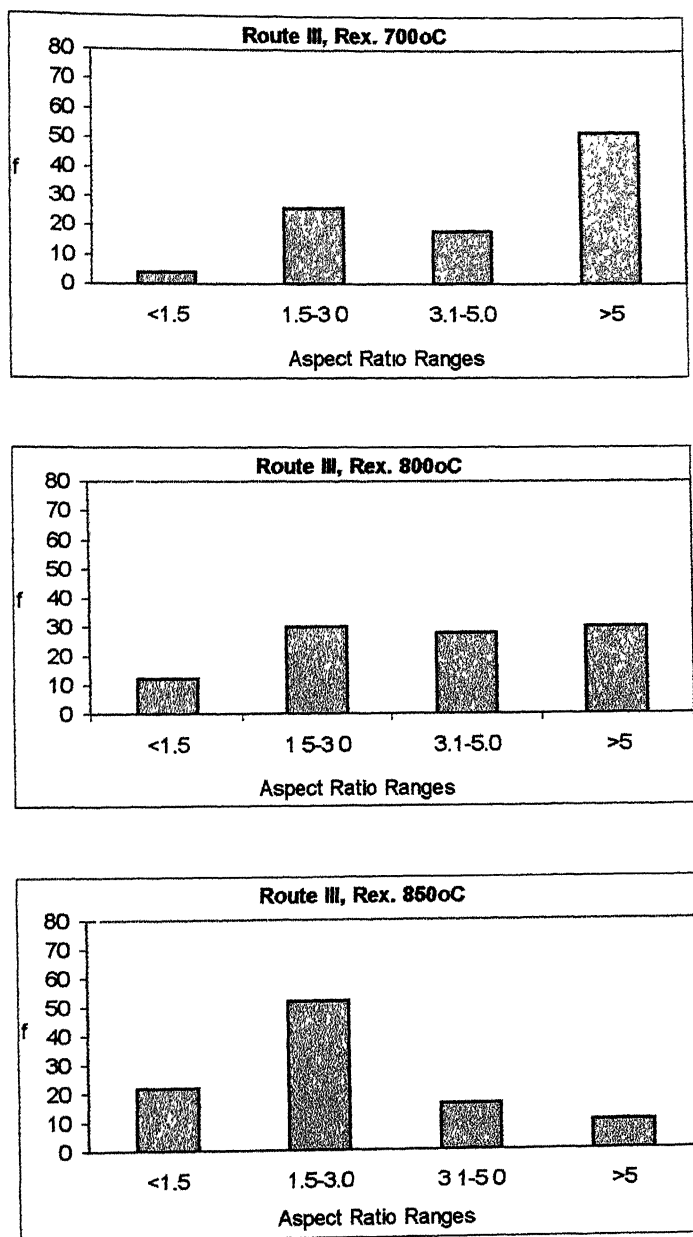


**Figure 4.34** Aspect Ratio Distribution of Samples Processed Through Route III and Recrystallized at Different Temperatures

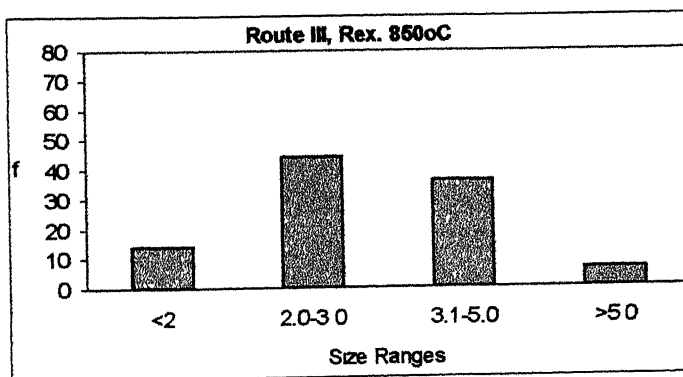
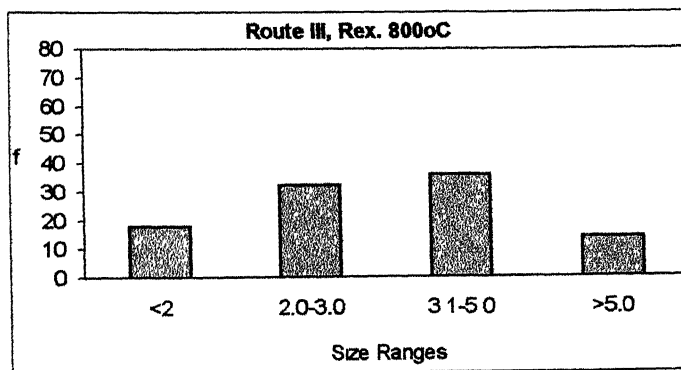
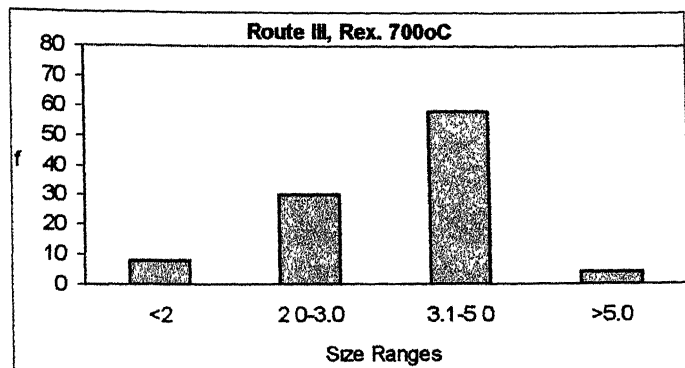


**Figure 4.35** Grain Size Distribution of Samples Processed Through Route III and Recrystallized at Different Temperatures

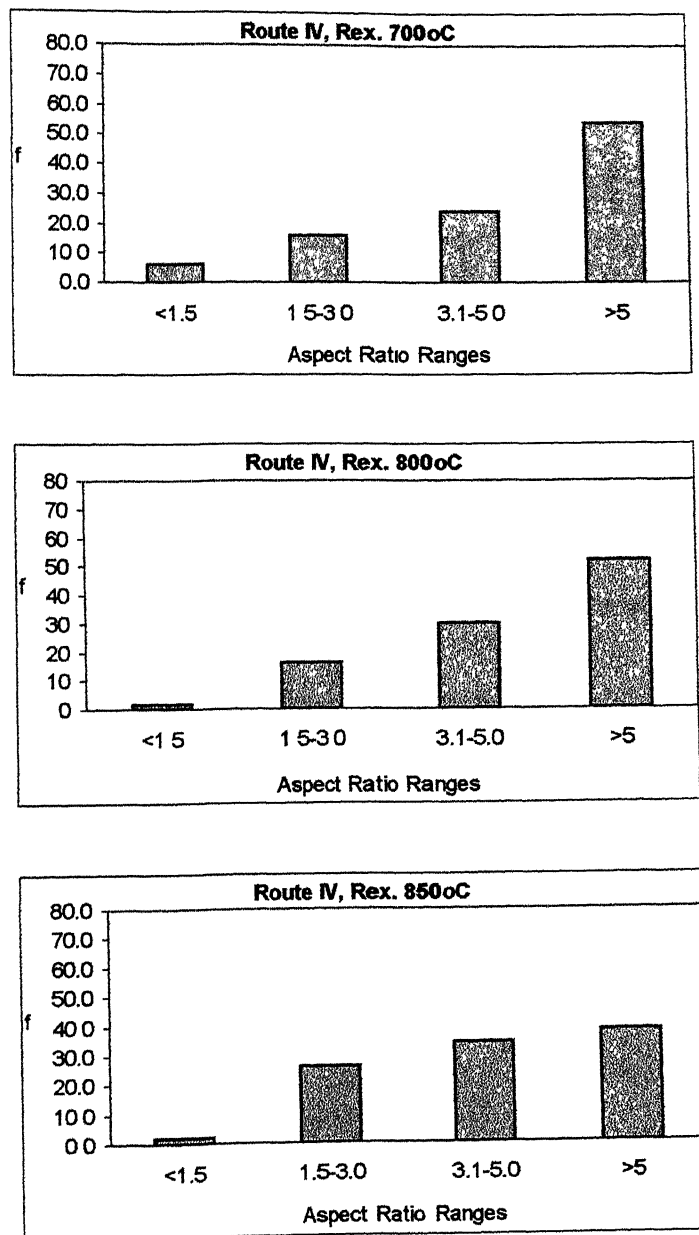


**Figure 4.36** Aspect Ratio Distribution of Samples Processed Through Route IV and Recrystallized at Different Temperatures

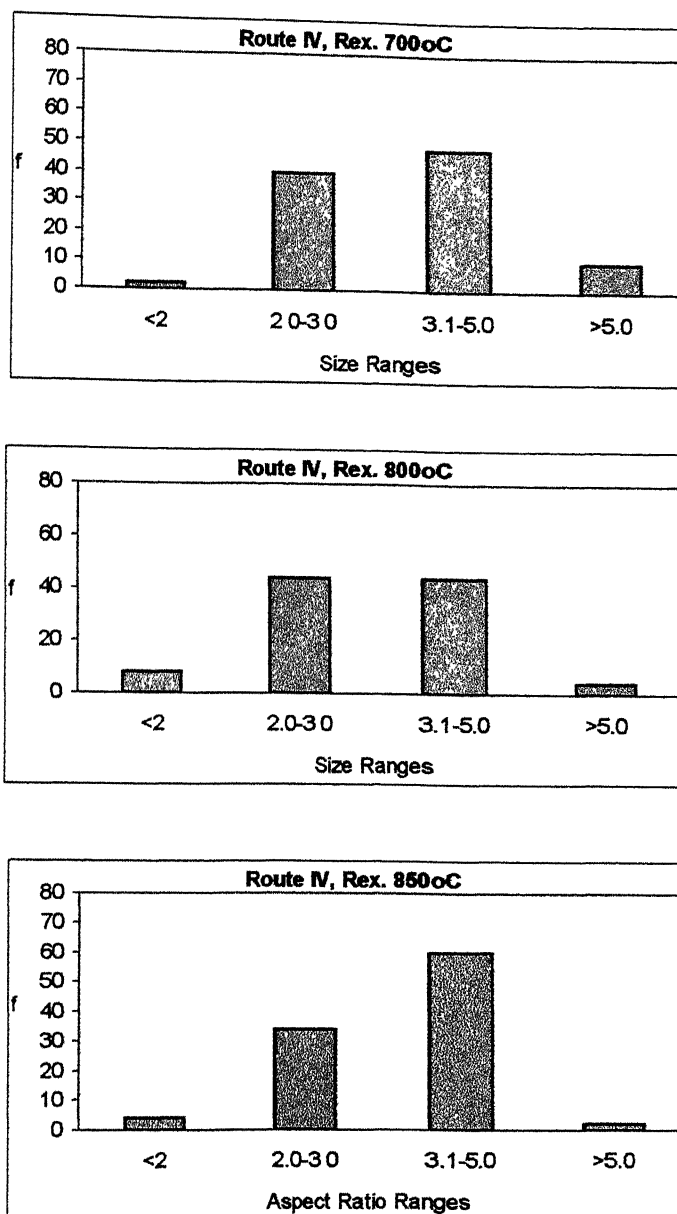


**Figure 4.37** Grain Size Distribution of Samples Processed Through Route IV and Recrystallized at Different Temperatures

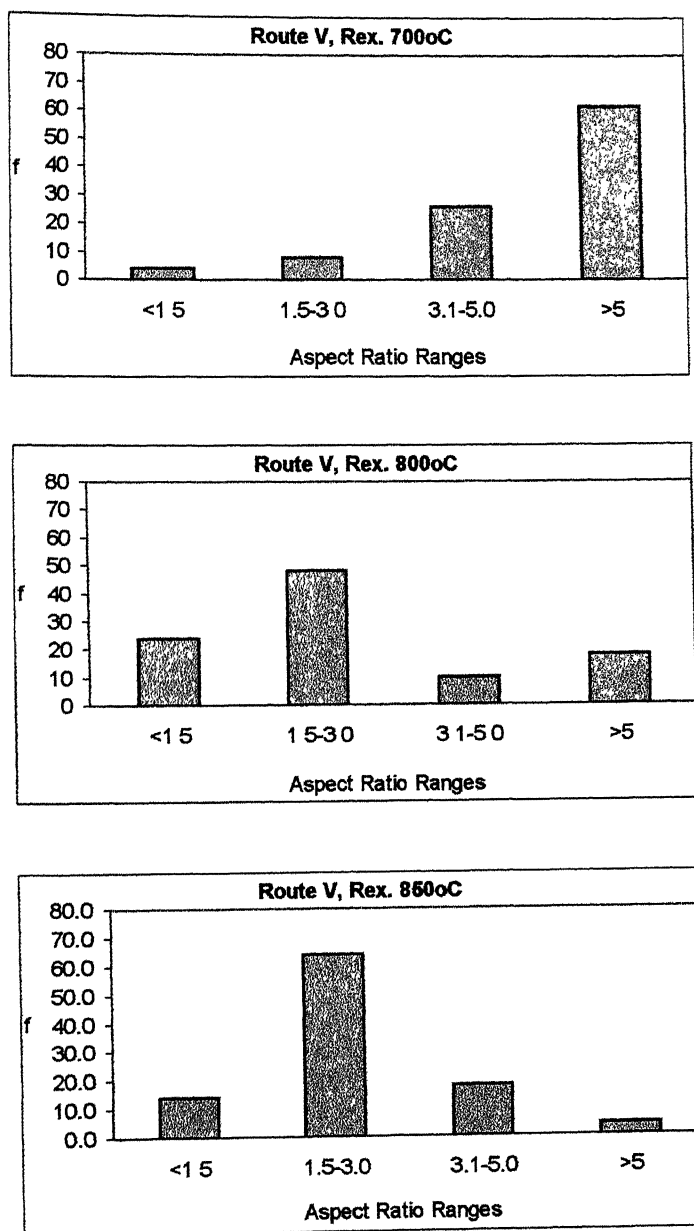


**Figure 4.38** Aspect Ratio Distribution of Samples Processed Through Route V and Recrystallized at Different Temperatures

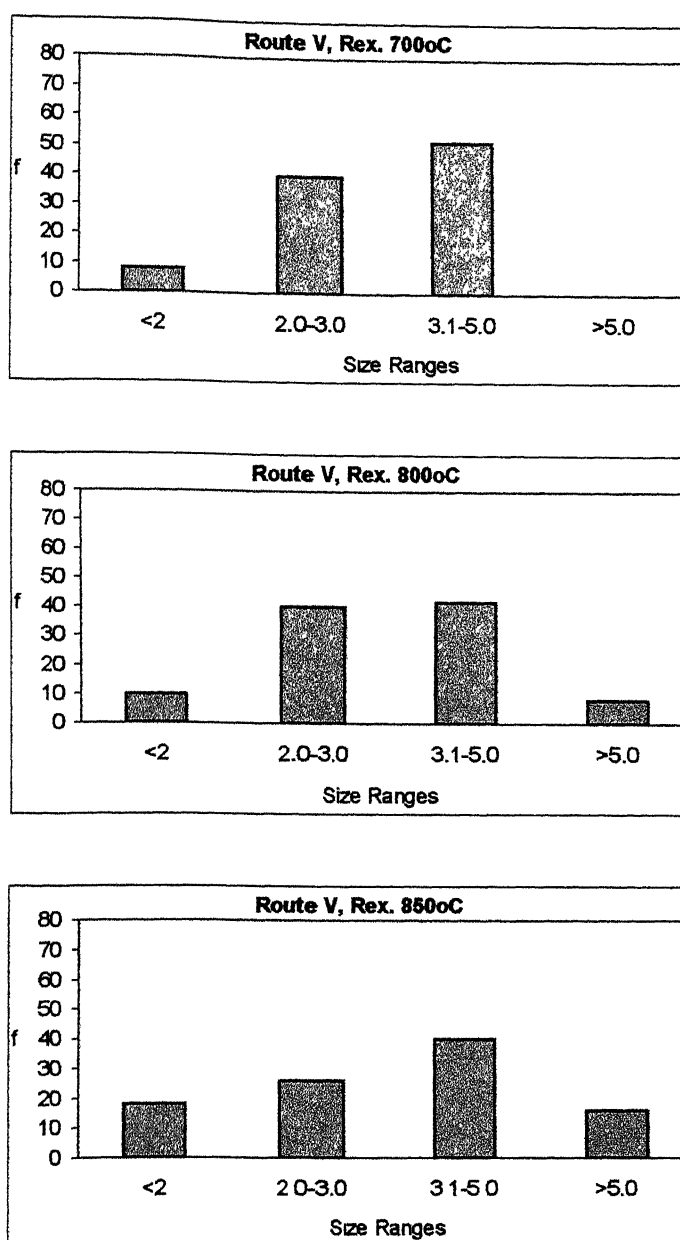


**Figure 4.39** Grain Sizeo Distribution of Samples Processed Through Route V and Recrystallized at Different Temperatures

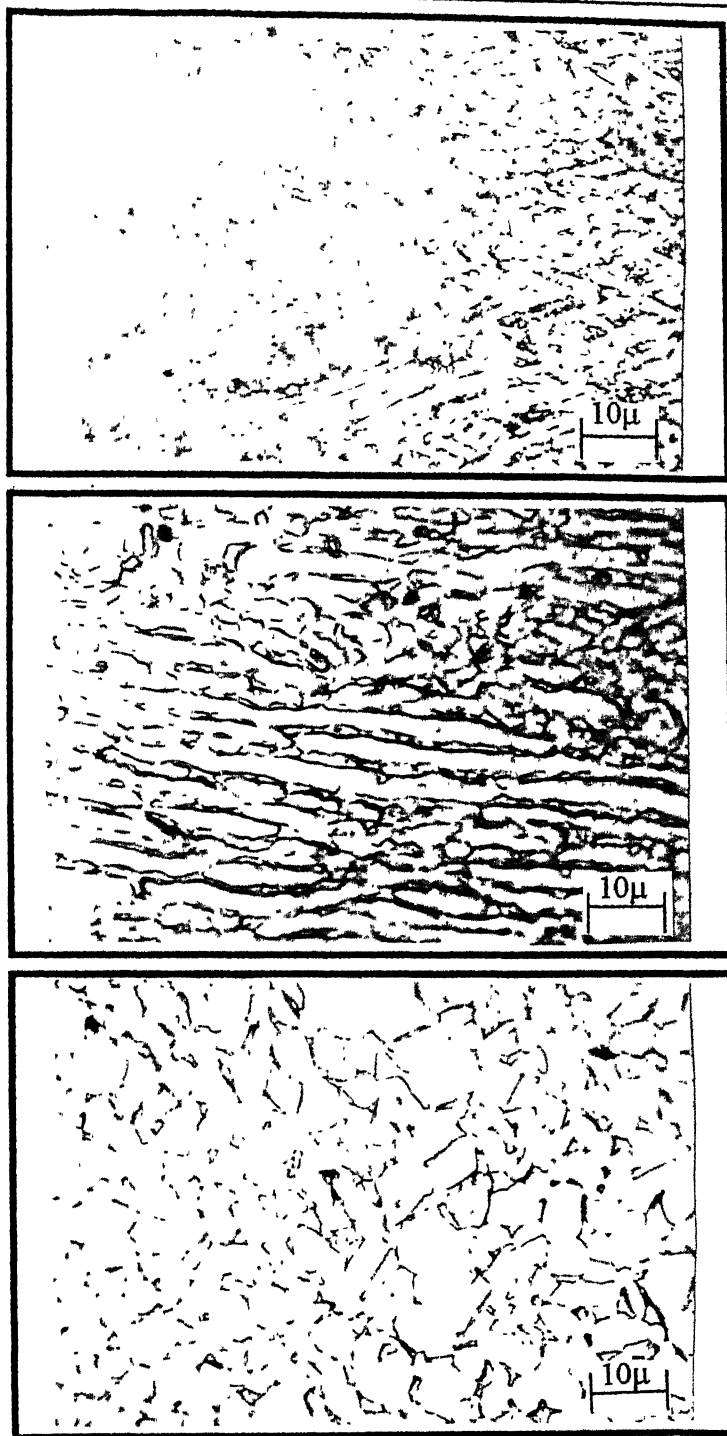


**Figure 4.40** Microstructure of Samples Processed Through Route II , and Recrystallized for 30 minutes at(in water quenched conditions)

- (a) 700°C
- (b) 800°C
- (c) 850°C

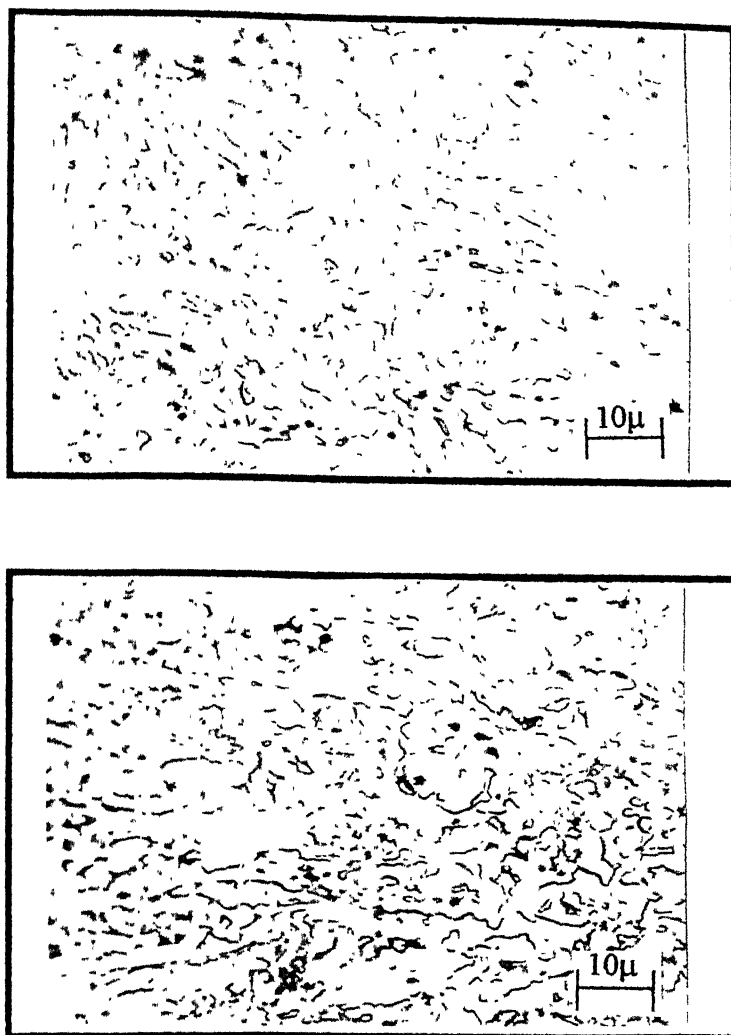


**Figure 4.41** Microstructure of Samples Processed Through Route III , and Recrystallized at 800°C for (in water quenched conditions)  
(a) 15 minutes  
(b) 30 minutes



#### 4.7 MECHANISM OF EVOLUTION OF EQUIAXED $\alpha$ STRUCTURE IN Ti-6-4 ALLOY

The hot rolling temperature of ( $\alpha+\beta$ ) titanium alloys in the two-phase field is important due to several reasons. Firstly, the volume fractions of equilibrium  $\alpha$  and  $\beta$  phases in the alloy change with temperature, with volume fraction of  $\beta$  phase increasing with increasing temperature. Secondly, the mean width of acicular  $\alpha$  plates, obtained by the transformation from  $\alpha'$ , changes with the transformation temperature. Finally, the deformation resistance and plasticity of  $\alpha$  and  $\beta$  phases change with temperature, with deformation resistance decreasing and plasticity increasing with increasing temperature. Since the  $\alpha$  phase undergoes morphological changes during working in the two-phase field all the above three factors play important role in fragmentation and refinement of the  $\alpha$  phase. In a previous work[5] it was concluded that rolling at lower temperatures improve the refinement of  $\alpha$  platelets. In the present work, all the samples processed through route I to V were heated at 820°C, 880°C and 920°C, soaked there for 20 minutes and deformed by 0%, 25%, 50% and 75% thickness reduction at each of these temperatures. Specimens in each case were immediately quenched in water after the last pass. The effect of hot rolling on the morphology and refinement of primary  $\alpha$  phase is shown in previous section in terms of lamellae length and thickness of  $\alpha$  phase. It is observed that on hot rolling in the two-phase field the mean aspect ratio of  $\alpha$  phase decreases in all the cases. This is mainly attributed to the breaking up of  $\alpha$  phase in shorter segments. This becomes clear from the figures, in which length and thickness distribution of  $\alpha$  lamellae are presented. A comparison of these figures clearly shows that for each route, the  $\alpha$  lamellae length decreases after higher amount of deformation in stage II than that after stage I, indicating that  $\alpha$  lamellae are breaking after heavy thickness reduction in the two-phase field. But the thickness of the  $\alpha$  lamellae increases first at 820°C than that from stage I, but with increasing temperatures it decreases. This can be explained by the fact that with increasing temperature equilibrium volume fraction of  $\beta$  increases, and hence,  $\alpha$

lamellae thickness decreases. So the microstructures come in equilibrium within the specific time period in this study. But this type of observation is just the opposite of what is found in standard literatures[72, 78]. This is probably due to non-attainment of equilibrium in the thick samples used in those studies

It is to be understood that  $\alpha/\alpha$  grain boundary energy increases with increasing strain and decreasing temperature of deformation. The formation of  $\beta$  cusps at  $\alpha/\alpha$  boundaries is likely to lower the energy of the system due to lower  $\alpha/\beta$  grain boundary energy. The most important analysis of breaking-up of  $\alpha$  lamellae during deformation is by Weiss et al.[78] and that during recrystallization is by Peters et. al.[72] It seems that the results of the present investigation clearly supports the mechanisms proposed by them.

In support with the mechanism proposed by Weiss et. al., it was observed that the morphological changes occurring during the modification of primary lamellar  $\alpha$  phase to more equiaxed configuration appear to be initially associated with the development of sub-boundaries across the  $\alpha$  plates. Depending on the amount of localized deformation, the  $\alpha$  lamellae can accumulate a relatively high dislocation density either homogeneously or heterogeneously. Dynamic and static recovery, which are softening processes than dynamic and static recrystallization are likely to occur during the high temperature deformation and subsequent cooling. This leads to formation of both low and high angle boundaries. This is considered to be the first step towards the break-up of lamellar structure followed by penetration of the  $\beta$  phase along the sub-boundaries or high angle boundaries. The  $\beta$  phase forms deep cusps at  $\alpha/\alpha$  boundaries with relatively high misorientation. It is also possible that the extent of cusp penetration along the  $\alpha/\alpha$  boundaries and shear bands is partially the result of  $\beta$  phase being left over after the advance of the  $\alpha$  phase upon cooling. If the  $\alpha$  lamellae width is small, then separation of the  $\alpha$  grains occur readily. The formation of cusps at the location where  $\alpha/\alpha$  interfaces intersect  $\alpha/\beta$  interfaces is a result of the balancing the interfacial energy between  $\alpha/\alpha$  and  $\alpha/\beta$  boundaries. The dihedral angle  $\theta$  is given by

It is assumed that the cusp penetration rate depends on the diffusion of Al and V through the volume or along the interfaces. In the presence of a high dislocation density, this process should be accelerated and fully developed cusps will form during deformation. A more complete separation into equiaxed  $\alpha$  grains can be achieved by post deformation annealing. This is a direct result of the  $\beta$  phase penetrating the  $\alpha/\alpha$  interfaces and shear bands by the cusp mechanism. This is also clear from Figure 4.40.

A more detailed description of the recrystallization behaviour of  $\alpha$  lamellae during post deformation annealing given by Peter et. al., claims that to establish a very fine equiaxed homogeneous microstructure, it is of advantage if the phases are not in equilibrium before deformation (Mechanism III, Figure 4.42). During subsequent heat treatment, the phase equilibrium will be obtained in combination with continuous recrystallization process. On the other hand, if the starting microstructure is in phase equilibrium, then both the phases recrystallize in themselves, so that their lamellar arrangement is maintained (Mechanisms I and II, Figure 4.42).

An almost similar mechanism of  $\alpha$  platelet refinement was proposed by Kaibyshev et. al.[84] which explained breaking of  $\alpha$  platelets during deformation. According to this mechanism (Figure 4.43), a laminate of  $\beta/\alpha/\beta$ , during rolling is consequently subjected to compressive forces perpendicular to the rolling direction and tensile forces along the rolling direction. Thus, a vacancy flux is directed towards the compressed side of the  $\alpha$  platelet and atoms of the alloying elements are moved to the extended region. Since, Al (an  $\alpha$  stabilizer) possesses higher diffusivity compared to that of V (a  $\beta$  stabilizer), it moves away from the compressed region towards the region of tensile stresses. Al depletion at the compressed surface of the  $\alpha$  platelets induces  $\alpha \rightarrow \beta$  transformation. Due to differential and localized thinning of  $\alpha$  plates, compressive stresses are not uniform over the length of the platelets. Therefore, during exposure to local stress concentration, the opposite fluxes of vacancies and Al atoms are more intense in

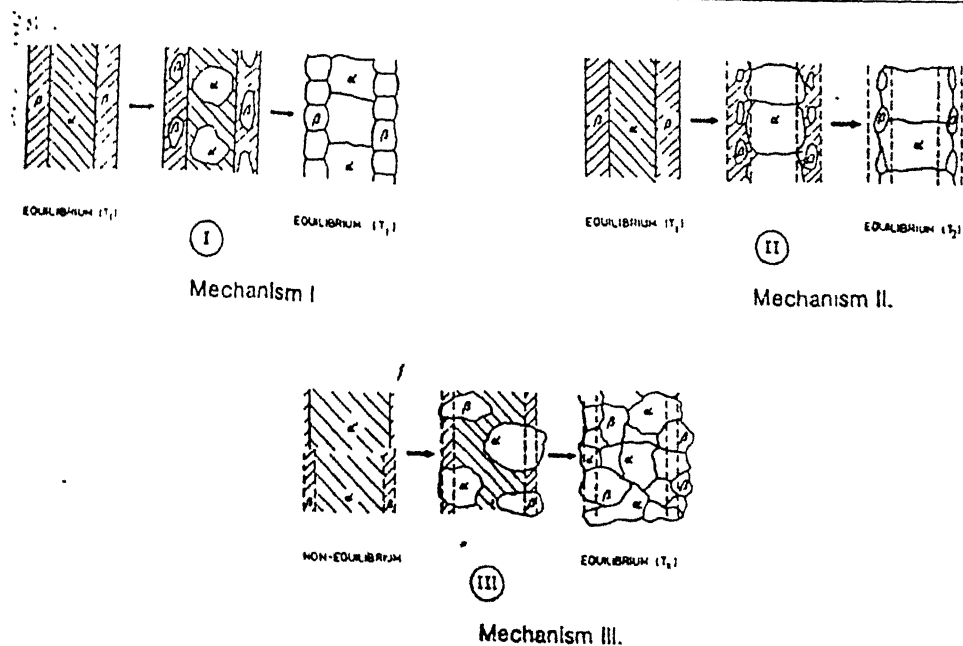


**Figure 4.42** Mechanisms of  $\alpha$  Lamellae recrystallization

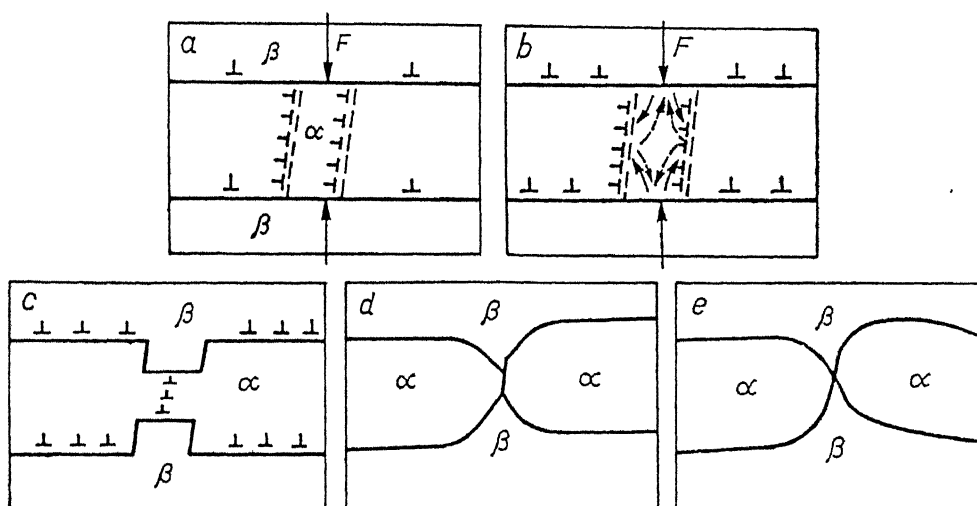


**Figure 4.43** Mechanism of Recrystallization During Deformation as Proposed by Kaibyshev et. al.

regions with enhanced defect density. The depletion of Al from the surface of the compressed part of the  $\alpha$  plate results in its transformation to  $\beta$  phase and forms groove on the  $\alpha/\beta$  interface. Under the continued operation of stresses, such a groove penetrates into the  $\alpha$  phase. In the presence of high dislocation density, this process gets intensified and complete penetration of the  $\beta$  phase occurs during hot deformation in the two-phase field. The frequency of occurrence of these cusps increases with decrease in deformation temperature. Further due to activation of diffusion processes, the breaking of  $\alpha$  plates is likely to be assisted by change in the interface from that of low angle to high angle ones. Therefore the model proposed by Kaibyshev for the refinement of  $\alpha$  platelets, explains explicitly the observations of the present investigation, in particular, the decrease in aspect ratio of  $\alpha$  platelets with deformation in two-phase field.

In the present investigation it is observed that the thickness of the martensitic needles and/or  $\alpha$  lamellae decreases in all the routes II to V as compared to the equilibrium structure obtained through route I. The structure heavily deformed at 880°C and then recrystallized at 850°C for 30 minutes shows that the grain size produced in the samples processed through the unconventional  $\beta$  processing routes is lower than that produced in the conventionally processed samples. Hence, it can be said that the newly conceived thermo-mechanical processing routes enhance the grain refinement behaviour of Ti-6-4 alloy, studied in this investigation.

## CHAPTER 5

### CONCLUSIONS

---

Ti-6Al-4V alloy was processed through five unconventional thermo-mechanical processing routes which essentially are designed with the aim of changing the pre- $(\alpha+\beta)$  deformation microstructure of the alloy by (i) conditioning of prior  $\beta$  grains and (ii) altering the morphology of  $\alpha$  lamellae prior to working in the two-phase field. The following conclusions can be drawn from the observations of the present study :

- (1) Ti-6Al-4V alloy, during its processing in the  $\beta$  phase field, does not undergo dynamic recrystallization upto the rolling temperature of 980°C, i.e., about 30°C above the  $\beta$  transus temperature even at a deformation as high as 60%.
- (2) The alloy undergoes rapid recrystallization and grain growth during subsequent annealing in the  $\beta$  phase field. For example, at a temperature of 960°C, i.e., just 10°C above the  $\beta$  transus temperature, the alloy recrystallizes within the short interval of 30 seconds only.
- (3) The size and morphology of  $\beta$  grains prior to their water quenching has considerable influence on (a) the morphology of the martensite needles and (b) acicular  $\alpha$  lamellae formed prior to hot rolling of the alloy in the  $(\alpha+\beta)$  phase field.
- (4)  $\beta$  processing through unconventional routes produces thinner and shorter martensite needles as compared to the conventional route.

- (5) Preheating of the martensitic structure for the rolling in the two-phase field produces acicular  $\alpha$  structure. With increasing temperature of treatment in the two phase field the thickness of  $\alpha$  lamellae decreases. However, the thickness of  $\alpha$  lamellae at all the temperatures is greater than that of martensite needles produced after stage I.
- (6) In the samples processed through route I and further heated at 820°C in  $(\alpha+\beta)$  region, breakage of  $\alpha$  lamellae is the dominant feature up to the higher degree of deformation given. But at higher temperatures, i.e., at 880°C and 920°C breakage of  $\alpha$  lamellae predominates up to about 75% deformation. Beyond this reduction some amount of elongation of the  $\alpha$  lamellae is observed. This trend is also observed in samples processed through routes IV and V respectively.
- (7) Samples processed through route II and III show somewhat different fragmentation behaviour. In these routes,  $\alpha$  lamellae elongate even at about 25% thickness reduction, but later with increasing amount of deformation undergo fragmentation.
- (8) Samples given 75% thickness reduction at 880°C upon recrystallization at 850°C for 30 minutes, samples processed through route II and III show finer grained structure than the other samples. On the other hand aspect ratio distribution of samples processed through route II and IV are alike and have wide range of distribution.
- (9)  $\beta$  processing of the alloy through unconventional routes increases the processing window and it is observed that very fine equiaxed  $\alpha$  structure can be obtained under several different conditions in Ti-6-4 alloy

## REFERENCES

1. H.T.Clerk ; "Trans. Amer. Inst. Min.(Metall.) Engrs.", v. 185, 1949, pp.588.
2. W.Burgers, F.Z.Jacobs ; "Kristallogr.", v. 94, 1936, pp.299.
3. A.D.McQuillon, M.K.McQuillon ; "Titanium", Butterworths Scientific Publications, 1956, London.
4. E.W.Collings ; "The Physical Metallurgy of Titanium Alloys", American Society for Metals, 1984, USA.
5. K.B.Mallikarjun; M.Tech. Thesis, I.I.T., Kanpur, 1998.
6. J.L.Everhart ; "Titanium and Titanium Alloys", Rein hold Publishing Corporation, 1954, New York.
7. G.Shujun, Q.Rongshi, Z.Suisheng, W.Xiaojng ; Fatigue crack growth for Ti-6Al-4V Alloy In Water, "Proc. of 1<sup>st</sup> Int. Conf. on Metallurgy and Material Science of W, Ti, RE, Sb", Ed. by F. Chongyue, v. II, pp.987.
8. European Productivity Agency of the organization for European Economic Co-operation ; "Titanium, Zirconium and Some Other Elements of Growing Industrial Importance", Project No. 247, Sept. 1956, Paris.
9. C.Sugui, M.Suland, L.Shizhuo ; Cavitation Damage of Ti-6Al-4V Alloy, "Proc. of 1<sup>st</sup> Int. Conf. on Metallurgy and Material Science of W, Ti, RE, Sb", Ed. by F. Chongyue, v.II, pp.906.
10. S.Ashley ; Boeing 777 Gets a Boost From Titanium, "Mechanical Engg.", v. 115, no. 7, July, 1993, pp.60.
11. "Titanium for Energy and Industrial applications", Ed. by D.Eylon, The Metallurgical Society of AIME, pp.19,71,84.
12. H.E.Friedrich, R.Furlon, M. Kullick ; SPF/DB on the way to the production stage for Ti and Al applications within military and civil projects, "Superplasticity and superplastic forming, Int. Conf. proc., Ed. by C.H.Hamilton,N.E.Patron; TMS, August,1988, Washington, pp.649.
13. R.Furlon, P.J.Winkler, D.Hagg, L.Reisinger ; Production of Ti-6Al-4V componenets for a new turbo-fan engine, ibid, pp.665.



## References

14. A.S.Ramamoorthy ; Titanium for underwater applications, "National seminar on titanium and superalloys", Conf Proc., Hyderabad, 28-29 July, 1996.
15. J.R.Myers, H.B.Bomberger, F.H.Froes ; Corrosion behaviour and use of titanium and its alloys, "Jornal of Metals", October, 1984, pp.50.
16. L.S.Richardson, N.J.Grant ; "Trans. Amer. Inst. Min. (Metall.) Engrs.", Vol. 200, 1954, pp.69.
17. E.S.Bumps, H.D.Kessler, M.Hansen ; "Trans. Amer. Soc. Metals", Vol.45, 1953, pp.1008.
18. L.Quingyun, L. Weihong ; Status for China's titanium processed materials, "Proc. 1<sup>st</sup> Int. Conf. on metallurgy and material science of W,Ti, RE, Sb", Ed. by F. Chongyue, Vol. 1, pp.23-33.
19. E.K.Molchanova ; "Phase diagrams of titanium alloys", Israel programme for scientific translations, Jerusalem, 1965.
20. U.Zwicker : "Titan and titanlegierungen" , Springer-Verlag, 1974(as cited in ref.4).
21. B.W.Levinger ; "Trans. Amer. Inst. Min. (Metall.) Engrs.", Vol.197, 1953, pp.195.
22. H.W.Rosenbarg ; Titanium alloying in theory and practice, "Sci. Tech. and Appli. Of titanium", Proc. 1<sup>st</sup> Int. Conf. on titanium, Ed. by R.I.Jaffee and N.E.Promisel, Pergamon press, London, 1970, pp.851-859.
23. "Facts about metalllography of titanium", RMI Company, Niles, Ohio.
24. R.A.Wood ; "Titanium alloys handbook", Metals and Ceramic information centre, Battelle, December, 1972.
25. D.R.Salmon ; "Low temperature data handbook, Titanium and titanium alloys", National Physical Laboratory, May, 1979.
26. I.V.Gorynin, B.B.Chechulin, S.S.Ushkov, A.I.Baluyev ; A study of the nature of the ductile-brittle transition in  $\beta$ -Titanium alloys, "Titanium Science and Tech.", Proc. 2<sup>nd</sup> Int. Conf. on Titanium, Ed. by R.I.Jaffee and H.M.Brute, Plenum press, 1973, pp.1109-18.
27. K.H.Mishra ; "Materials Engineering", Reinhold Publishing Company Inc., . 1974, pp.61-80.

28. S.M.L.Shastri, P.S.Rao, K.K.Shankaran ; High Temperature Deformation of Ti-6Al-4V, "Titanium'80 Science and Technology", Conf. Proc., Ed. by Kimura and Izumi, Japan, May 1980, pp.873-86
29. S.Abkowitz, J.J.Burke, R.H.Hiltz ; "Titanium in Industry", D.Van Norstand Company Inc., USA, January 1955.
30. "Emerging Materials for Automotive Applications", An ISTE Course package developed by S.Bhargava, Dept. of MME, IIT Kanpur, pp.24.
31. H.D.Kessler, R.P.Sullivan ; Seamless Ti-15V-3Cr-3Sn-3Al Alloy Tubing for Aerospace and Other Applications, "Titanium 1986, Int. Conf. Proc. on Titanium Products and Applications", Titanium Development Association, Dayton, Vol-1, 1987, pp.72-83.
32. J.Charles, A.Suiger, J.P.Doucet ; Corrosion Behaviour And Use in Offshore Applications of Ti-6Al-4V Titanium Alloy, *ibid*, pp.256-81.
33. M.Sen ; Development of a Titanium Base Alloy for Medical Implants, *ibid*, Vol. 2, pp. 712-20.
34. T.Shepard, J. Norley ; Deformation Characteristics of Ti-6Al-4V, " Mat. Sc. And Tech.", Vol. 4, No. 10, Oct 1988, pp. 903-8.
35. F.D.Rosi, C.A.Dube, B.H.Alexandar ; "Trans. Amer. Inst. Min.(Metall.) Engrs.", Vol.197, 1953, pp.257.
36. A.T.Churchman ; "Nature", London, Vol.171, 1953, pp.706.
37. F.D.Rosi, F.C.Perkins ; "Journal of Metals", Vol.5, 1953, pp.1083.
38. C.J.McTargue, J.P.Hamond ; "Acta Met.", Vol.1, 1953, pp.700.
39. Metals Handbook, 8<sup>th</sup> Edition, Vol. 4, ASM, pp. 437-46.
40. S.L.Semiatin, D.Lahoti ; The Occurance of Shear-Bands in Non-isothermal Hot Forging of Ti-6Al-2Sn-4Zr-2Mo-0.1Si, "Met. Trans. A", Vol.14A, January1983, pp.105-15.
41. Metals Handbook, 9<sup>th</sup> Edition, Vol.3, ASM Committee on Ti and Ti alloys, 1980, pp.361-71.
42. Microstructural Standards for  $\alpha+\beta$  Titanium Alloy Bars, Prepared by The Technical Committee of European Titanium Producers,1979.
43. W.A.Reinsch ; Terminology for Titanium Microstructures, "Metal Progress", Vol.121, No.2, February1982, pp.51-56.

## References

44. G.Welsch, R.Boyer , Technical Note 1: Metallography and Microstructure, pp.1051-60.
45. D.R.Thornburg, H.R.Piehler , Cold Rolling Texture Development in Ti and Ti-Al Alloys, "Titanium Sc. And Tech.", Int. Conf. Proc. on Titanium, Ed. by R.I.Jaffee, H.M.Burte, Boston, 1973, pp.1187-97.
46. H.Inagaki ; Development of Cold Rolling Textures in Pure Ti, "Z. Metalkd.", October 1991, pp.79-89.
47. H.Inagaki ; Hot rolling Textures in Ti, "Z. Metalkd.", April 1990, pp.282-92.
48. H.Inagaki ; Hot rolling Textures in High strength Ti alloys, "Z. Metalkd.", August 1990, pp.540-55.
49. H.Inagaki ; Evolution of Textures and Microstructures in TMP of Ti-6Al-4V, "Z. Metalkd.", June 1990, pp.433-45.
50. S.F.Frederick, G.A.Lenning ; Producing Basal Textured Ti-6Al-4V Sheet, "Met. Trans.", Vol.6B, December 1975, pp.601-5.
51. A.A.Babreko, I.V.Egiz, O.S.Belova, M.M.Dobrodeyeva ; The Formation of a Basal Texture of Sheets of a Psedo  $\alpha$  Alloy of the Ti-Al-V System in Different Conditions of Rolling, " Phys. Met. Metallo.", Vol.65, No. 5, 1988, pp.100-7
52. R.A.Adanesku, G.I.Denisenko, A.S.Kudryavtsev, G.V.Turchaninova, Ye.V.Chudakov ; Influence of Annealing on The Texture of a Titanium  $\alpha+\beta$  Alloy, "Phys. Met. Metallo.", Vol.63, No.5, 1987, pp.139-43.
53. M.F.Amateau, D.L.Dull, L.Reymond ; The Effect of Processing on Plastic Anisotropy of Ti-6Al-4V, "Met. Trans. A", Vol.5A, March 1974, pp.561-64.
54. G.V.Shakhanova, O.G.Ukolova ; Features of The Texture of Hot Upsetting and Its Influence on The Structure of Titanium Alloy VTZ-1, "Phys. Met. Metallo.", Vol.71, No.4, 1991, pp.143-48.
55. H.Liping ; The Study of Reducing Superplastic Temperature in Titanium Alloys, "Superplasticity and Superplastic Forming", Int. Conf. Proc., Ed. by C.H.Hamilton, N.E.Paton, TMS, 1988, pp.435-39.
56. G.Sridhar, D.S.Sarma ; On The Influence of Microstructure on The Room-temperature Deformation Behaviour of a Near  $\alpha$  Ti Alloy, " Met. Trans. A", Vol.22A, No.5, May 1991, pp.1122-25

## References

57. K.A.Padmanabhan, G.J.Davies ; "Superplasticity – Mechanical and Structural Aspects, Environmental Effects, Fundamentals and Applications", Springer-Verlag, Berlin, Heidelberg, 1980.
58. M.M.I.Ahmed, T.G.Langdon ; Exceptional Ductility in The Superplastic Pb-62%Sn Eutectic, "Met. Trans.A", Vol.8A, No.11, November1977, pp.1832-33.
59. K.Higashi, T.Ohnishi, Y.Nakatani ; Superplastic Behaviour of Commercial Aluminium Bronze , "Scr. Met.", Vol.19, no.7, July1985, pp.821-24.
60. G.J.Davies, J.W.Edington, C.P.Cutler, K.A.Padmanabhan ; "J. of Mater. Sc.", Vol.5, 1970, pp.1091-
61. J.Pilling, N.Ridley ; "Superplasticity in Crystalline Solids", The Institute of Metals, London, 1989.
62. H.Inagaki, Enhanced Superplasticity in High Strength Ti Alloys, "Z. Metallkd", Vol.87, No.3, 1996, pp.179-86.
63. H.Inagaki, Mechanism of Enhanced Superplasticity in Thermomechanically Processed Ti-6Al-4V, "Z. Metallkd", Vol.86, No.9, 1995, pp.643-50.
64. M.E.Rosenblum, P.R.Smith, F.H.Froes ; Microstructural Aspects of Superplastic Forming of Titanium Alloys, "Titanium'80 Sc. And Tech.", -Int. Conf. Proc., Ed. by H. Kimura, O.Izumi, 1980, pp.1015-24.
65. A.K.Ghosh, C.H.Hamilton ; Influences of Material Parameters and Microstructure on Superplastic Forming, "Met. Trans.A", Vol.13A, May1982, pp.733-43.
66. A.Arieli, A.Rosen, Superplastic Deformation of Ti-6Al-4V Alloy, "Met. Trans.A", Vol.8A, Oct.1977, pp.1591-96.
67. M.T.Cope, N.Ridley ; Superplastic Deformation Characteristics of Microduplex Ti-6Al-4V Alloy, "Mat. Sc And Tech.", Vol.2, Feb.1986, pp.140-45.
68. M.T.Cope, D.R.Evetts, N.Ridley ; Superplastic Deformation Characteristics of Two Microduplex Titanium Alloys, "J.of Mat. Sc.", Vol.21, 1986, pp.4003-08.

## References

69. E.Girault, J.J.Blandin, A.Verloteaux, M.Surey, Y.Combres ; Low Temperature Superplasticity of A Metastable  $\beta$ -Ti Alloy, "Scr. Met.", Vol.29, No.4, 1993,pp. 503-08.
70. S.Yamazaki, T.Oka, Y.Mae, Superplastic Properties of The Cold Formable Ti Alloy SP35, "Superplasticity And Superplastic Forming", Int. Conf. Proc., Ed. by C.H.Hamilton, N.E.Paton, TMS, 1988, pp.407-11.
71. M.j.Donachie ; " Titanium And Titanium Alloys: A Source Book", ASM, 1982.
72. M.Peters, G.Lutjering, G.Ziegler ; Control of Microstructures of  $\alpha+\beta$  Titanium Alloys, "Mat. Sc. And Tech.", Vol.4, No.903, Oct.1988, pp.274-82.
73. D.Bourell, H.J.McQueen ; "J. of Applied Metal Work", Vol.5, 1987, pp.53-73.
74. J.C.Chesnutt, C.G.Rhodes, J.C.Williams ; Relationship Between Mechanical Properties, Microstructure And Fracture Topography in  $\alpha+\beta$  Titanium Alloys, "Fractography – Microscopic Cracking Processes", ASTM, 1976, pp.99-138.
75. M.A.Greenfield, C.M.Pierce, J.A.Hall ; The Effect of Microstructure on The Control of Mechanical Properties in  $\alpha+\beta$  Titanium Alloys, "Titanium Science And Technology", Proc. of 2<sup>nd</sup> Int. Conf., Ed. by R.I.Jaffee, H.M.Burte, Vol.3, 1973, pp.1731-43.
76. V.Shukla, S.Bhargava ; Effect of Thermomechanical Treatment on Microstructural Refinement in Ti-6.8Al-3.2Mo-1.8Zr-0.3Si Alloy, "National Seminar on Titanium And Superalloys", Hyderabad, July1996.
77. G.Wirth, K.J.Grundhoff, A TMT For The Improvement of Microstructure of PM And IM Ti-6Al-4V Possessing A Combination of High RT Fatigue Strength And Good Creep Rupture Strength, "6<sup>th</sup> World Conference on Titanium", France, 1988, pp.1307-18.
78. I.Weiss, F.H.Froes, D.Eylon, G.E.Welsch ; Modification of  $\alpha$  Morphology in Ti-6Al-4V by Thermomechanical Processing, " Met. Trans.A", Vol.17A, Nov.1986, pp.1935-46.

79. G.Lutjering, J.Albrecht, O.M.Ivasishin ; Influence of Cooling Rate and  $\beta$  Grain Size on the Tensile Properties of ( $\alpha$ + $\beta$ ) Ti-alloys, "Titanium '95: Science and Technology", Pub. By TMS, 1995, pp.1163-1170.
80. M.A.Greenfield, H.Margolin ; The Interrelationship of Fracture Toughness and Microstructure in a Ti-5.25Al-5.5V-0.9Fe-0.5Cu Alloy, "Met. Trans.", Vol. 2, March 1971, pp.841-847.
81. R.I.Jaffee ; Critical Review : Metallurgical Synthesis, "Titanium Science And Technology", Proc. of 2<sup>nd</sup> Int. Conf., Ed. by R.I.Jaffee, H.M.Burte, Vol.3, 1973, pp. 1665-1693.
82. D.Banerjee, D.Mukherjee, R.L.Saha, K.Bose ; Microstructure and Tensile Ductility in a  $\beta$  Heat Treated Titanium Alloy, "Met. Trans. A", Vol. 14A, March 1983, pp. 413-420.
83. R.M.German ; "An Introduction to Powder Metallurgy", p.78.
84. O.A.Kaibyshev, R.A.Lutfullin, G.A.Salishchev ; Influence of Superplastic Deformation Conditions on Transformation of Plate-like Microstructure in Titanium Alloy VT9 , "Phys. Metal. And Metallo.", Vol 66, No.6, 1988, pp.109-117.